Stony Brook University

Biomechanical Promotion of Mesenchymal Stem Cell Proliferation as a Countermeasure to the Development of Obesity and Osteoporosis

A Dissertation Presented

by

Yen Kim Luu

to

The Graduate School

in Partial fulfillment of the

Requirements

for the Degree of

Doctor of Philosophy

in

Biomedical Engineering

Stony Brook University

May 2008

Stony Brook University

The Graduate School

Yen Kim Luu

We, the dissertation committee for the above candidate for the
Doctor of Philosophy degree,
hereby recommend the acceptance of this dissertation

Dr. Clinton T. Rubin, Advisor
Chair, Department of Biomedical Engineering

Dr. Stefan Judex, Chairman of Defense
Associate Professor, Department of Engineering

Dr. Peter Brink, Member
Chair, Department of Physiology
Adjunct Faculty Department of Biomedical Engineering

Dr. Jeffrey E. Pessin, Member
Director, Diabetes Research Center
Albert Einstein College of Medicine

This dissertation is accepted by the Graduate School.

Lawrence Martin
Dean of the Graduate School

Abstract of the Dissertation

Biomechanical Enhancement of Stem Cell Populations can Prevent Obesity and Counter Osteoporosis

by

Yen Kim Luu

Doctor of Philosophy

in

Biomedical Engineering

Stony Brook University

2008

Pluripotent mesenchymal stem cells (MSCs) are considered ideal therapeutic targets in regenerative medicine, as they hold the capacity to differentiate into osteoblasts, adipocytes, fibroblasts, chondrocytes, and myocytes. The potential to harness MSCs as a means of prevention and treatment of disease is dependent on an improved understanding of the means by which exogenous signals regulate their activity, and the ability of these stimuli to influence either/both proliferation and differentiation This work addressed the hypothesis that MSCs represent a common mechano-responsive element upstream of osteoblast and adipocyte differentiation that could potentially be targeted for the control and treatment of both obesity and osteoporosis. We proposed that low magnitude mechanical signals (LMMS) could non-pharmacologically and non-invasively promote stem cell proliferation, and thus an organism's healing and regenerative potential.

In light of the increased health complications experienced by obese individuals, we assessed the impact of a high fat diet on the resident stem cell population, as a possible contributing factor in the pathophysiology of obesity. We show that the MSC

population was significantly diminished in animals fed a high fat diet for six weeks. Data from flow cytometry and real-time PCR provided clear indication that while the high fat diet decreased the MSC population, LMMS increased the proliferation of MSC's and was able to recover the diet-induced decrease in cell numbers. In addition, the marrow environment in LMMS animals had shifted towards osteogenesis both in cell number and gene expression, providing a mechanism of LMMS action based on the selective differentiation of MSC's into osteoprogenitors.

To characterize the phenotypic effects of twelve weeks of LMMS stimulation on a young adult animal, we developed a methodology for *in vivo* micro-computed tomography (microCT) for the precise determination of fat quantity, and more importantly fat distribution in the body. We applied these *in vivo* imaging methods to a complete characterization of the phenotypic fat suppression under normal dietary conditions, and several models of dietary induced obesity. Finally, data from a long term study (36 week of LMMS treatment) provided preliminary evidence of the benefit of LMMS in mitigating some the deleterious effects of dietary induced obesity and aging.

The experiments and results presented herein indicate that MSCs respond to LMMS by increasing proliferation. A developmentally mediated mechanism by which fat was suppressed and bone was enhanced, was implicated and was linked to the mechanically-based biasing of the mesenchymal stem cells to preferentially differentiate towards osteoblasts over adipocytes. The mechanical promotion of the number of progenitor cells, as well as driving commitment choices, suggests a means to enhance an organism's regenerative capacity as achieved by exploiting stem cell sensitivity to physical signals.

For those that inspired, and believed.

I prepare this manuscript in honor of, and dedication to, the

memories of my grandmother, Mrs. Luu Banh Bao,

and my beloved friend, Dr. Scott H. Swaner.

Table of Contents

List of Symbols and Abbreviations

BM: bone marrow

BMI: body mass index

BMC: bone mineral content

BMD: bone mineral density

BV: bone volume

BV/TV: bone volume fraction

CDC: Centers for Disease Control

CON: control group/animals

Conn.D: connectivity density

Dlk1: delta-like 1 (aka. Pref 1)

DXA or DEXA: dual energy x-ray absorptiometry

DIO: dietary induced obesity

ECM: extracellular matrix

EGF: epidermal growth factor

FA1: fetal antigen 1 (aka. Pref-1)

FD: fat diet

FDA: Food and Drug Administration

FFA: free fatty acid

FSC: forward scatter

GFP: green fluorescent protein

HFD: high fat diet

HSC: hematopoietic stem cell

LMMS: low magnitude mechanical stimulation

microCT or μCT: micro-computed tomography

MRI: magnetic resonance imaging

MSC: mesenchymal stem cell

NAFLD: non-alcoholic fatty liver disease

NMR: nuclear magnetic resonance

PTH: parathyroid hormone

Pref-1: preadipocyte factor-1

RD: regular diet

ROI: region of interest

RT-PCR: reverse transcription polymerase chain reaction

SAT: subcutaneous adipose tissue

Sca-1: stem cell antigen-1

SC: stem cell

SMI: structural model index

SSC: side scatter

TAT: total adipose tissue

Tb.N: trabecular number

Tb.Sp: trabecular separation

Tb.Th: trabecular thickness

TG: triglyceride

TV: total volume

VAT: visceral adipose tissue

List of Figures

(macrovesicles) infiltrated within and between the hepatocytes, whereas LMMS livers show a more typical packing of cells, with smaller and fewer lipid vacuoles.

Figure 27 (pg 107). The reduction in liver size and weight can be somewhat accounted for by the reduction of fatty infiltration (as approximated by TG and NEFA content) in LMMS animals. The concentration (per mg of tissue) of these compounds were both decreased by ~25% (**a,c**), and taken in parallel with the 29% decrease liver weight translated into 46.2%, (p=0.013) reduction in total triglycerides in the liver (**b**) and 42% overall decrease in total liver NEFA (**d**) of LMMS animals, compared to the sham CON group. Based on the concentrations of TG levels and % decreases, the reduction in just the triglyceride component of the liver accounted for 132 mg of the decrease in liver weight.

Figure 28 (pg 108). Flow cytometry data tracking the surface labeling of Sca-1, a marker present on both HSC and MSC, illustrate the age-related decline in the number of multipotent progenitor cells (**a**). Data were compared between CON subjects (6 wk: n=8 , 36 wk: n=7), fed a high fat diet for either 6 or 36 weeks. Comparing the effect of the LMMS signal on either the overall stem cell population (**b**) or specifically the MSC population (**c**) it was evident that the MSC cell population exhibits a greater responsiveness to mechanical stimulation over the long term. While overall stem cells were non-significantly affected by LMMS, MSCs saw a 36.4% (p=0.039) increase highlighting the ability of the LMMS signal to some degree counter the age-induced loss of stem cells and regenerative potential.

List of Tables

Acknowledgements

This dissertation and project would not have been possible but for the support, advice, and encouragement of many people. While I can not thank everyone enough, I'd like to acknowledge (in no particular order) all the people who have in some way contributed to this work and to its completion. Bhavin Busa performed the initial animal studies and taught me how to "bounce" mice when I first started. The data reported in Chapter 4 on fat volumes were in part collected by Bhavin, and some of his data were combined with the additional animals and analyzed to comprise the full data set. Dr. Encarnacion "Encarni" Capilla, was my partner in crime through many of the initial experiments, and through her patience, guidance, and generosity I learned some of the various assays that were critical to establishing and understanding of the implications of this work. The biochemical data reported in Chapter 4 were in part generated by Encarni. Of course, my interaction with Encarni was through a collaboration with Dr. Jeff Pessin, external committee member and mouse handler extraordinaire (especially in front of a film crew)! Dr. Pessin's input and expertise really helped to shape the various aspects of the experiment as they related to obesity and diabetes, and allowed this project to move beyond "only" bone and address the big "fat" questions.

I'd like to thank Dr. Stefan Judex for serving as the chair of my dissertation committee, and for his invaluable input into the various experimental designs and data analysis. Surely these experiments are more rigorous and statistically sound for his expertise, even if the advice was given over (and bargained for with,) beers at John Harvards. In addition, he graciously shared the resources of his lab both in terms of space and personnel. For all matters microCT related, Svetlana Lublinsky has come to my rescue on many occasions. Whether it be to help develop algorithms which have saved me many hours/days/weeks of drawing contour lines or helping to instruct

students on proper technique, your assistance has always been generously offered. My eyes, and sanity, thank you.

The expertise and advice of various other experts was eagerly sought and found in numerous conversations with Drs. Peter Brink, Michael Hadjiargyrou, Anil Dhundale, Cliff Rosen, Janet Rubin, and Mark Horowitz. The speedy responses to even general protocol questions saved more than one experiment from complete disaster. Dr. Brink, thank you for serving on my dissertation committee even as a 100+ page dissertation is probably the last thing you'd like to return to after a long trip.

The other members of the Judex and Rubin lab team, in particular Engin Ozcivici and Ben Adler made the incredibly draining task of animal work and unfortunate yet necessary act of sacrifices and tissue harvests bearable. Rest assured, of the many random, entertaining, and sometimes controversial conversations we have had, "what happens in DLAR, stays in DLAR." After several prior interactions with mentoring students that could best be described as "interesting," in the end I was fortunate enough to have encountered two that were motivated and bright. BME undergraduates Pooja Parekh and Elizabeth Fievisohn contributed to the adipocyte quantification experiments (preliminary data reported in Chapter 3) and analysis of spine data from the various animal groups (data not yet reported). My tenure in the BME department at Stony Brook has allowed to me cross paths with some very cool people, fellow graduate students to commiserate and celebrate the various travails of the academic life. Dr. David Komatsu, and soon to be Drs. Hoyan Lam, Rob Gersch, Suzanne Ferreri, and Chiung Yin Chung.

I owe a huge "thank you" to Ms. Annemarie Dusatko, who has saved me from drowning in the university bureaucracy too many times to count. Your patience with my constant comings and goings, and the entangled paper trail that each action further complicated is much appreciated.

The true brains behind this madness, aka “research” is Dr. Clinton Rubin, who is the mentor that I was incredibly fortunate to have found. Clint has been supportive of my still-developing abilities as a scientist, even when I was a fledgling graduate student trying to tissue engineer bone in a structure that he described as reminiscent of a “Whatchamacallit” candy bar. He provided support and encouragement when I was feeling downtrodden, and “motivation” when I was lacking drive or direction. In the end, he has taught me that you have to believe in whatever it is that you are doing. While the comment was made in specific reference to research and experiments, it will certainly be useful in the coming days.

And lastly, to my parents My Linh and Nghiep – for your patience and sacrifices, support and unconditional love, I owe you thanks today and my whole life through.

Finally, the text of this dissertation in part is a reprint of the materials as they appear in Luu et al (2008) *In Vivo Quantification of Subcutaneous and Visceral Adiposity by Micro Computed Tomography in a Small Animal Model (*in press, accepted March 2008, Medical Engineering Physics) and Rubin et al (2007) *Adipogenesis is Inhibited by Brief, Daily Exposure to High Frequency, Extremely Low Magnitude Mechanical Signals, an Attribute Achieved by Suppressing Mesenchymal Stem Cell Commitment to Adipocytes*. Proceedings of the National Academy of Science, v104, no 45, 17879-17884. The co-authors listed in the publications contributed to the direction and supervision of the research that forms the basis for this dissertation.

List of Publications

The following publications were produced during the course of this dissertation.

REFEREED PAPERS (PUBLISHED OR IN PRESS)

Y. K. Luu, S. Lublinsky, E. Ozcivici, E. Capilla, J. E. Pessin, C. T. Rubin S. Judex. (2008) *In Vivo Quantification of Subcutaneous and Visceral Adiposity by Micro Computed Tomography in a Small Animal Model (*in press April 2008, Medical Engineering Physics).

S. Lublinsky, **Y. K Luu**, S. Judex. (2008) *Automated Separation of Visceral and Subcutaneous Adiposity in Micro Computed Tomographies* (in press May 2008, Journal of Digital Imaging).

Rubin, C.T., Capilla, E., **Luu, Y. K**., Busa, B., Crawford, H., Nolan, D.J., Mittal, V., Rosen, C., Pessin, J.E., Judex, S. (2007) *Adipogenesis is Inhibited by Brief, Daily Exposure to High Frequency, Extremely Low Magnitude Mechanical Signals, an Attribute Achieved by Suppressing Mesenchymal Stem Cell Commitment to Adipocytes*. Proceedings of the National Academy of Science, v104, no 45, 17879-17884.

REFEREED PAPERS (IN REVIEW)

Y. K. Luu, E. Capilla, C. Rosen, V. Gilsanz, J. E. Pessin, S. Judex, C. T. Rubin. (2008) *Mechanical Promotion of Mesenchymal Stem Cell Proliferation and Differentiation Prevents Dietary Induced Obesity while Promoting Osteogenesis* (under review, submitted April 2008, Journal of Bone and Mineral Research).

CONFERENCE PROCEEDINGS AND ABSTRACTS (PEER REVIEWED)

Y. K. Luu E. Capilla, J. E. Pessin, S. Judex, C. T. Rubin (2008). *Mechanical Stimulation of Mesenchymal Stem Cell Differentiation to Enhance Bone Formation: Are Osteoblasts the Only Way to a Better Skeleton?* Orthopedic Research Society Annual Meeting, San Francisco, CA.

Y. K. Luu, E. Capilla, B. J. Lee, J. E. Pessin, S. Judex, C. T. Rubin. (2007) *Mechanical enhancement of bone quality is paralleled by suppression of fat production. Can osteoporosis and obesity be countered through the same mechanism?* American Society of Bone and Mineral Research Annual Meeting, Honolulu, HI.

Lee BJ, Judex S, **Luu YK**, Thomas JB, Gilsanz V, Rubin C. (2007) *Skeletal complications of Duchenne's muscular dystrophy: Can they be mitigated by extremely low level mechanical signals?* International Bone and Mineral Society Annual Meeting, Montreal, Canada. BONE 40 (6): S247-S247 Suppl. 2 JUN 2007

Yen Kim Luu, Encarni Capilla, Jeffrey E. Pessin, Stefan Judex, Clinton T. Rubin. (2007) *Daily Low Magnitude Mechanical Signal Reduces Adiposity in Male Mice.* Northeast Bioengineering Conference, Stony Brook University.

C. T. Rubin, B. Busa, E. Capilla, **Y.K. Luu**, C. Rosen, J. Pessin, S. Judex. (2006) *Low-Level Mechanical Signals Anabolic to Bone Suppress Adiposity in Growing Mice.* American Society of Bone and Mineral Research Annual Meeting, Philadelphia, PA.

BOOK CHAPTERS

Ozcivici, E., **Luu, Y.K**., Rubin, C., Judex, S**.** (in press) High-resolution imaging of organs and tissues by in vivo micro-computed tomography. In: *The Protocols in Musculoskeletal Research: A Practical Manual for Laboratory Techniques.* Qin, Y.X (ed.). The Humana Press, Totowa, NJ

Chapter 1

INTRODUCTION AND LITERATURE REVIEW

OBESITY AND OSTEOPOROSIS

Obesity is a condition in which the natural energy reserve stored in fatty tissue exceeds healthy limits. For humans, it is commonly defined as a body mass index (BMI) of 30 kg/m^2 or higher. It is currently estimated that almost 65% of adult Americans are overweight (BMI of 25 kg/m^2 or higher), translating into approximately $100 billion per year in direct health care costs. (1)

Another major health problem, osteoporosis, is characterized by a decrease in bone, due to reductions in bone mineral density (BMD) and disruption of bone micro-architecture. The diagnosis of osteoporosis is typically made on measurement of BMD by methods such as dual energy X-ray absorptiometry (DXA or DEXA). Osteoporosis results in over 1.5 million fractures each year in the United States, with direct costs estimated at approximately $18 billion dollars in 2002. (2)

The presentations of these two diseases are markedly disparate, and yet at the cellular and molecular level several similarities emerge. As reviewed by Zhao *et al*, both obesity and osteoporosis are affected by genetic and environmental factors. Mechanical forces, such as those experienced during exercise can suppress the development of both diseases, and can to some degree “treat” excess adiposity and reduced bone mass. Bone remodeling and adiposity are both regulated through the hypothalamus and the sympathetic nervous system. (3) Perhaps most significantly, mature adipocytes and osteoblasts both derive and differentiate from the same multipotent mesenchymal stem cells (MSCs). Many researchers have noted an inverse dependency between the development of osteoblasts and adipocytes, and consequently the processes of osteogenesis and adipogenesis appear to be interdependent. (4) Yet clinically, it has been reported that obese individuals tend to have higher bone mineral density than normal weight individuals, and are less prone to osteoporosis. (5) Clearly, the

interaction between bone and fat is complex, and highly contingent on a multitude of factors including genetic, biochemical, and mechanical inputs that coordinate the overall interaction and resulting phenotype.

However, what is clear is that the increasing prevalence of, and costs associated with, osteoporosis and obesity represent major health concerns. Further, for obese individuals the excess adiposity actually puts them at risk for developing a multitude of additional diseases such as diabetes, cardiovascular disease and cancer. Pharmacological treatments for both have met with limited success, and carry lots of associated risks. Rather than simply exploring treatments for the compromised state once the disease has developed, it is generally accepted that primary prevention should be emphasized. With this, fundamental understanding of the some of the interacting factors that drive the differential development of stem cells down either a bone or fat lineage holds promise for the discovery of new prevention and treatment strategies.

CURRENT TREATMENTS FOR OBESITY

The strategies for obesity treatment generally aim at shifting the balance between energy consumption and energy expenditure. (6) The act of "dieting" undertaken by an individual or more rigorous diet restriction prescribed by a doctor represent the simplest method to combat obesity, and yet limiting caloric consumption is difficult for a variety of societal and lifestyle reasons. As reviewed in Kirk *et al*, the treatment options for pediatric obesity are rather limited. (7) In the US, there are currently only two prescription treatments approved for long term use by the Food and Drug Administration (FDA) for obesity. Orlistat blocks absorption of up to 30% of ingested fat in the intestine, to create a negative energy balance. The second approved

drug, sibutramine, inhibits the reuptake of neurotransmitters to promote satiety and prevent overconsumption, and is only approved for patients over the age of 18. Adverse effects of the these treatments include gastrointestinal complications (orlistat), increases in blood pressure and heart rate (sibutramine) and high attrition rates for both drugs. (8)

In cases of severe obesity, bariatric surgery for adults has been shown to be effective, and is gaining prominence for use with adolescents. Obese adolescents with a BMI of 40 or more and serious medical complications associated with their obesity are considered good candidates for the technique. (7) The costs and risks of this procedure, and its indication only in severe cases, limit its applicability to the general population. Further, as both pharmacologic control and surgical intervention are designed to reduce the caloric load with the intent to reduce the existing adipose deposits, these treatments do not address the actual cascade of events whereby adipocytes develop and accumulate into fat tissue.

CURRENT TREATMENTS FOR OSTEOPOROSIS

Treatment options for osteoporosis and low bone density can be categorized as those designed to promote new bone growth (anabolic treatments), or to prevent bone resorption/loss (anti-catabolic treatments). Within these two approaches, the majority of current treatment options are pharmacologic, although non-pharmacologic therapies are under development. Bisphosphonates such as alendronate, risedronate, and ibandronate are antiresportive compounds that are widely prescribed for bone loss and associated diseases. (9) A different class of compounds is the selective estrogen-receptor modulators, which include drugs such as raloxifene, lasofoxifene, bazedoxifene, and arzoxifene. Complications of these agents vary, from osteonecrosis of the jaw to

increased risk of breast cancer and stroke. (10) In terms of anabolic agents, parathyroid hormone (PTH), PTH-like compounds, and strontium ranelate have all been shown to decrease fracture risk with varying degrees of success. PTH is the only currently FDA approved anabolic drug, but can only be administered by injection and only for up to 24 months. (11)

In the category of non-pharmacologic interventions for bone loss, exercise in the form of short, repetitive mechanical loads has been established as leading to the greatest increases in bone strength, especially in childhood before peak bone mass is achieved. (12) In adults, regular exercise helps in maintenance of bone mass, but additional gains in bone are relatively small and are contingent upon continued activity.

TREATMENT AND PREVENTION BY TARGETING THE COMMON PROGENITOR

The current treatments are predominantly designed to treat obesity and osteoporosis once symptoms have already manifested, and a major shortcoming of these pharmacologic interventions is that they are not well suited for prevention of disease. In addition, the majority of these strategies offer treatments aimed at acting on the fat and bone cells themselves, to try to modify the activity of these cells whether it be to reduce the lipid accumulation (adipocytes) or to prevent activation (osteoclasts) and matrix resportion. With the increasing knowledge of the developmental pathways by which these diseases develop, new targets for primary prevention are being evaluated. For example, recent findings show that targeting adipocyte apoptosis pathways might potentially provide treatment for obesity and osteoporosis, as high adipocyte counts in bone marrow are directly related to bone loss, due to fat cells replacing osteoblasts in the bone marrow compartment. (13) Strategies targeting diseases of bone and fat at the

developmental level, by targeting the progenitor cells (such as mesenchymal stem cells) that have yet to commit and differentiate into the mature cell types is a relatively new strategy. (14;15)

MESENCHYMAL STEM CELLS (MSCs)

Studies examining the therapeutic potential of mesenchymal stem cells have greatly increased in recent years. (16-18) MSCs are primarily found in the bone marrow, and are able to differentiate into various cell types including osteoblasts, adipocytes, fibroblasts, chondrocytes, and myocytes (**Fig 1**). (19) Further, along with the classical mesenchymal lineages, the bone marrow cells actually exhibit great multipotency, and have recently been induced into functional myocardial cells. (20) It is important to note that the bone marrow houses a diversity of cells, including hematopoietic stem cells (HSC) which also exhibit mulitpotent differentiation capacity. In addition to development into the various cells that coordinate the immune response, HSCs are the progenitor cell to mature osteoclasts. (21)

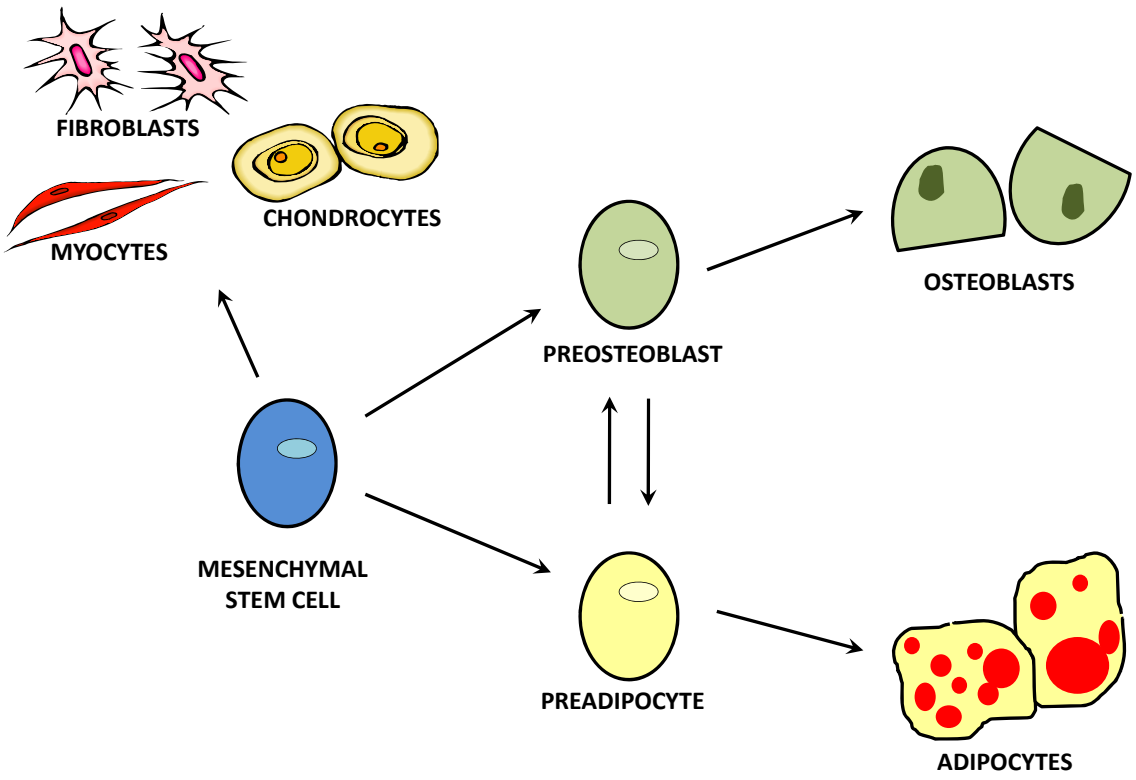

Fig 1. Schematic representation of the lineage potential of multipotent mesenchymal stem cells in the bone marrow. The development of mature cells such as adipocytes and osteoblasts proceed through intermediate "progenitor" cells, preosteoblasts and preadipocytes. The processes of commitment and differentiation are complex and not fully characterized.

IDENTIFICATION OF MSCS

While the interest in mesenchymal stem cells and their application to regenerative therapy and molecular medicine has been great, the understanding of these cells is still in the nascent stages. Even the identification of the MSC population is under debate as stem cells and their neighboring cells within tissues are difficult to delineate based on current histological methods. Illustrating the difficulty of cellular identification, using a combination of markers that distinguish HSCs from 99.9% of other cells in the bone marrow yields a population estimated at 3% purity. (22)

The expression of surface markers is not well characterized and to date markers exclusively defining MSCs have not been reported. Cell populations obtained in the current isolation methods are essentially heterogeneous mixtures of several cell types. (23) Although consensus is lacking, there are several markers such as stem cell antigen (Sca-1) and CD117 (c-kit) that are commonly used for identification of stem cells in murine models. (24;25) Additionally, many studies utilize negative selection, with stem cells identified as cells not expressing lineage surface markers (Lin^-), but Sca-1 and c-kit positive. (26;27) When harvested from bone marrow, MSCs are typically defined as the non-hematopoietic fraction, either for adherence to plastic (hematopoietic cells do not adhere) or by negative selection for HSC markers such as CD34, CD45, etc.

In vitro assays to identify stem cells are useful, but inherently limited in that culture environments can artificially modify stem cell development. (28). The classical assay to demonstrate the "stemness" of an isolated population is via transplantation into immunodeficient mice, and induction to differentiation towards tissues of mesodermal origin. (29) Recent studies employing the technique of bone marrow transplantation using fluorescently tagged cells injected into a live animal to track cell fate and to determine lineage commitment have been reported with the potential to provide valuable information. (30)

CELL LINEAGE DETERMINATION

Not surprisingly, the question of what determines whether a MSC differentiates into either an adipocyte or osteoblast or other cell type remains unknown and is the focus of intense research. Of the various signals capable of inducing differentiation, various biochemical factors have been reported that typically drive the differentiation

towards one cell type, with a parallel suppression of another cell. Recent work on the differentiation of osteoblasts from MSCs highlights the finding that cell fate decisions can be made by preferentially activating a very small subset of a particular signaling network, rather than requiring large or dramatic shifts on gene expression. (31)

Certain molecules, such as Pref-1 (also known as Fetal antigen 1 (FA1) and delta-like 1 (Dlk-1)) of the epidermal growth factor (EGF)-like protein family, have been identified as promoting the maintenance of a bipotential stem cell population. (32) In their native bone marrow environment, mesenchymal stem cells express small amounts of both adipogenic and osteogenic factors, which cross regulate each other to keep the cell in its undifferentiated state. For example, PPARγ down-regulates Runx2 expression to suppress osteogenesis whereas MSX2 binds to C/EBPα to repress adipogenesis. (33) As such, the relative expression levels of the molecules PPARγ and Runx2 in the marrow can be taken as general indicators of either adipogenic or osteogenic environments.

MECHANICAL STIMULATION TO INDUCE CELL DIFFERENTIATION

In addition to the biochemical factors capable of altering cell fate, mechanical forces can also play key and interacting roles in the cellular environment. Mechanotransduction is the process by which cells transduce physical force-induced signals into electrical and/or biochemical responses, resulting in altered gene expression, cell morphology, and extracellular matrix production. This process is critical for mediating adaptations to mechanical loading in many tissues. (34) The basis for mechanotransduction lies in that cells form networks, which are connected by intercellular adhesion complexes such as adherens junctions, gap junctions or by local

paracrine signals. (35) These networks are capable of acting as integrated units to transduce various stimuli, such as mechanical loading, into coordinated tissue responses. Not surprisingly, to transduce the mechanical signal requires the interaction of many signaling pathways, (35) and due to the complexity is still not well characterized. Various pathways such as cell-extracellular matrix interactions, cytokines, second messenger transmission through gap junctions and intercellular adhesive junctions enable cells to transmit mechanical signals to other cells. (36)

As an example of cellular mechanotransduction in lineage determination, the role of mechanical forces in the control of adipogenesis has been linked to changes in extracellular matrix (ECM) proteins and matrix metalloproteinases. (37) ECM components play an important role in regulating adipose tissue remodeling during adipocyte differentiation, by transducing cellular signals which can alter adipocyte gene transcription during adipogenesis. (38) Examples of the importance of mechanical signals to bone and bone marrow are highlighted in the following section.

MECHANOTRANDUCTION IN BONE AND BONE MARROW

Underlying the essence of mechanotransduction is the necessity that certain cells in the biological environment can act as receptors, which in turn can generate secondary, cytogenic signals that are aimed at target cells. How mechanical factors are sensed in the bone comprises a large body of active research, with many differing hypotheses regarding the mechnosensory element. (39;40) The prevailing view is that osteocytes are responsible for detecting mechanical signals, and respond by signaling the effector cells, osteoblasts and osteoclasts, that modulate actual bone formation and resportion. (41) Equally complex is the multitude of forces generated in the bone

marrow cavity in response to mechanical loading. (42) Even as mechanotransduction by cells in the musculoskeletal system has long been observed, the ability of mechanical signals to affect and alter the differentiation patterns of mesenchymal stem cells was only recently noted. (43;44)

Enmeshed within the bone/bone marrow interaction is the concept of a stem cell "niche", a specialized location where cells reside and are regulated. The thought that the marrow cavity represents such a niche has gained traction within recent years, with the endosteal bone surface providing the primary location for marrow regeneration. (45;46) Several models utilizing transgenic mice have shown that increases in hematopoiesis occur in conjunction with increases in both osteoblasts and trabecular bone, as an increased niche size is necessary to provide support for the increase in hematopoietic stem cells. (47) Within this niche, it has been suggested that osteoblasts can play a direct role on stem cell function by providing support for hematopoietic stem cells. (48) Thus, the ability of mechanical forces to effect changes in the bone and bone marrow are interlinked, and perhaps the responsiveness of bone to mechanical signals might provide insight into the ability of cells in the bone marrow to respond.

MECHANISMS OF MECHANOSENSING IN BONE

The ability of bone as a tissue to respond and adapt to mechanical signals has long been explored by researchers interested in harnessing the benefits of physical activity as a means to the prevention of bone loss and osteoporosis. While the understanding of the interaction of exercise and bone is yet incomplete, among the various effects of exercise, there is evidence that the mechanical component can regulate bone maintenance and stimulate bone formation and the accumulation of

mineral to strengthen existing bone. (49) Insights from animal models including turkeys, rats, and mice have revealed several key features that illuminate some of the mechanisms of mechanosensing in the bone. It has been hypothesized that the interconnected network of osteocytes and of the periosteal and trabecular lining cells is mechanosensitive to shear stress and streaming electrical potentials generated by extracellular fluid forced through the bone canaliculi when cortical bone undergoes compression, bending, or torsion during mechanical loading. (50;51) Further, the increased fluid flow provides circulatory enhancement to bones through increased supply of nutrients, hormones and oxygen. (49)

As such, it is intuitive that static loads do not play a role in mechanotransduction, and to be anabolic to bone the applied load should be dynamic and time varying. This effect has been demonstrated in turkeys and rats where static (isometric), loading provides very little stimulus to mechanotransduction (52-54) and under certain circumstances actually inhibits normal appositional growth. (55) Researchers have also noted that for a mechanical signal to activate new bone formation, a threshold level of loading needs to be exceeded. (56) This loading threshold and the osteogenic potential of mechanical signals is modulated by the interaction between strain rate and strain amplitude. (57;58) In terms of exercise, this means that activities that create relatively high strain rates (i.e. jumping) will be more osteogenic than loads applied gently, or in which a strain magnitude is held constant for a period of time (i.e. walking or strength training). (59)

A key characteristic of loading, revealed in early work by Rubin and Lanyon is that very few loading cycles are actually required to elicit new bone formation. (58) This anabolic effect saturated very quickly in turkey ulnae such that increasing the duration of loading beyond approximately 40 cycles per day had little additional effect. Similar saturation effects were seen in rat tibiae for just 5 loading cycles per day. (60) Further, a

given number of loading cycles will also be more osteogenic if they are broken up into shorter bouts with rest periods in between, as bone cells can re-sensitize to a stimulus after a rest period. Robling *et al* demonstrated that for 360 cycles of tibial loading divided into 1 bout of 360, 2 bouts of 180, 4 bouts of 90 or 6 bouts of 60 cycles per day for 2 weeks, the bone formation rate in the loaded tibia saw an 80% increase in the groups that received the most inserted rest periods (4 to 6 bouts). (61)

Translating these findings on the various types of load that are most effectively sensed and mechanotransduced in animal studies to young children, controlled trials with a loading regime incorporating short bouts of relatively high loading with rest periods inserted in between demonstrated increased bone strength in the distal tibia (62) and 2-4% increases in spine and total body BMC of prepubertal boys and peripubertal girls. (63) At the opposite end of the spectrum, with the sensitivity of bone to mechanical loading increasing rapidly with frequency, the application of low strain magnitudes are also sufficient to maintain bone mass. It is predicted that minimum strain magnitudes required to maintain bone mass could be lower than 70 microstrain, given a high enough loading frequency. (64)

LOW MAGNITUDE MECHANICAL SIGNALS (LMMS)

Accepting that mechanical forces can play a critical role in the normal development and maintenance of numerous tissues, and that these forces need not be large to be sensed at the cellular level to enact large tissue level changes, we now examine how these forces can be applied as a potential strategy to control cell fate. Based on work done by researchers in the field of bone biology and mechanics, it is know that the skeleton responds to low magnitude mechanical signals (LMMS) by

increasing both bone quantity and quality. (65;66) This significant tissue level response to a relatively small signal highlighted the potential of this method as a non-pharmacologic intervention for osteoporosis (67-69) and demonstrated influence to at least one cell population (perhaps osteoblasts or osteocytes) by the applied stimulus. However, there were persistent inconsistencies on how and why mechanical factors stimulate bone in some, but not all cases. Differential responsiveness at different skeletal sites within the same animal to the same stimulus further complicates the understanding of the interaction. (70)

The physiologic relevance of high frequency, low magnitude mechanical signals becomes evident upon examination of the contractile spectra of muscle. Type IIa muscle fibers fire in the range of 20-50 Hz, (71) at very low magnitude. Compared to the high amplitude, lower frequency peak signals generated by strenuous activities such as running, the high frequency signals over time comprise a predominant component of the mechanical energy in the musculoskeletal system. (72) The responsiveness of bone to LMMS has been shown to be dependent on the applied frequency, with a 90 Hz signal stimulating greater bone growth than a 45 Hz signal at the same strain magnitude. (73)

RESEARCH QUESTION

As the bone exerts a large influence to the marrow cavity, it is intuitive that the cells in the marrow cavity likewise exert control over the bone. Therefore, is the ability of the bone to respond to a mechanical stimulus being influenced by the ability of the marrow to sense and respond to the same mechanical signal? Further, if the bone marrow derived stem cells respond to the signal by differentiating into bone, does it

affect the potential of the stem cell to differentiate into other cell types, specifically fat? These questions form the basis for this project, which stems from preliminary work that demonstrated that the introduction of a low magnitude mechanical signal that was anabolic to bone could in effect alter the balance of bone and fat development at the tissue level. The precise mechanism by which this effect occurred was the focus of this dissertation, as outlined based on four key questions.

First, what is the effect of diet induced obesity to the bone marrow derived stem cell population? Specifically, of the complications engendered by obesity, how much influence is exerted by the increased adiposity or are there other factor that are affected by the high fat diet?

Second, can LMMS alter the fat phenotype in normal animals, and what changes are experienced at the biochemical and cellular levels? Specifically, can reductions in adiposity reduce key biochemical factors such as triglycerides, free fatty acids, and adipokines that are known to be elevated in obesity?

Third, can LMMS prevent and/or treat obesity and osteoporosis, and what changes were occurring in the bone marrow environment in obese animals? Specifically, how was the mechanical stimulation affecting the proliferation and differentiation of mesenchymal stem cells, osteoblasts, adipocytes to elicit the phenotypic bone and fat response?

Fourth, what are the long term effects of LMMS and dietary induced obesity as the animal ages? Specifically, can LMMS prevent or counteract the deleterious effects of aging and obesity?

OBJECTIVE AND HYPOTHESIS

The overall objective of this dissertation was to develop a better understanding of the divergence down the osteogenic and adipogenic lineages from a single precursor stem cell type, thus providing the scientific foundation for a unique, non-pharmacologic intervention for the prevention and/or treatment of *both* osteoporosis and obesity with the same therapeutic modality. The research questions were addressed in experiments designed based on four sub-hypotheses.

Hypothesis 1: Diet induced obesity negatively effects the stem cell population. The increased adipose burden not only increases risk of obesity related complications, but diminishes the ability of the organism to combat disease because of compromised stem cell numbers.

Hypothesis 2: LMMS phenotypically suppresses fat formation and adipose tissue growth, while simultaneously promoting bone formation at the level of cellular development.

Hypothesis 3: Mechanical signals (either directly or indirectly) are able to stimulate increased proliferation of MSCs, and in addition increase the differentiation towards osteoprogenitor cells.

Hypothesis 4: By promoting the proliferation of MSCs, the beneficial effects of LMMS in overall ability to resist disease, even in response to aging and obesity, are sustainable over time, and result in systemically “healthier” animals.

ANIMAL MODEL AND RESEARCH DESIGN

Small animal models such as the mouse, are the model of choice in obesity and diabetes research. (74) In particular, the general purpose C57BL/6J inbred mouse strain was chosen as the animal model for these studies due to 1). Their broad application in research and 2). C57BL/6J mice have a high susceptibility to diet induced obesity and Type 2 diabetes.

The responsiveness of bone to LMMS has been shown to be dependent on the applied frequency, with a 90 Hz signal stimulating greater bone growth than a 45 Hz signal at the same strain magnitude (73) and thus the 90 Hz stimulation was adopted. All experiments were conducted with a whole body oscillatory signal at the same magnitude (0.2 g acceleration) and frequency (90 Hz) applied for 15 minutes a day without additional optimization. It is important to note that associations persist between vibration and adverse health conditions, including low-back pain, cartilage erosion, circulatory disorders and neurovestibular dysfunction, (75;76) leading to International Safety Organization advisories to limit human exposure to these mechanical signals. (77) At the frequency and amplitude used in these studies the exposure would be considered safe for over four hours each day.

Chapter 2

*IN VIVO QUANTIFICATION OF SUBCUTANEOUS AND VISCERAL ADIPOSITY BY MICRO COMPUTED TOMOGRAPHY IN A SMALL ANIMAL MODEL**

---

*Reprinted from Luu et al. from Medical Engineering Physics (paper in press)

ABSTRACT

Accurate and precise techniques that identify the quantity and distribution of adipose tissue *in vivo* are critical for investigations of adipose development, obesity, or diabetes. Here, we tested whether *in vivo* micro computed tomography (microCT) can be used to provide information on the distribution of total, subcutaneous and visceral fat volume in the mouse. Ninety C57BL/6J mice (weight range: 15.7 - 46.5 grams) were microCT scanned *in vivo* at 5 mo of age and subsequently sacrificed. Whole body fat volume (base of skull to distal tibia) derived from *in vivo* microCT was significantly ($p<0.001$) correlated with the *ex vivo* tissue weight of discrete perigonadal ($R^2 = 0.94$), and subcutaneous ($R^2 = 0.91$) fat pads. Restricting the analysis of tissue composition to the abdominal mid-section between L1 – L5 lumbar vertebrae did not alter the correlations between total adiposity and explanted fat pad weight. Segmentation allowed for the precise discrimination between visceral and subcutaneous fat as well as the quantification of adipose tissue within specific anatomical regions. Both the correlations between visceral fat pad weight and microCT determined visceral fat volume ($R^2=0.95$, $p<0.001$) as well as subcutaneous fat pad weight and microCT determined subcutaneous fat volume ($R^2=0.91$, $p<0.001$) were excellent. Data from these studies establish *in vivo* microCT as a non-invasive, quantitative tool that can provide an *in vivo* surrogate measure of total, visceral, and subcutaneous adiposity during longitudinal studies. Compared to current imaging techniques with similar capabilities, such as microMRI or the combination of DEXA with NMR, it may also be more cost-effective and offer higher spatial resolutions.

INTRODUCTION

The current obesity epidemic has spurred efforts to identify its etiology as well as prophylaxes and potential treatments for this health crisis. Because the accumulation of fat in different body compartments carries differential metabolic risks (78), spatial information on the distribution of adipose tissue is important. Increased total adiposity across the abdomen promotes a high risk of metabolic disease (79) and type 2 diabetes (80) but visceral adipose tissue (VAT) is more closely correlated with obesity-associated pathologies and complications than either total adipose tissue (TAT) or subcutaneous adipose tissue (SAT) (81;82). Nevertheless, the quantification of both VAT and SAT accumulation is also relevant as they have been associated with many metabolic risk factors including fasting plasma insulin, triglycerides, low-density lipoprotein, or cholesterol levels (83;84).

In humans, the use of magnetic resonance imaging (MRI) and computed tomography (CT) to assess body composition and determine fat content is well established (85;86). However, the ability to spatially discriminate different types of adipose tissue in small animal models such as the mouse, the model of choice in obesity and diabetes research (74), is limited by most of the current measurement techniques. The resolution and signal-to-noise ratio required to selectively quantify adipose tissue depots in mice that weigh as little as ten grams presents a unique challenge. MicroMRI has been successfully used to phenotype mouse models of obesity (87), but this technology is not readily available to most researchers. Dual energy x-ray absorptiometry (DEXA) and quantitative nuclear magnetic resonance (QMR) based scanning of the whole animal have been used to effectively characterize lean and fat volume in the mouse, but they do not provide detailed spatial information on fat distribution (88;89).

Over the past ten years, high-resolution micro-computed tomography (microCT) scanners have become widely available. MicroCT distinguishes itself from other imaging techniques in its ability to acquire high-resolution images based on the physical density of the tissue. Because of the much greater density of calcified tissue, this technique has been used extensively in biomedical research to quantify the morphology and micro-architecture of the skeleton (68;90;91). However, microCT also provides a three-dimensional density map with sufficiently large density gradients (contrast) to distinguish adipose tissue from other tissues, fluids, and cavities without contrast agents. As the resolution of *in vivo* microCT scans can be selected to fall into an isometric voxel range of approximately ten to two hundred microns, the system can not only measure the total volume of adipose tissue within an animal, but can also identify and quantify very small volumes of fat cells residing in discrete deposits. While perhaps not necessary for adipose imaging, the capability of high-resolution microCT scan confers specificity for describing adipose tissue that can currently only be obtained by combining DEXA with MRI technology (92).

The ability to use *in vivo* microCT imaging to describe altered levels of total fat content based on low-resolution scans has been recently suggested (93;94). Herein, we tested whether microCT can provide a surrogate measure of *in vivo* visceral, subcutaneous, or total fat pad mass and whether adipose information obtained from the abdominal region is equivalent to that derived from whole body scans. Data from these studies establish and validate *in vivo* microCT as a non-invasive, quantitative tool that provides a robust, reliable, simple and cost-effective alternative with higher resolution and selectivity than previous methods to precisely determine total and regional adipose volumes.

MATERIALS AND METHODS

Experimental Model. All procedures were reviewed and approved by Stony Brook University's Animal Care and Use Committee (IACUC). Twenty-four female and 66 male C57BL/6J mice were obtained from The Jackson Laboratories (Bar Harbor, ME) at 6wk of age, housed in conventional cages, and given free access to food and water. Of this population, fifty mice received a regular chow (Lab Diets, RMH 3000, Richmond, IA) diet (12 female, 38 male) or a 45% kcal high-fat (Test Diets, 58V8, Richmond, IA) diet (12 female, 28 male). At 7wk of age, half of the mice within each group (regular diet and fat diet, male and female), were subjected to a non-pharmacological prophylaxis for adiposity (short daily durations of very low-level mechanical signals applied via vertical whole body oscillations for 12 wk), further amplifying differences in body composition within the group of mice (93). At 19wk of age, mice were scanned *in vivo* by microCT. Animals received a 2wk recovery from the exposure to anesthesia to facilitate biochemical analyses unrelated to this study. Upon sacrifice, the perigonadal fat pad (epididymal in male and parametrial in female mice) and a subcutaneous fat pad spanning the lower back (mesenteric) region were harvested and weighed. The perigonadal fat pad is regarded as part of the visceral compartment (95). The mesenteric fat pad is considered subcutaneous, starting at the lesser curvature of the stomach and ending at the sigmoid colon (96) but is external to the abdominal capsule delineated by the muscle fascia (**Fig. 2**).

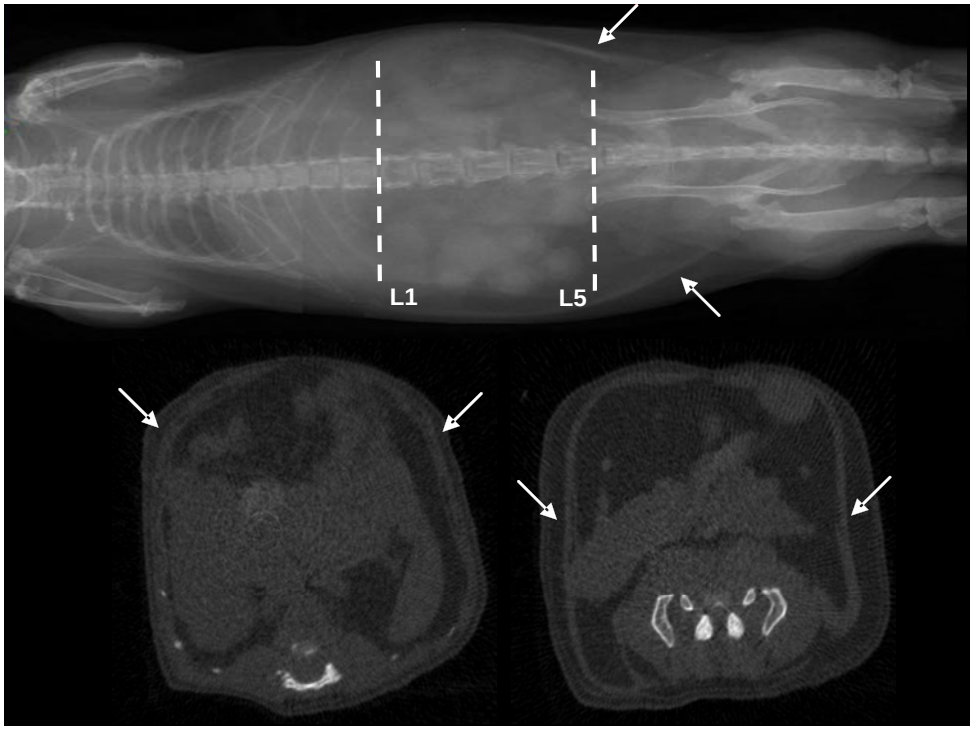

Fig 2. MicroCT scout view of a mouse (top). The abdominal region of interest between the proximal end of L1 and the distal end of the L5 vertebrae is shown between the dotted lines. At the level of the dotted lines, cross-sectional view through the proximal and distal that were used to identify the abdominal region of interest are shown (bottom). Arrows indicate the muscle layer that separates visceral from subcutaneous fat.

***In Vivo* Scanning.** For *in vivo* scans, mice were anesthetized by 1% isoflurane inhalation and positioned with both legs fully extended. The entire torso of each mouse was scanned at an isotropic voxel size of 76 microns (45kV, 133μA, 300ms integration time) with a vivaCT 40 scanner (Scanco Inc, SUI). Selection of the scan energy and voxel size (scanning increment) was based on optimizing the requirements of scanning time and tissue detail, and to minimize exposure to radiation. Based on the scan parameters, the estimated radiation exposure is on the order of 190-380 mGy for each scan (based on values provided by Scanco, SUI). Two-dimensional gray-scale image slices were reconstructed into a three-dimensional tomography. Density values for soft tissue were calibrated from a 5-point linear fit line with mixtures in various ratios of two

liquids, ranging from 0.78mg/ml (100% ethanol, Sigma, St. Louis, MO) to 1.26mg/ml (100% glycerol, J.T. Baker, Phillipsburg, NJ). Density values for bone tissue were calibrated via a commercially available phantom containing hydroxyapatite rods of different densities (Scanco, SUI). Scans were reconstructed for either the whole body (base of the skull, as the spinal canal begins to widen and the distal end of the tibia) or the abdominal region (between the proximal end of L1 and the distal end of L5, **Fig. 2**). The head and feet were not scanned and/or evaluated because of the relatively low amount of adiposity in these regions, and to allow for a reduction in scan time and radiation exposure to the animals. The region of interest (ROI) for each animal was defined based on skeletal landmarks from the gray-scale images.

In Silico Evaluation, Total Fat Volume. A custom script written in image processing language (IPL) was used to analyze total fat volume. Briefly, the algorithm separated the mouse body from the background to provide the total tissue volume (TV) of the mouse. A Gaussian filter (sigma = 1.5, support = 3.0) was used to reduce the background noise in the image. A preliminary threshold segmenting fat from other tissue and background (voids) was determined by *ex-vivo* microCT imaging of a freshly harvested fat pad from a C57BL/6J mouse. The harvested fat pad only served to provide a broad estimate of the threshold, and would not be necessary for future studies using the same genetic mouse strain. Subsequently, the lower and upper threshold values were adjusted by selecting only those voxels within a histogram of all grayscale values of a given region of interest (ROI) that represented either adipose tissue and muscle/internal organs (lean tissue). This is readily accomplished as the distribution of tissue grayscale values from a microCT scan is bimodal in nature, with one mode representing adipose tissue voxels and the other mode representing lean tissue voxels (**Fig. 3**). For our analyses, we selected regions from an animal with average body mass in which the tissue

composition consisted of approximately 50% fat, 50% lean volume, and was of sufficient size to ensure that the histogram had sufficient data points to provide two distinct peaks within the distribution. Thus, thresholds can be set to selectively visualize fat volume, lean volume, or both. By comparing raw to segmented images, the selected threshold was visually confirmed for animals on the extremes of low- and high body mass. These thresholds were fixed thresholds and applied consistently across all animals and regions of interest.

Quantifying Visceral and Subcutaneous Fat. For determinations of abdominal adipose volume, a subset of 45 animals was randomly selected from the total animal population of 90. The total adipose tissue (TAT) volume was first evaluated, and then further subdivided into compartments. The abdominal muscular wall was used as the demarcation line to separate visceral adipose tissue (VAT) from subcutaneous adipose tissue (SAT) (97). Histologically, the muscle fascia is distinct and easy to identify (**Fig. 2**). In microCT density based images of an animal, this muscle layer appears brighter because of its higher density. To separate the lower density fat compartments on both sides on either side of the muscle, the fascia can either be traced manually by drawing contour lines, or detected automatically to increase processing speed and reduce user-variability (98;99). The separation of fat regions was performed on segmented images. Here, the fat compartments in the abdominal region were separated and quantified using a custom IPL script based on the Canny method for edge detection (100;101).

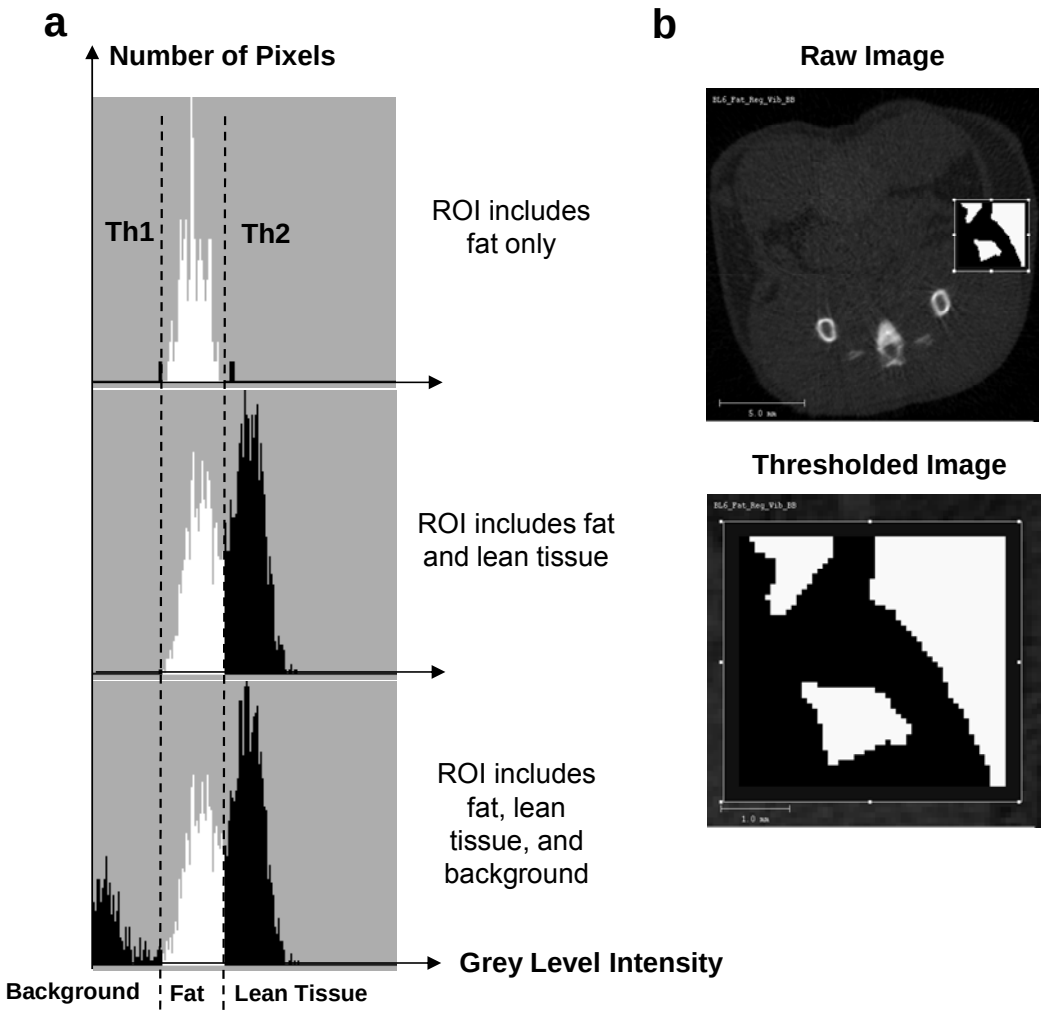

Fig 3. Selection of threshold values for each tissue type to separate fat and bone from other tissues. **(a).** Representative regions of interest (ROI) of known composition were selected. Histograms of the gray-level intensities (x-axis) within these representative ROIs were generated. The top histogram presents a histogram for a ROI in which only one tissue type (fat) was present. The relatively homogenous fat tissue is represented by a narrow distribution of gray level intensities (densities), allowing the selection of an upper and lower thresholds (Th1 and Th2) specific for fat. For the histogram below, an ROI was selected in which two tissue types - fat and lean tissue (muscles and/or internal viscera) – were present, causing a bimodal intensity distribution. The bottom histogram shows a trimodal distribution of density values from a ROI with two tissue types and background. **(b).** A reconstructed image from the mid-torso areas was utilized in the selection of the ROI with known tissue types (top). The enlarged image (bottom) provides an example for a ROI which yields a bimodal distribution.

Statistics. Across all mice (n = 90 for whole body evaluations, n=45 for abdominal evaluations), linear regressions were used to determine the association between the microCT-determined adipose volumes and explanted fat pad weights. For the abdominal region of each animal, total adipose volume in (TAT) was divided into visceral (VAT) or subcutaneous (SAT) adipose volume and regressed against fat pad weight individually. All data were reported as mean ± standard deviation, and statistical significance was defined at $p<0.05$.

RESULTS

Validation of Scan Data. The *in vivo* microCT scans provided a sufficiently high contrast and signal-to-noise ratio to identify and isolate adipose tissue throughout the body of the mouse (**Fig. 4**). As expected, the degree of adiposity varied greatly across the group of 90 mice. The use of skeletal sites as anatomical landmarks allowed the precise definition of the region of interest, both for measurements between different animals as well as for multiple measurements within the same animal. This was particularly important because we found that adipose and other soft tissues were poor landmarks because of their variable location due to physiological factors (e.g., gastrointestinal status) and variability associated with positioning (e.g., stretching) the animal in the scanner.

Across the ninety mice, total adipose values of the body (minus head and feet) exhibited a very strong and positive correlation with the physiologic weight of the discrete visceral and subcutaneous fat pads that were explanted at sacrifice (2wks after the scans). The coefficient of determination (R^2) for the correlation between the harvested subcutaneous fat pad and microCT fat volume of the entire body was 0.91

($p<0.001$) while the correlation between the harvested visceral fat pad and whole-body fat volume ($R^2 = 0.94$, $p<0.001$) was similarly high (**Fig. 5a**).

The length of time required to scan an entire mouse with our scanner at the specified settings was approximately 40 minutes and, inherently, proportional to the length of each mouse. To decrease the scan time and the exposure of the animal to anesthesia and radiation, it was investigated whether similar information on fat volume can be gained by reducing the length of the region of interest from the whole body to the abdominal area. Selection of this much smaller abdominal region, encompassing the mid-torso between the L1 and L5 vertebrae, reduced the scan-time by two thirds, from 35-40 minutes to 12-13 minutes. Whole-body fat volume was very highly correlated with abdominal fat volume across the 45 mice ($R^2 = 0.99$, $p<0.001$, **Fig 5b**) and, therefore, the R^2 values between microCT fat volume and fat pad weight did not change significantly by restricting the region of interest to the abdominal area ($R^2 = 0.92$ for subcutaneous fat pad and $R^2 = 0.96$ for epididymal fat pad, $p<0.001$ each).

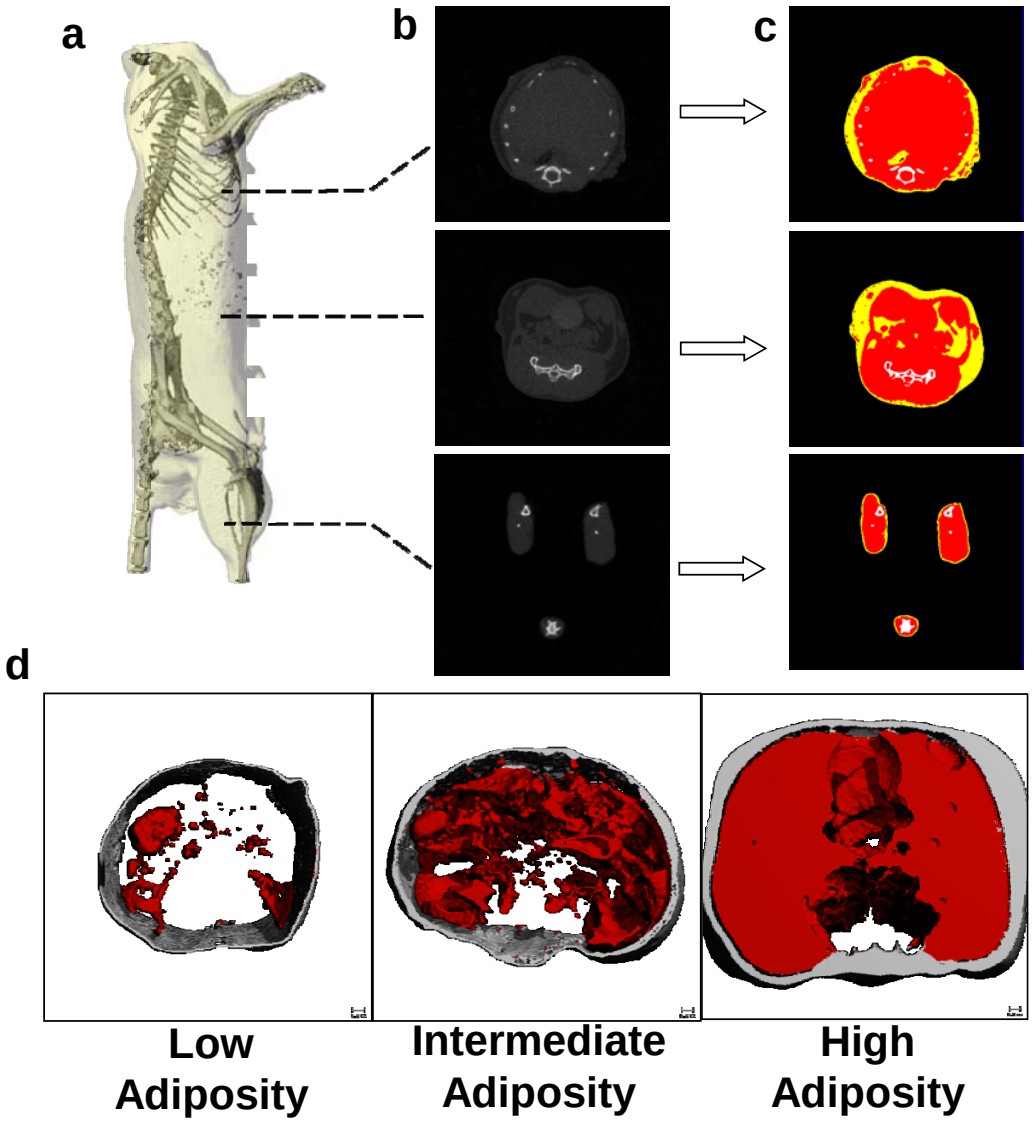

Fig 4. **(a)** Reconstructed microCT scan of a mouse in which the skeleton can be readily identified to define the region of interest. **(b)**. The majority of the adipose tissue in the mouse is localized in the abdominal region, as the thoracic cavity and legs show lower prevalence of low density (fat) tissue. **(c)**. To quantify fat volume in these different body compartments, tissues of different density were segregated and categorized as either fat (yellow) lean mass (red) or bone (white). **(d)**. Representative images from three different animals with either low, intermediate, or high adiposity, with the threshold specific to fat applied. Subcutaneous fat is shown in gray, visceral fat in red.

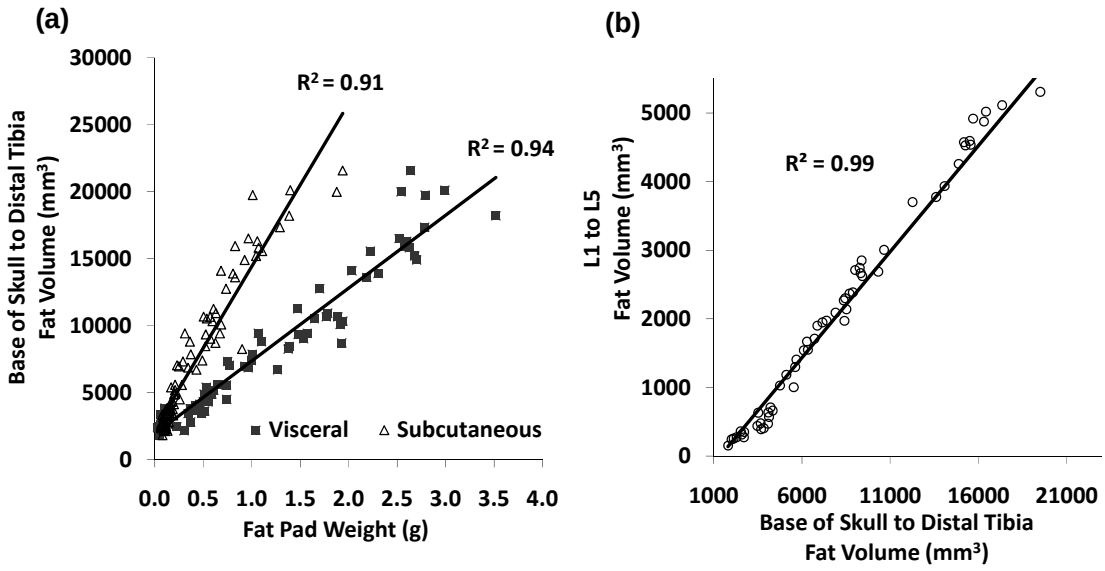

Fig 5. (a) Total fat volume (from the base of the skull to the distal tibia) determined by *in vivo* microCT was highly correlated with both the visceral and subcutaneous tissue weight of the fat pads harvested at sacrifice (n=90). **(b).** A scan of the *abdominal* region reduced the scan time by two-thirds. Despite the much smaller region, fat volume of the abdomen (spanning between L1 and L5 vertebrae) was highly correlated with total fat volume of the entire mouse body (n=45).

Visceral and Subcutaneous Fat Discriminations. To investigate any potentially different relations between the subcutaneous/visceral adipose tissue compartments and fat pad weights, visceral fat volume was automatically separated from subcutaneous fat volume by customized algorithms for the abdominal region encompassing L1 to L5. The weight of the visceral fat pad weight was highly correlated with the microCT determined VAT volume (R^2 =0.95, p<0.001, **Fig. 6a**). The correlation between the subcutaneous fat pad weight and the microCT determined SAT volume was equally high (R^2 =0.91, p<0.001, **Fig. 6b**). Further, VAT volume was highly correlated with SAT volume (R^2 = 0.98, p<0.001, **Fig. 6c**), similar to the correlation between visceral fat pad weight and subcutaneous fat pad weight (R^2 =0.95, p<0.001).

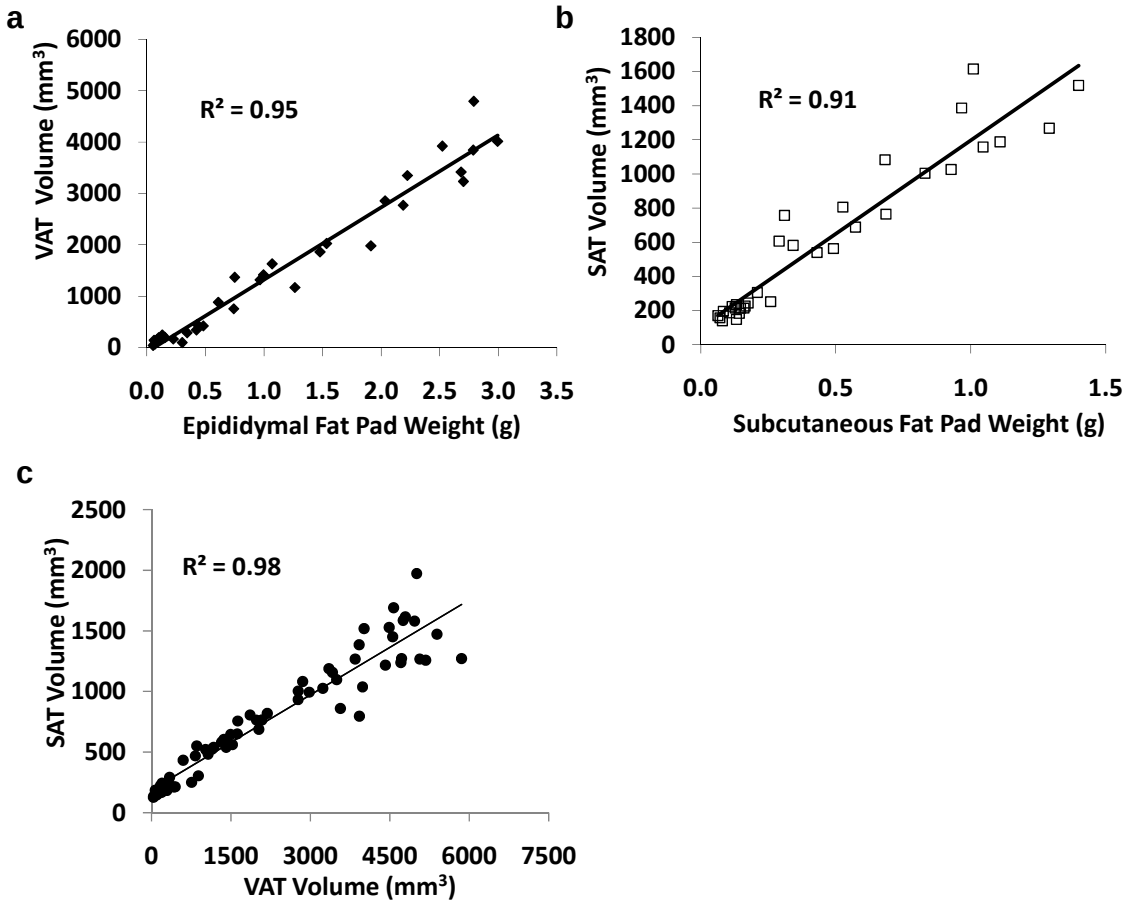

Fig 6. Evaluation of abdominal adiposity separating visceral adipose tissue (VAT) from subcutaneous adipose tissue (SAT). For these analyses, data from 45 animals were randomly selected from the entire population. **(a).** Visceral adipose tissue volume was highly correlated with the weight of the visceral (perigonadal) fat pad ($p<0.001$). **(b).** Subcutaneous adipose tissue volume was highly correlated with the weight of the subcutaneous (from the lower back) fat pad ($p<0.001$). **(c).** As the microCT calculated volumes for both fat deposits correlated well with the weights of the respective fat pads, VAT and SAT area were also correlated to each other ($p<0.001$).

DISCUSSION

With the high current, and projected, activity in obesity and diabetes related research, the ability to non-invasively image different types and locations of adipose tissue in small animal models has become increasingly important. The primary aim of this study was to validate the methodology of *in vivo* microCT scanning as a substitute for the *ex vivo* measurements of fat pads. Mice used in this study were of the most commonly utilized inbred strain in biomedical research and displayed differences in body fat volume by an order of magnitude. The very high correlations between total / subcutaneous / visceral fat volume with the specific subcutaneous and visceral fat pad weights demonstrated the utility of this technique in providing real time data on adiposity in the mouse, in a quick, non-invasive manner. That the correlations using fixed thresholds that were consistent across this very diverse sample of mice (body mass, body fat, diet, gender, and treatment) attests to the robustness of this method. While this study was performed in mice, it can be readily adapted to any animal model that fits into a microCT scanner.

All evaluated data for visceral and subcutaneous adipose tissue showed strong correlations to the weight of the explanted fat pads. However, the perigonadal (visceral) fat correlations were slightly higher than the mesenteric (subcutaneous) correlations even though the R^2 values for either type of fat were not significantly different from each other. This difference may have been caused by the location of the isolated mesenteric fat pad which, in contrast to the perigonadal fat pad, was not entirely within the evaluated abdominal region. Moving the distal anatomical landmark further distally may further enhance the coefficient of determination. The high R^2 values for the linear regressions between microCT-calculated fat volumes and fat pad weights over a large range of data demonstrates the utility of *in vivo* microCT to determine differences in body

composition between different groups but it is important to note that the absolute values of the calculated fat volumes were entirely dependent on the region of interest. As the cross-sectional fat content varies greatly along the longitudinal axis of the mouse torso, the regressions cannot be used for future studies to predict the specific weight of visceral or subcutaneous fat pad weights based on the microCT data.

Our data showed that the information derived from whole-body microCT scans was equivalent to scans of only the abdominal region between the L1 and L5 vertebrae. In clinical studies, relatively few (typically one to five) CT slices in the abdominal area between the L2 and L3 vertebra are analyzed to assess adiposity (102). While this suggests that it may be possible to further reduce the length of the region of interest in the mouse, it may cause inaccuracies in the discrimination between visceral and subcutaneous fat, particularly in small and lean animals, as the total volume of evaluated fat deposits would be greatly decreased. Regardless, our data demonstrate that the scanning and evaluating of only the mid-torso of a mouse, encompassing the majority of the intra-abdominal fat, will provide a precise relative assessment of total, subcutaneous, and visceral adipose tissue.

For our analyses, the calculated SAT value also included the volume of the skin, as the density of skin is similar to the density of fat (103) and is therefore assigned to fat within the selected threshold values. The full thickness of skin for the C57BL/6J inbred mouse strain is approximately 120 microns (104). Based on the resolution of the microCT scans, the skin encompassed up to two voxels in the radial direction and this volume was included in our reported fat volumes. For the spatial analyses of SAT and VAT, the skin volume defaulted as part of the subcutaneous compartment (based on location). Because skin voxels contributed a relatively small and consistent volume to the SAT, no efforts were made to subtract them either from SAT or TAT. Nevertheless,

in very lean mice or in mice with very little subcutaneous fat, algorithms could be used to adjust SAT volume to exclude the contribution from skin.

Adipose mass and increased adiposity can alter systemic physiology by changing the endocrine and metabolic state of the tissue (105) and the measurement of *in vivo* fat volume and adipose burden may be an important surrogate indicator of metabolic health. Thus, the ability to determine this parameter non-invasively in a live animal will not only provide longitudinal data without the need to sacrifice the animal, but will also increase the statistical power by the ability to perform intra-animal comparisons. Our data indicate that *in vivo* microCT of small animals can quickly and reliably provide data on adipose volume at spatial resolutions that are high enough to quantify specific and very small deposits of fat within animals of varying adiposity.

Chapter 3

EXCESS ADIPOSITY COMPROMISES THE NUMBER OF BONE MARROW DERIVED STEM CELLS

ABSTRACT

Parallel to the growth of the obesity epidemic, the number of medical conditions associated with and/or caused by excess adiposity has also increased dramatically. Caloric intake and dietary composition play a large role in the development of obesity, but the contribution of these factors to the cells involved in adipogenesis, specifically the bone marrow derived stem cell population, has not been defined. We hypothesized that in addition to promoting adiposity, dietary induced obesity (DIO) also reduces the stem cell pool, compromising the ability to repair and regenerate after tissue damage. Our data indicated that in response to 6 wks of a high fat diet beginning at 7 wks of age, FD animals (n=8) exhibited a 13% ($p = 0.010$) increase in body mass, 113% ($p<0.001$) increase in fat volume, and a -54.8% ($p<0.001$) decrease compared to age matched regular diet animals (RD, 13 wks old at sacrifice, n=8) in the total bone marrow derived stem cell number, which included both hematopoietic (HSC) and mesenchymal stem cells (MSCs). Further, comparison of the FD animals fed 6 wks of a fat diet to a SFD group (n=8) fed 9 wks of a fat diet beginning at 4 wks age demonstrated an additional stem cell reduction (-59.9%, $p<0.001$), highlighting that the age of obesity onset and duration of obesity contribute greatly to the stem cell reduction. Linear regression of number of stem cells to the epididymal fat mass demonstrated a significant suppression of stem cells with increasing adipose burden ($R^2 = 0.59$, $p = 0.03$). Overall, a high fat diet greatly disrupts the stem cell population, both in terms of number and differentiation patterns, providing evidence of the toxicity of obesity to stem cells. This negative correlation of increased adiposity to diminished number of stem cells can be seen as a contributing factor to the impaired ability of obese individuals, who are more prone to certain diseases, to also resist and fight disease.

INTRODUCTION

As the incidence of obesity continues to increase, the medical conditions that are associated with adiposity likewise become more prevalent. Conditions such as osteoarthritis and obstructive sleep apnea are often attributed to an increased adipose burden in obese individuals, whereas the increased number and size of adipocytes are considered key etiologic factors in the development of diabetes, cardiovascular disease, and various cancers.(106) Not surprisingly, the impact of excessive caloric intake and a poorly balanced diet are major foci of obesity research, clinical practice, and public policy.(107) Diets high in saturated and trans fat typically promote weight gain, which in turn engenders complications such as metabolic syndrome.(108) In addition, diet patterns high in fat cause activation of the immune response and an increase in inflammation.(109)

The role of obesity and excess fat mass in the progression of bone loss and osteoporosis is another active area of investigation. It is often presumed that the load bearing challenges inherent to obesity will have a beneficial impact on the skeleton, (110) as heavier individuals adapt greater density in their bones to withstand the increased loading. There is increasing evidence, however, that overweight individuals do not realize a proportionally greater bone mass, and are at a greater relative risk of fracture when falling. (111). In a review of risk factors for fractures in normally active children and adolescents, excess adiposity was shown to increase the fracture risk to 33.3% in obese children, up from 15.5% in normal weight children (112;113).

That an association exists between a high fat diet and obesity, and obesity and osteoporosis, is becoming clear, but the full impact and interaction of the dietary signal and fat and bone development is far from characterized. The effect of diet on the molecular responses that drive adipocyte formation is an area of active research, with

recent evidence that the adipose burden increases not only due to adipocyte hypertrophy, but also adipogenesis.(114) The effect of diet on bone has been noted in epidemiological studies, which indicate that high fat diets result in low bone mass and poor bone quality.(115) Based on *in vitro* studies and animal models, researchers have suggested that excess dietary fat (and their metabolites) can inhibit bone formation by blocking differentiation of osteoblast progenitor cells (116) and by inducing apoptosis of osteoblastic cells.(117)

Conclusive evaluations on the interaction of a high fat diet and stem cells are lacking in the literature. Herein we examine the effect of a high fat diet on the marrow mesenchymal stem cell population, the progenitor population to the mature adipocyte and osteoblast, as a potential contributing factor to the pathophysiology of obesity. We hypothesized that in addition to promoting adiposity, dietary induced obesity (DIO) also reduces the mesenchymal stem cell (MSC) pool, which would compromise the ability to repair and regenerate in response to tissue damage. This finding lends support for a preventative approach towards obesity, as not only does excess adiposity increase the risk factors for disease, obesity-induced loss of stem cells to resist and fight disease could potentially decrease the efficacy of treatment.

MATERIALS AND METHODS

Experimental Design. The overall experimental design consisted of two similar protocols, differing in the duration that animals were fed the respective diets. To characterize the development of dietary induced obesity three groups were established: 12 wks on either a regular (RD, n=15) or high fat diet (FD, n=10), and 15 wks on a high fat diet (SFD, n=7). *In vivo* measurements were made at 19 wks of age, and *ex vivo*

values established at sacrifice at 21 wks of age. The second study, designed to assess mechanistic responses of cells to the duration of the high fat diet feeding period and amount of adiposity are likewise referred to as RD (n=8) FD (6 wks on high fat, n=8) and SFD (9 wks on high fat, n=8), and all animals in this study were sacrificed at 13 weeks of age.

Animal Model. Male C57BL/6J mice were obtained from Jackson Laboratories (Bar Harbor, ME), and were acclimated (single-housed) in our facilities for a week. For the study to characterize phenotypic responses, mice were randomized by weight into two groups to either receive a regular chow diet (Lab Diet, Richmond, IN) or a high fat diet (45% kcal fat, # 58V8, Research Diet, Richmond, IN, n=8 for RD, n=16 for high fat diet). The high fat diet group was further segregated into animals that began the high fat at 4 wks of age (SFD, n=8) or those that began high fat at 7 wks of age (FD, n=8). Body mass and food intake were monitored weekly. Animals were allowed free access to food and water, and were sacrificed by cervical dislocation under deep anesthesia at 21 weeks of age.

For the study to assess the effect of duration of high fat feeding and amount of adiposity, animals were fed a high fat diet beginning at either 4 wks of age (SFD, n=8) or 7 wks of age (FD, n=8). A RD group (n=8) was age-matched to FD animals. All animals were sacrificed at 13 wks of age. All animal procedures were reviewed and approved by the Stony Brook University animal care and use committee

***In Vivo* Microcomputed Tomography and Determination of Adiposity.** Total adipose volume for each animal was established at 19 wks of age. Refer to Chapter 2 for detailed scanning and data evaluation methodology, as well as method validation. Briefly, the entire torso of each mouse was scanned at an isotropic voxel size of 76

microns (45kV, 133μA, 300ms integration time) with a vivaCT 40 scanner (Scanco Inc, SUI). The region of interest was defined by two anatomical landmarks, one at the distal end of the tibia and the other at the base of the skull. At the end of each scan x-ray impressions of the whole body were reconstructed as a three dimensional grey scale image. A custom script written in image processing language (ipl) was used to contrast and analyze fat tissue. Gaussian filtering (sigma = 1.5, support = 3.0) was used to reduce the noise in the separated image, followed by an image segmentation to contrast fat from bone and lean tissue.

Estimation of Adipocyte Size and Number. At sacrifice, the epididymal fat pad was harvested and fixed in 10% formalin. The fixed tissue was paraffin embedded, sectioned at 8 μm thickness, and stained with hematoxylin and eosin (H&E) to visualize cell morphology. H&E stained slides from each individual animal were imaged on a Zeiss Axiovert 200M. For each animal, average cell radius was calculated based on images of 5 random fields, and with the simplifying assumptions of homogenous cell size and spherical cell shape. The number of adipocytes that comprise the total adipose volume (determined by in vivo micro-computed tomography) of the animal was estimated based on the average adipocyte cell volume determined from histological images.

Status of MSC Pool by Flow Cytometry. Cellular and molecular changes in the bone marrow resulting from 6w of regular or high fat diet (n=8 animals per group) were determined at sacrifice from bone marrow harvested from the right tibia and femur by flushing (animals at 13w of age). Red blood cells in the bone marrow aspirate were removed by room temperature incubation with Pharmlyse (BD Bioscience) for 15 mins. Single cell suspensions were prepared in 1% sodium azide in PBS, stained with the appropriate primary and (when indicated) secondary antibodies, and fixed at a final

concentration of 1% formalin in PBS. Phycoerythrin (PE) conjugated rat anti-mouse Sca-1 antibody and isotype control were purchased from BD Pharmingen and used at 1:100. Rabbit anti-mouse Pref-1 antibody and FITC conjugated secondary antibody were purchased from Abcam (Cambridge, MA) and used at 1:100 dilutions. Flow cytometry data was collected using a Becton Dickinson FACScaliber flow cytometer (San Jose, CA).

Flow Cytometric Analyses. Regions were defined for flow cytometry data based on clustering of cells with similar forward (FSC) and side scatter (SSC) profiles. FSC correlates with the cell size/volume and SSC depends on the inner complexity of the cell (i.e. shape of the nucleus, the amount and type of cytoplasmic granules or the membrane roughness). Reported stem cells quantities are from region R1 (smallest, least granular cells), which typically comprised the population with the highest positivity for the Sca-1 marker. Sca-1 positive cells in region R3 (largest size, most internal complexity) were quantified as osteoprogenitors. The preadipocyte population was identified as all cells positive for surface staining of preadipocyte factor-1 (Pref-1).

Statistical Analyses. All data are shown as mean ± standard deviation. To determine significant differences between RD, FD, and SFD groups (multiple comparisons), one way ANOVAs with two-tailed Dunnett post-hoc tests were used. For comparisons between FD and SFD groups, two-tailed t-tests were performed. Significance value set at 5% was used throughout for all analyses.

RESULTS

Development of Diet Induced Obesity. Increases in body mass and fat volume were used to assess the development of obesity in the animals. Weight-based randomization of animals at the beginning of the study ensured that all groups were of similar weight at baseline. Body mass at the time of *in vivo* microCT scanning (all animals 19 wks of age) demonstrated significant increases between all groups (**Fig 7a**). RD animals weighed on average 28.6 ± 2.5 g, FD animals 32.4 ± 3.8 g (+ 13.3%, $p = 0.010$) and SFD animals 39.2 ± 3.0 g (+37.0%, $p < 0.001$). Percentage changes are reported relative to RD. MicroCT calculated fat volumes demonstrated even larger differences, with FD and SFD animals exhibiting increases of 113.4% and 171.7% respectively (both $p<0.001$) over the RD group (**Fig 7b**).

At sacrifice, differences in epididymal fat pad and liver weights for all groups were determined. The epididymal fat mass in regular diet animals averaged 0.62 ± 0.22 g, and FD animals saw a 190.1% ($p<0.001$) increase in fat mass over the RD group. Epididymal fat mass in SFD animals were 240.6% ($p<0.001$) higher (**Fig 7c**) than RD. In contrast to the relatively small yet significant increases in animal weight and large increases in total fat volume and fat pad weight, the weight of the liver was not affected by the high fat diet (**Fig 7d**). Compared to RD (1.12 ± 0.11 g), FD animals saw a non-significant decrease (0.98 ± .016 g, $p = 0.196$). Likewise, SFD animals (1.10 ± 0.38 g, $p = 0.301$) were similar to RD. Tibial lengths measured with a digital micrometer indicated that both fat diet groups had slightly shorter tibia than RD animals (17.7 ± 0.13 mm for RD, 17.5 ± 0.14 mm for FD and 17.4 ± 0.36 mm for SFD, $p = 0.020$ for multiple comparison). The 1% difference between RD and FD animals was not significant ($p = 0.103$), but the 1.5% difference between RD and SFD was ($p = 0.017$).

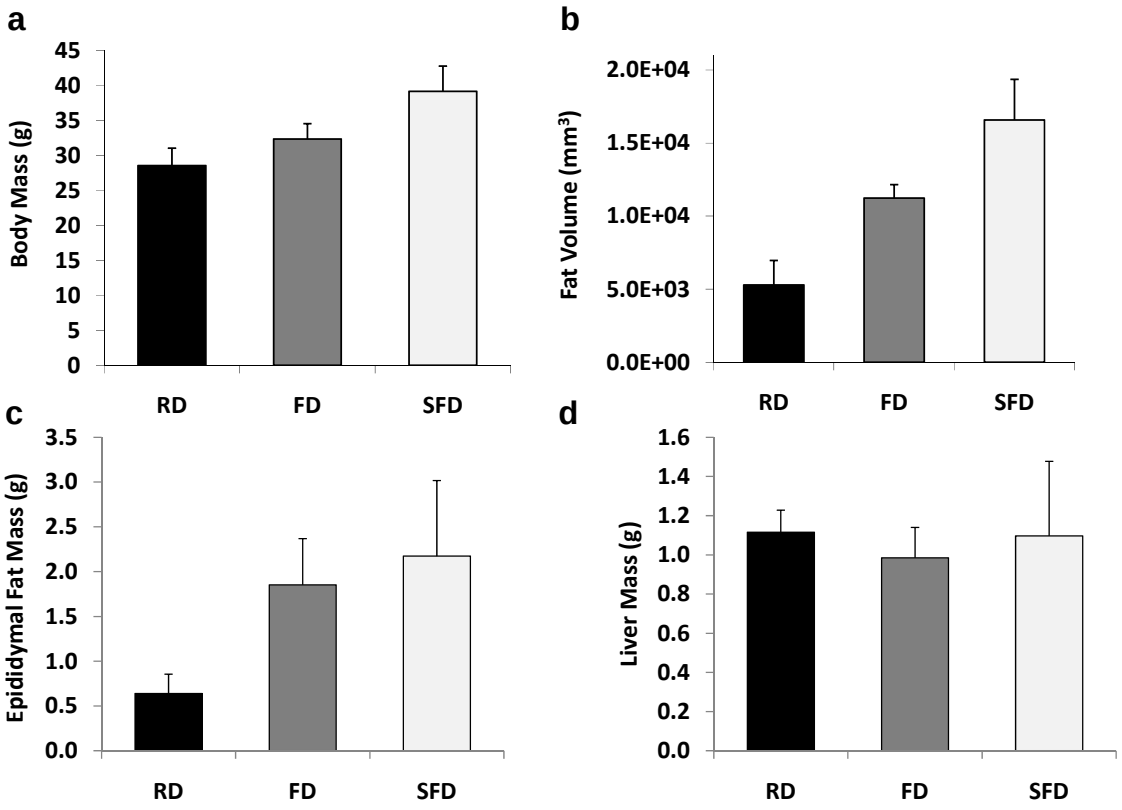

Fig 7. A high fat diet readily induces obesity in male C57BL/6J mice, such that animals fed high fat for 12 wks (FD) increased body mass 13%. Animals fed high fat for 15 wks (SFD) saw a 37% increase relative to RD animals (**a**). Percentage increases in fat volume (113% and 172% respectively, both $p<0.001$, **b**) and epididymal fat mass (190% and 241% respectively, both $p<0.001$, **c**) were much larger than the change in body mass. The increase in animal mass is largely due to the increase in adipose burden, as liver mass (**d**) shows no differences between groups.

In addition to the various measurements of weight and volume of fat at the organismal (microCT volume) and tissue (epididymal fat mass) levels, qualitative results based on image analysis of histological sections from epididymal fat from RD and FD animals indicate that adipocyte size was increased by 30%, and the total number of adipocytes in the animal based on volume increase by 93% (**Fig 8**) due the 12 weeks of a high fat diet. Standard deviations and p-values are not reported for the qualitative data due to the small sample size (n=2), and will be reported once all samples are analyzed. Adipocyte size and number in SFD animals has not yet been determined for this study.

High Fat Diet Reduces Marrow Mesenchymal Stem Cells. To assess the effect of a high fat diet on the process of adipogenesis in terms of the developmental response, the progenitor cell populations upstream of mature adipocyte formation (preadipocytes and mesenchymal stem cells) were examined. To elucidate potential changes in the cell population that would precede the large phenotypic changes seen after 12 weeks on a high fat diet, animals fed high fat for 6 wks were utilized. Flow cytometric analyses of the total marrow cell population harvested from the femurs and tibias of animals after six weeks of either a regular chow diet or a high fat diet indicated that the number of stem cells present had been significantly diminished in response to the fat diet (**Fig 9**). The overall bone marrow derived stem cell pool representing all cells expressing the surface marker stem cell antigen-1 (Sca-1), including both hematopoietic and mesenchymal stem cells, was decreased by -54.8% ($p<0.001$). More specifically, the undifferentiated MSC population was decreased by -59.6% ($p<0.001$).

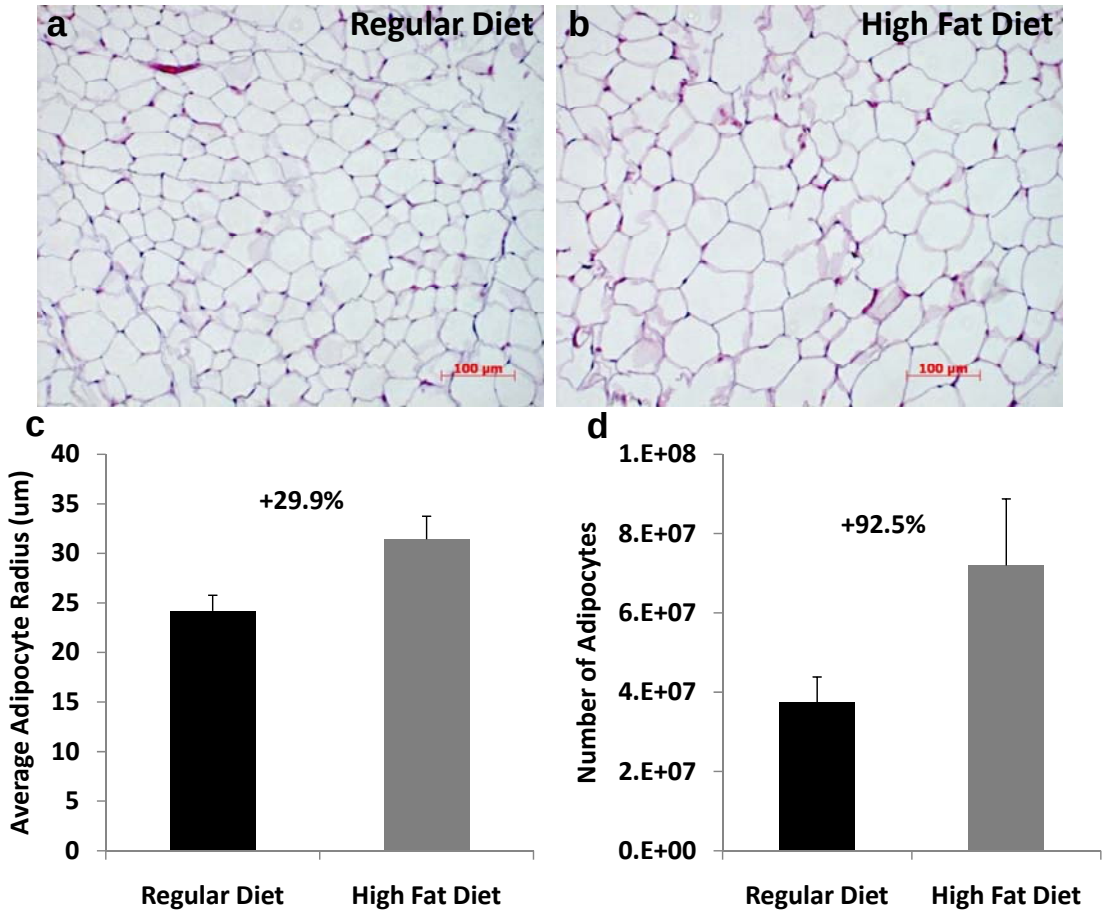

Fig 8. Representative images from a regular diet (a) and fat diet (b) animal show clear differences in adipocyte morphology. Qualitative assessments of average adipocyte size based on images from 5 random fields from each animal (n=2 animals per group) demonstrated a 30% increase in cell radius (**c**). Based on microCT calculated adipose volumes for the entire animal (neck to distal tibia), the total number of adipocytes was determined to be 93% greater in fat diet animals (**d**).

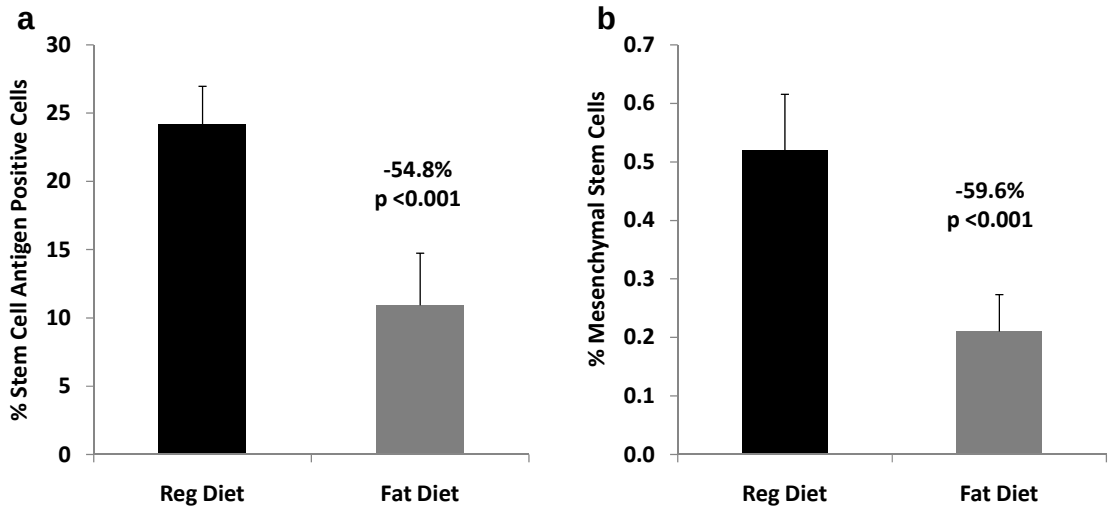

Fig 9. To determine the effect of high fat diet on the bone marrow derived stem cell populations, animals were fed a high fat diet for 6 weeks. The overall stem cell pool containing both hematopoietic and mesenchymal stem cells was significantly suppressed by six weeks of a high fat diet (**a**). Demonstrating that a high fat diet exerts significant consequences on the process of adipogenesis, the mesenchymal stem cell population that gives rise to osteoblasts and adipocytes was reduced by -59.6% (**b**) due to the dietary challenge introduced to a young animal.

Distribution of Size and Granularity of Preadipocytes is Altered by High Fat Diet. Identified by the expression of Pref-1 surface protein, the distribution of the preadipocyte cells for animals fed a high fat diet showed a clear shift from the regular diet animals (**Fig 10**), in that there was an increase of smaller, less granular preadipocytes (region R1). The preadipocyte population in region R2 (-1.5%, p=0.92) remained consistent, but in conjunction with the increase in R1 (+555%, p=0.001) due to the high fat diet, there was a large decrease in R3 (-58.6%, p=0.003).

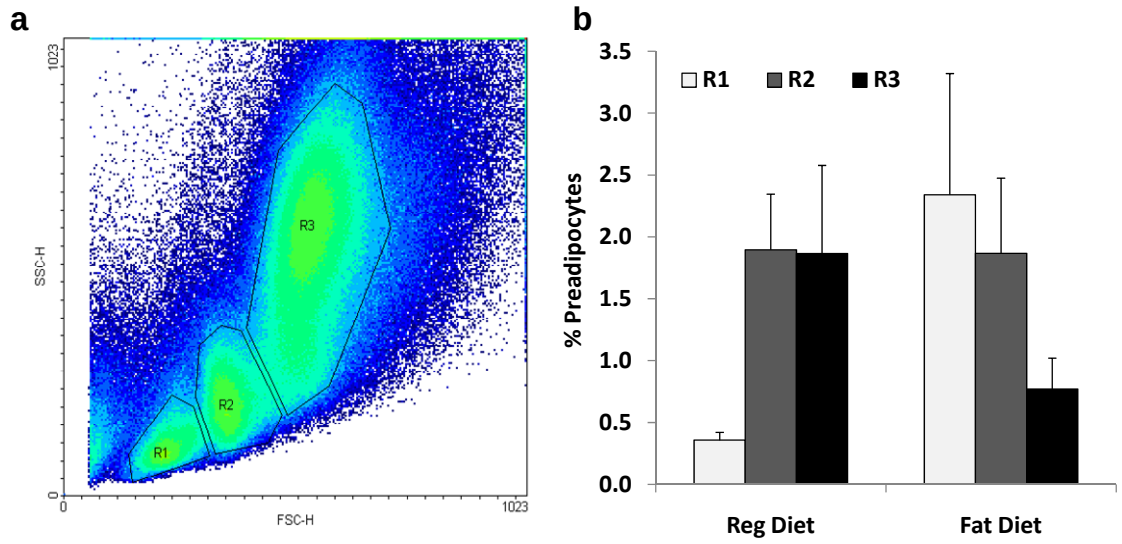

Fig 10. Representative image of a flow cytometry plot (forward scatter = FSC on x-axis, side scatter = SSC on y-axis) for a bone marrow sample (**a**) showing the 3 distinct populations of similar FSC and SSC. Within each of the three regions, the percentage of preadipocyte factor-1 (Pref-1) positive cells shows clear differences in distribution for animals fed a high fat diet (**b**). Mechanistically, the high fat diet increases the commitment of preadipocytes (R1) and the differentiation pattern, perhaps with more preadipocytes converting to adipocytes and losing the preadipocyte marker (decrease in R3).

Longer Duration of Obesity Causes Greater Loss of Stem Cells. Examining the effect of the duration of the high fat diet demonstrated that SFD animals that began the high fat at 4 wks of age and persisted for 9 wks were on average 30.0 ± 1.5 g, which represented a 9.4% (p=0.017) increase over the FD group (27.4 ± 2.4 g, **Fig 11a**), that began the high fat diet at 7 wks age and persisted for 6 wks. In addition to the longer time frame over which to accumulate fat, the weekly food consumption of animals was also altered (**Fig 11b**). Compared to SFD animals, the FD animals consistently ate less with the difference being significant at weeks 9 and 11 of age.

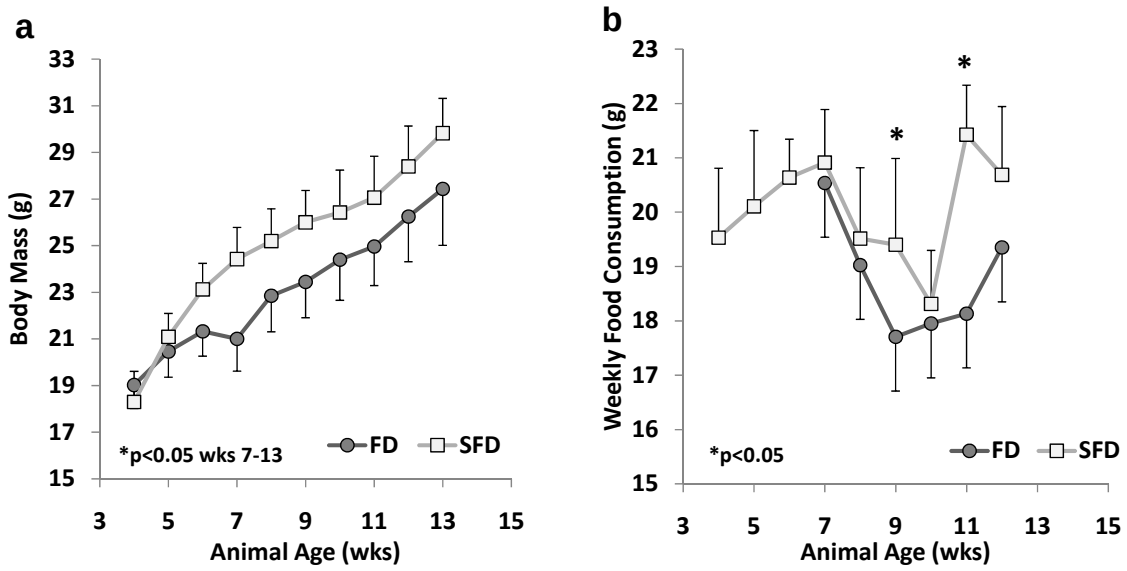

Fig 11. Animals fed a high fat diet for 9 wks demonstrated a 9.4% (p=0.017) over animals that were fed the high fat diet for 6 wks (**a**). The significant divergence in weight was actually evident beginning at 7 wks of age when the FD group commenced the fat diet. In addition to the increased adiposity of SFD animals, the earlier onset of obesity increases the metabolic demands of the animal, as evidenced in greater weekly food consumption (**b**) FD animals consistently ate less with the difference being significant at weeks 9 and 11 of age.

The consequences of the increased high fat diet duration on the stem cell population are evident from flow cytometry data quantifying the stem cell populations Compared to FD animals, SFD animals had fewer cells bone marrow derived stem cells (-59.9%, p=0.001, **Fig 12a**). The relationship between increasing fat mass (epididymal fat) and total stem cell number is shown as a linear regression between these two variables for both the FD and SFD groups (**Fig 12c**). For the FD animals, increasing fat mass demonstrates a strong negative correlation to the stem cell number (R^2 = 0.589, p = 0.026) whereas the SFD animals show no relationship between these two parameters (R^2 = 0.010, p = 0.081). However, the osteoprogenitor population was increased in SFD (+78.8%, p=0.098) as compared to FD animals (**Fig 12b**). Differences between groups in the osteoprogenitor population were not attributed to changes in body mass (data not

shown) or epididymal fat mass, as correlations for the SFD group (R^2 = 0.18, p = 0.31) and the FD group (R^2 = 0.05, p = 0.59) both demonstrated that increases in fat mass did not account for the differences in the osteoprogenitor population (**Fig 12d)**.

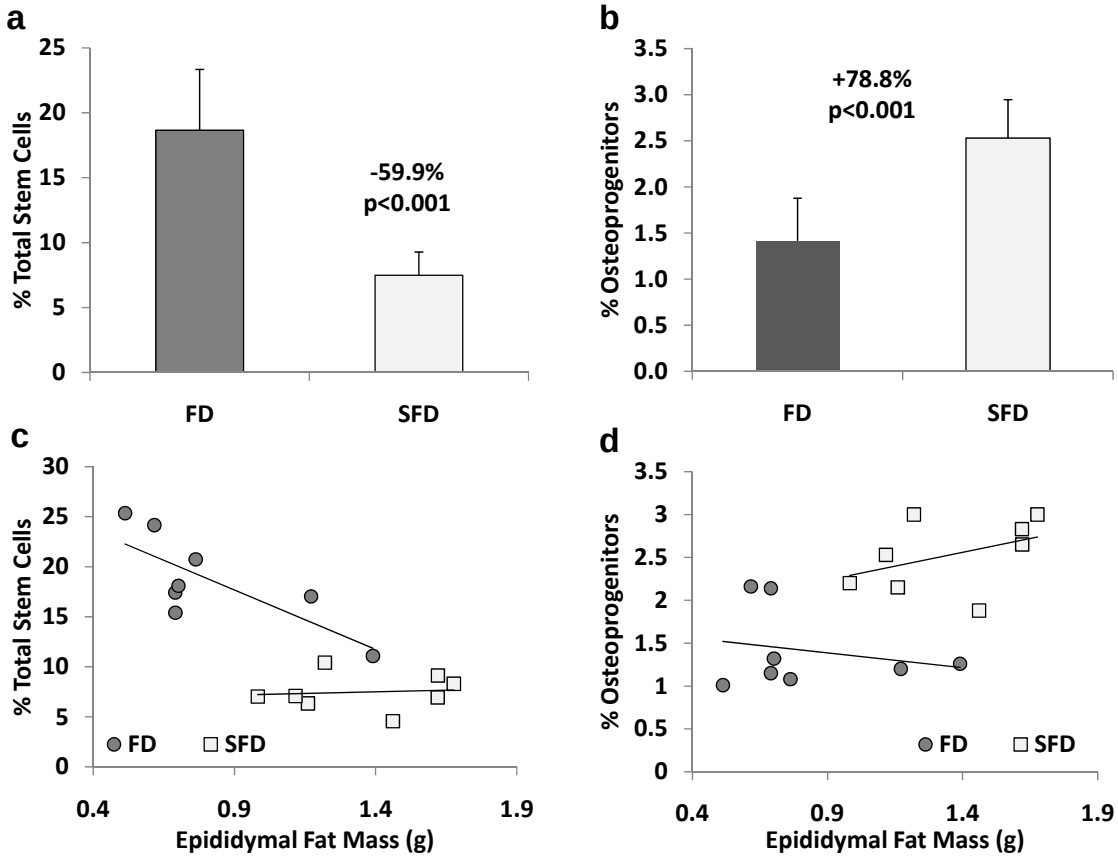

Fig 12. Flow cytometry data indicated that the number of stem cells present in the marrow had been significantly decreased in SFD animals compared to FD (**a**). Considering that FD animals already demonstrate compromised numbers of stem cells compared to regular diet animals, the additional 60% reduction caused by the duration of the high fat diet highlights the negative effect of excessive fat mass. However, even as the stem cells pool was diminished, the osteoprogenitors in the SFD group demonstrated a significant increase (**b**). Linear regressions between the adipose burden (represented by epididymal fat mass) and the % of stem cells further demonstrate the suppression of stem cells by increasing adiposity in FD animals (p=0.03), but not SFD (p=0.81, **c**). Neither group saw any relationship between % and osteoprogenitors and fat mass (p = 0.59 and 0.31 for FD and SFD respectively, **d**).

DISCUSSION

Data reported in May 2007 indicate that 15 percent of children and adolescents can be labeled as having childhood obesity in the U.S, which according to the Centers for Disease Control and Prevention (CDC) is associated with more severe complications of obesity, such as diabetes, cardiovascular disease, and cancer later in life. (118) This steadily increasing incidence of childhood obesity raises serious concern about the health of these youth as they approach adulthood, and understanding the cellular effects of negative dietary factors, such as a high fat diet, could provide potential insight into preventions and treatments for obesity. Specifically, of the complications engendered by obesity, how much influence is exerted by the increased adiposity, or are there other factors that are influenced by elevated fat intake? We show that in addition to creating a caloric excess, a high fat diet negatively affects the number of marrow derived stem cells and would likewise influence and contribute to obesity related complications. This data implies that for individuals that are obese, especially early in life, their long term health would be compromised as they would simultaneously be more prone to developing certain diseases, and less capable of fighting disease and repairing damage.

Our *in vivo* microCT analyses and assessments of *ex vivo* tissue weights clearly demonstrate that the relatively small increases in body mass (~10-30%) somewhat mask the >100% changes in adiposity between the regular diet and fat diet groups. The relatively short duration of the dietary challenge in this study, was not long enough to enact changes in the major organs, as 12 weeks of high fat did not affect liver size. Liver enlargement and fatty liver disease are associated with obesity, (119) but are typically changes seen over the longer term. The average adipocyte size observed is consistent with the reported range of 60-100 μm for white adipose tissue (120) even as

the analysis of adipocyte size and number were qualitative and relied on simplifying assumptions of homogeneity in size and uniformity of distribution.

The characterizations of the effects of high fat on the cellular milieu demonstrate that the bone marrow derived stem cell populations, and committed but not fully differentiated “progenitor” populations are largely influenced by diet, with the introduction of a high fat diet exerting significant negative consequences to the *in vivo* marrow environment. Osteoprogenitors and preadipocytes are considered progenitor cells, as they are committed to the lineage but have not achieved full differentiation. The drastic percentage decreases in the number of both hematopoietic and mesenchymal stem cells is observed in parallel to percentage increases in the committed progenitor populations, with the possible implication being that the resident bone marrow derived stem cell population would have diminished plasticity to respond to various biological challenges such as injury. Indeed, researchers have noted that with age, the number of bone marrow derived stem cells diminish as the marrow cavity increasingly fills with mature adipocytes.(121) That these changes are observed in parallel with the increased fragility and reduced capability of elderly individuals to heal is perhaps not coincidental.

In terms of the increase quantified in the osteoprogenitor population, some biomechanical factor surely is in effect, where larger loads due to the increased animal weight and adiposity engender greater bone mass. However, in humans only 27-38% of total body weight is attributed to fat,(3) and estimates based on our microCT calculated volumes and the reported density of fat (122) show that FD animals in this study were similar to these values (~32% of body weight attributed to fat). As such, increased loading due to increased fat mass does not entirely account for the increased in osteoprogenitors. The large excess in caloric intake serves as a dominating signal for differentiation towards adipogenesis, and in response to six weeks of a high fat diet, the number of early commitment preadipocytes increased by several orders of magnitude

indicating that the differentiation pathway of the stem cells was shifted towards adipogenesis. The decrease in R3 preadipocytes, which we believe to be further progressed towards the mature adipocyte morphology, is perhaps indicative of a change in rate of adipogenesis. As it is inhibitory of terminal adipocyte differentiation, the disappearance of surface expression of Pref-1 marks the transition to a mature cell phenotype. (37) The actual role of the preadipocyte, specifically of those residing in the marrow space, is not clearly understood and the full differentiation pathway of adipogenesis from the mesenchymal stem cell to the preadipocyte to the mature adipocyte is yet unclear. Additional studies are needed to definitively confirm the early identification of both the osteoprogenitors and preadipocytes, as well as address the rate of conversion into the mature cell types.

The negative correlation between adiposity and stem cell number is evident, but surely a bottom "limit" to the loss of stem cells must surely be achieved, as a basal level of cells is necessary for survival. Further decreases in the stem cell population might herald an early death if animals experience any sort of immune challenge or injury. Animals that start a high fat diet earlier in life and are therefore obese for a longer amount of time show drastic reductions in the stem cell population even compared to age-matched animals that began a high fat diet slightly later in life. For these animals there is no correlation between increasing fat mass and stem cell number as likely they are at the bottom limit of number of stem cells needed to survive, considering that they began the high fat diet essentially right after weaning.

In a similar manner by which osteoprogenitors are needed to maintain a "healthy" state of bone as animals age (122), the findings of this study indicate that at least some component of the pathophysiology of obesity and increased susceptibility of obese individuals to disease is likewise due to a lack of progenitor cells, mesenchymal or otherwise, to replenish the various tissues as damage (including that induced by the

excess adiposity) accumulates. There is increasing evidence that MSCs are protective of tissue damage and can help regenerate liver and pancreatic islet cells (123) with MSCs recruited to sites of injury and tumor microenvironments due to the secretion of various inflammatory factors. (124) Studies have shown that obesity compromises this immune response, and increases susceptibility to tumorigenesis, with one report showing a 30% increase in tumor development in DIO mice one week after subcutaneous injection of cancer cells compared with normal mice. (125;126) In humans, excess body weight is responsible for an estimated 14% of all cancer deaths in men and up to 20% in women. (127) Our results demonstrate the profound effects of diet on the stem cell population, in part providing explanation for how and why choices made early in life regarding diet can impact an individuals long term health, growth, and regenerative potential. This insight into another potential factor contributing to the pathphysiology of obesity, at the stem cell level that affects the repair and regeneration mechanism rather than a causality of fat to the development of disease, illuminates that in addition to therapies to “simply” reduce adiposity there is a need for treatments that can promote and protect the number of pluripotent stem cells resident in the bone marrow.

Chapter 4

ADIPOGENESIS IN A NORMAL MOUSE IS SUPPRESSED BY LOW MAGNITUDE MECHANICAL STIMULATION (LMMS)

---

*Reprinted in part from Rubin, *et al* from Proceedings of the National Academy of Science (v104, no 45, 17879-17884)

ABSTRACT

Obesity, a global pandemic which debilitates millions of people and burdens society with tens of billions of dollars in health care costs, is deterred by exercise. While it is presumed that the more strenuous a physical challenge the more effective it will be in the suppression of adiposity, here we show that 15 weeks of brief, daily exposure to high frequency mechanical signals, induced at a magnitude well below that which would arise during walking, inhibited adipogenesis by 27% in C57BL/6J mice. The mechanical signal also reduced key risk factors in the onset of type II diabetes, non-esterified free fatty acid and triglyceride content, in the liver by 43% and 39%, respectively. Irradiated mice receiving bone marrow transplants from heterozygous GFP^{+} mice revealed that 6wks of these mechanical signals reduced the commitment of mesenchymal stem cell differentiation into adipocytes by 19%, indicating that obesity in these models was deterred by a marked reduction in stem cell adipogenesis. Translated to the human, this may represent the basis for the non-pharmacologic prevention of obesity and its sequelae, achieved through developmental, rather than metabolic pathways.

INTRODUCTION

With the escalating incidence and associated cost of obesity, the need to develop effective interventions is prevalent.(128) Even the *control* of obesity and diabetes has proven difficult, as the principal etiologic factors are built into lifestyle choices that are increasingly sedentary. As a deterrent to the accumulation of adiposity, exercise suppresses obesity and the onset of type II diabetes by metabolizing calories that accumulate through the diet (6) and regulating insulin, free fatty acids and triglyceride production through physiologic control of sugar in the bloodstream.(129;130) This implies that the more strenuous and extended the exercise, the greater the benefit in metabolizing fat.(131;132) While the exact mechanism remains unknown, the pathways by which exercise suppresses adipogenesis are certain to involve both metabolic (133;134) and mechanical (135) factors, and a more complete understanding is necessary to help define physical and biochemical pathways which will more efficiently, effectively and uniformly control the pathogenesis of these diseases.(136)

In some contrast to paradigm that “more is better,” short daily durations of high frequency, extremely low-level mechanical signals, at least two orders of magnitude below those induced by exercise,(137) can positively influence other biologic systems, including bone (65) and muscle.(69) Considering that adipocytes, osteoblasts and myocytes all derive from a common progenitor, marrow derived mesenchymal stem cells,(138) it was hypothesized that these low-level mechanical signals which are anabolic to the musculoskeletal system would, in parallel, suppress adiposity. This would be achieved not by metabolizing existing adipose tissue, but by inhibiting stem cell differentiation into adipocytes, thus curbing obesity via a developmental pathway, at a

physical input far below that currently considered necessary to suppress obesity via exercise.(139)

METHODS

Mechanical Influence on Adiposity in the Normal Mouse: To examine the potential of high frequency, low magnitude mechanical signals to influence adipogenesis, forty C57BL/6J male mice, seven weeks of age and given free access to a normal chow diet, were randomized by weight into either LMMS (n=20) or their age-matched sham controls (CON; n=20). Animal weights, as well as their individual food consumption, were measured on a weekly basis. All procedures were reviewed and approved by the university's institutional animal care and use committee.

Low Magnitude Mechanical Stimulation (LMMS). For fifteen weeks, five days per week, LMMS mice were subjected to fifteen minutes per day of a 90Hz, 0.2g peak acceleration (1g = earth's gravitational field, or $9.8 m \cdot s^2$), induced by vertical whole body vibration via a closed-loop feedback controlled, oscillating platform (modified from Juvent, Inc, Somerset, NJ).(140) A sinusoidal vibration at this magnitude and frequency causes a displacement of approximately 12 microns and is barely perceptible to human touch. Sham CON animals were placed on an inactive vibrating platform each day.

Determination of Adiposity by *In Vivo* microCT. Twelve weeks into the protocol (19w of age), *in vivo* micro-computed tomography was used to quantify fat and lean volume of the torso (n=15 in each group, method detailed in Chapter 2). Data was evaluated by

defining the torso as the entire animal from the neck to the distal tibia, and reported adipose volumes are considered as representative of the total adipose tissue (less any fat contained in the head and feet).

Biochemical Assays. At 15w into the protocol (22w of age), eight mice from each group were fasted overnight before blood collection. Samples were collected by cardiac puncture with the animal under anaesthesia and the plasma harvested by centrifugation (14,000 rpm, 15min, 4ºC). Mice were sacrificed by cervical dislocation and the different tissues (i.e., epididymal fat pad, a subcutaneous fat pad from the torso, liver, and heart) quickly excised and weighed and frozen in liquid nitrogen and stored at –80ºC for further analyses. Glycerol, triglycerides (TG), free fatty acids (FFA) and insulin were measured in the plasma, and TG and non-esterified free fatty acids (NEFA) were measured on lipid extracts from adipose tissue (n=8 per group) and liver (n=12 per group). Plasma insulin levels were measured using an ELISA kit (Mercodia Inc., Winston-Salem, NC). TG and FFA/NEFA from plasma and tissues were measured using enzymatic colorimetric kits: Serum Triglyceride Determination Kit (Sigma, Saint Louis, MO) and NEFA C (Wako Chemicals, Richmond, VA), respectively. Total lipids from white adipose tissue (epididymal fat pad) and liver were extracted and purified following the chloroform-methanol method with some modifications,(141) while liver glycogen content was determined by the anthrone method.(142)

Cell Fate Determination after Bone Marrow Transplant: Sixteen male C57BL/6J mice, 8w of age, were irradiated in a Gamma Cell Irradiator with a Cs137 source at a total dose of 15Gy (dose rate of 1.07 Gy/min). The following day, irradiated mice were injected through the tail vein with 1 x 10^7 cells (total injection volume of 100 µl) harvested

from the bone marrow of the GFP^+ donor B6 mice. Heterozygous C57BL/6J^{GFP} mice (GFP expression controlled by constitutive actin promoter) were utilized as bone marrow donors.(30) After one week of recovery, GFP^+ transplanted mice were randomized into either CON or LMMS groups (n=8 each). Animals were sacrificed following 6w of the respective protocol, and the epididymal fat pad and marrow from the tibia were harvested for examination.

Identification of GFP+ Cells by Flow Cytometry. Single cell suspensions from the direct isolation of the tissue were prepared in PBS and fixed at a final concentration of 1.5% formalin in PBS. Adipocytes were isolated from the epididymal fat pad by collagenase digestion and centrifuged to remove the stromal vascular compartment. Bone marrow was harvested from the tibia and femur by flushing of the marrow cavity with PBS (0.5% bovine serum albumin). Red blood cells in the bone marrow aspirate were removed by room temperature incubation with Pharmlyse (BD Bioscience) for 15 mins. Single cell suspensions were prepared in 1% sodium azide in PBS, and fixed at a final concentration of 1% formalin in PBS. Flow cytometry data were collected on adipocytes and bone marrow cells on a Becton Dickinson FACScan flow cytometer (San Jose, CA) based on the GFP fluorescence signal.

Statistical Analyses. All data are shown as mean ± standard deviation. To determine significant differences between CON and LMMS groups, two-tailed t-tests were performed. For microCT calculated volumes (fat, lean, and bone) analyses were performed taking into account body mass as a covariate. Significance value set at 5% was used throughout for all analyses.

RESULTS

LMMS Suppression of Adiposity in Normal Mice: Throughout the study, body mass of both CON and LMMS groups increased at similar rates (**Fig. 13a**). At 12w, when the *in vivo* CT scans were performed, the body mass of LMMS animals was comparable to CON (4.0% lower in LMMS, p=0.2, **Table 1**). Throughout the course of the protocol, weekly food intake between LMMS (26.4 $\pm$ 2.1 g/w) and CON (27.0 $\pm$ 2.1 g/w) were essentially identical (**Fig 13b**).

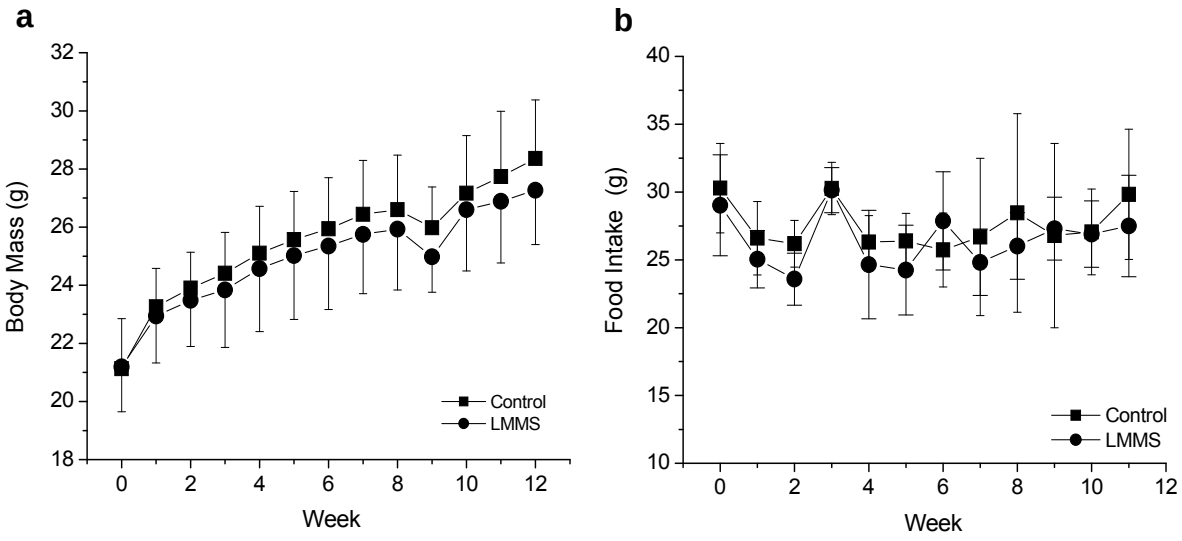

Fig. 13. Over the course of the experimental period, no significant differences were measured in average body mass (**a**) or weekly food intake (**b**) between controls (■) and LMMS mice (●). n≥15 in each group.

In vivo CT fat volume measured at 12 wk was 27.4% lower in LMMS animals than that measured in CON mice (p=0.008; **Fig 14**). With body mass of the animals as a covariate increased the P value to 0.013 whereas food intake as a covariate to fat volume does not alter the P value for the difference between CON and LMMS. With

body mass a covariate, total lean volume of the torso was greater in LMMS than CON (+1.2%, p=0.035), and bone volume was also indicated a trend towards increase (+0.6%, p=0.081). No differences in tibial length (p=0.6), the length of the torso (p=0.6), heart (p=0.7) or liver weights (p=0.6), were measured between groups (**Table 2**).

Parameters	CON	LMMS	% Diff.	P
Body Mass @ 12 weeks (g)	28.6 ± 2.49	27.4 ± 2.21	-4.0	0.20
Fat Volume (cm^3)	5.20 ± 1.67	3.85 ± 0.93	**-27.4**	**0.013 (0.008 w/o body mass covariate)**
Bone Volume (mm^3)	521.9 ± 39.0	518.6 ± 34.8	+0.6	0.081
Lean Volume (cm^3)	17.3 ± 1.2	17.5 ± 1.5	**+1.2**	**0.035**
Skeletal Length (cm)	8.13 ± 0.15	8.15 ± 0.18	+0.3	0.682
Fat Mass (g) (density = 0.92)	4.87 ± 1.5	3.54 ± 0.9	**-27.4**	**0.008**
Bone Mass (g) (density = 1.80)	0.93 ± 0.06	0.94 ± 0.07	+0.6	0.809

Table 1: Mean and standard deviation, as well as percentage difference and p-values, of body habitus parameters of the CON and LMMS mice at 12w, as defined by *in vivo* microcomputed tomography (n=15 in each group, p-values <0.05 are in bold). Significance values for reported volumes are based on analyses using body mass as a covariate.

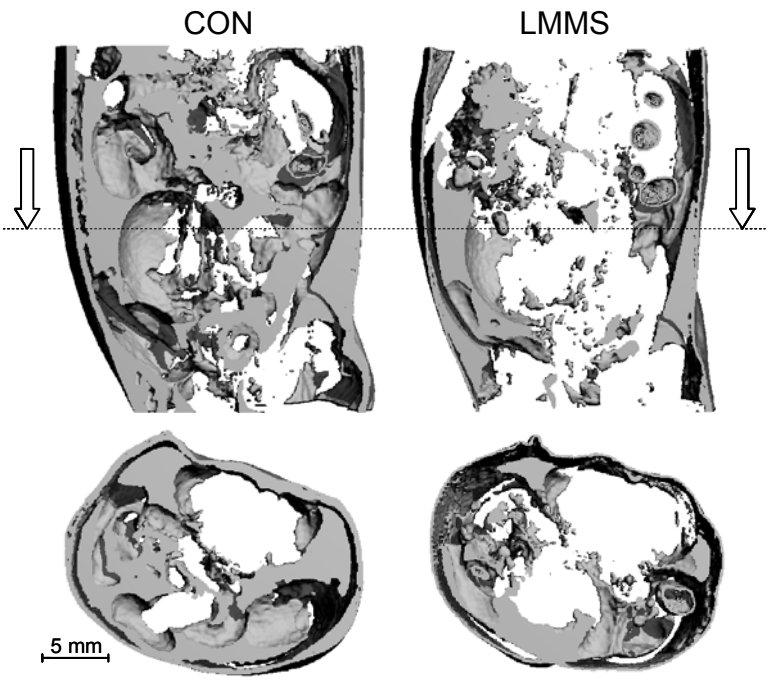

Fig. 14. Following twelve weeks of daily, 15 minute low-level mechanical signal, the average amount of fat within the torso is 27% lower than that of age-matched control animals. Representative longitudinal (top) and transverse (bottom, taken at level of dashed line) reconstructions of total fat content through the torso of a control (left) and LMMS (right) mouse.

Fat volume data derived from *in vivo* CT were supported by the weights of the dissected fat pads harvested post-sacrifice at 15w, where LMMS had 26.2% less epididymal ($p=0.01$) and 20.8% less subcutaneous ($p=0.02$) fat than CON mice (**Table 2**; **Fig 15**). Normalized to animal mass, there was 22.5% less epididymal and 19.5% less subcutaneous fat mass in LMMS than CON ($p=0.007$).

Parameters	CON	LMMS	% Diff.	P
Epididymal Fat weight (g)	0.63 ± 0.21	0.47 ± 0.12	**-26.2**	**0.014**
Subcutaneous Fat weight (g)	0.21 ± 0.06	0.17 ± 0.03	**-20.8**	**0.016**
Heart weight (g)	0.120 ± 0.010	0.122 ± 0.015	+1.6	0.707
Liver weight (g)	1.11 ± 0.11	1.09 ± 0.09	-1.7	0.581
Tibial Length (mm)	18.2 ± 0.17	18.1 ± 0.27	-0.4%	0.43
Plasma Glycerol (mg/dL)	17.37 ± 6.63	18.75 ± 9.31	+7.9	0.64
Plasma Insulin (ng/mL)	0.54 ± 0.09	0.48 ± 0.07	-10.8	0.068
Plasma TG (mg/dL)	38.74 ± 15.67	39.44 ± 12.4	+1.8	0.89
Plasma FFA (mmol/L)	0.69 ± 0.32	0.63 ± 0.20	-8.9	0.53

Table 2. Mean and standard deviation, as well as percentage difference and p-values, of body habitus ($n \geq 15$ in each group) and biochemical parameters (n=8 in each group for adipose, n=12 in each group for liver) of the Control and LMMS mice, measured at sacrifice (p-values <0.05 are in bold).

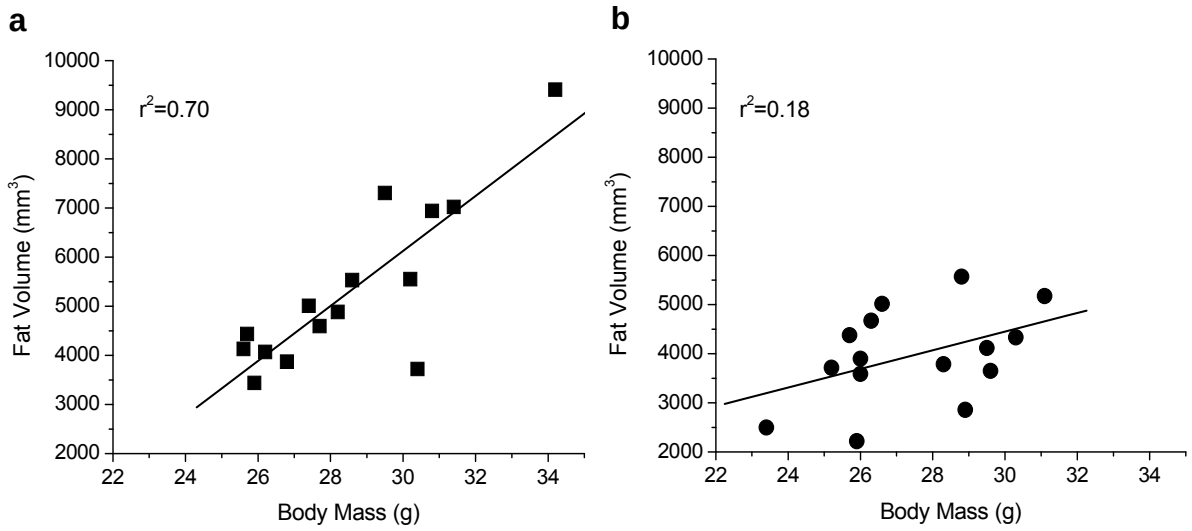

Fig. 15. Fat volume, as a function of body mass, for both the CON (**a**) and LMMS (**b**) mice. While the control animals demonstrated a strong positive correlation between fat volume and weight (R^2 = 0.70; p=0.0001), the correlation in the LMMS animals was weak (R^2 = 0.18; p=0.1). A comparison between slope and intercept shows the control and LMMS conditions to be significantly different (p<0.001). Considered along with the similar food intake between groups, these data indicate that the mechanical signals suppressed adipogenesis. (n=15 in each group).

Correlations between food intake and either total body mass (R^2 = 0.15; p = 0.7) or fat volume (R^2=0.008; p = 0.6) were weak, and indicated that the lower adiposity in LMMS animals could not be explained by differences in food consumption between the groups. While variations in body mass of the CON mice correlated strongly with fat volume (R^2 = 0.70; p = 0.0001), no such correlation was observed in LMMS (R^2 = 0.18; p = 0.1), indicating that fat mass contributed to weight gain in the controls, but failed to account for the increase in body mass in the mechanically stimulated animals (**Fig 15**).

To account for the 1.2g body mass difference between LMMS and CON mice measured at 12w, *in vivo* CT measurements of fat volume were converted to mass equivalents. Using a density of 0.9196 $g \cdot cm^{-3}$ to convert fat volume to fat mass (143) indicated that 3.54g ± 0.9 of the average LMMS mouse mass came from fat (13% of

total mass), while 4.87g ± 1.5 of the mass of the average CON mouse came from fat (17% of total mass). Thus, the lack of fat in the LMMS animals was, in essence, able to account for the "missing mass" between the groups (p=0.01).

Although there was a slight decrease in fasting glucose and insulin levels in the LMMS group (p=0.07), this was not significantly different (**Table 2**). Similarly, there was no significant change in glucose tolerance, insulin signaling or fatty acid oxidation in muscle, liver or adipose tissue (data not shown). However, triglycerides in adipose tissue of LMMS mice were 21.1% (p=0.3) lower than CON, and 39.1% lower in the liver (p=0.02; **Fig 16c, d**). Total non-esterified free fatty acids (NEFA) in adipose tissue were 37.2% less in LMMS mice as compared to CON (p=0.01, **Fig 16e**), while NEFA in the liver of LMMS mice was 42.6% lower (p=0.02) than CON (**Fig 16f**).

Influence of LMMS on the Differentiation of GFP Marrow Cells into Adipocytes: It has recently been reported that the adipogenic precursors in mice are derived from bone marrow stem cells,(138) the presumable site of mechanical signal recognition. Thus, we used GFP-labeled recipient mice to determine if LMMS suppressed adiposity in the growing animal by redirecting bone marrow derived adipogenic stem cells. This was accomplished by examining the production of adipocytes following GFP-labeled bone marrow transplant. Sacrificed following 6w of loading (animal age 15w), the animal mass of LMMS was not significantly different from CON. Flow cytometry demonstrated the ratio of GFP^+ adipocytes in the epididymal fat pad to GFP^+ marrow-based mesenchymal stem cells to be 19% lower (p=0.018) in animals subjected to LMMS relative to controls (CON: 101.2% ± 16.1%; LMMS 82.0% ± 11.1%; **Fig 17**). These data indicating reduced commitment to adipocytes were supported by the weight of the epididymal fat pad following 6w of LMMS, which was 12.2% less than CON (p=0.029).

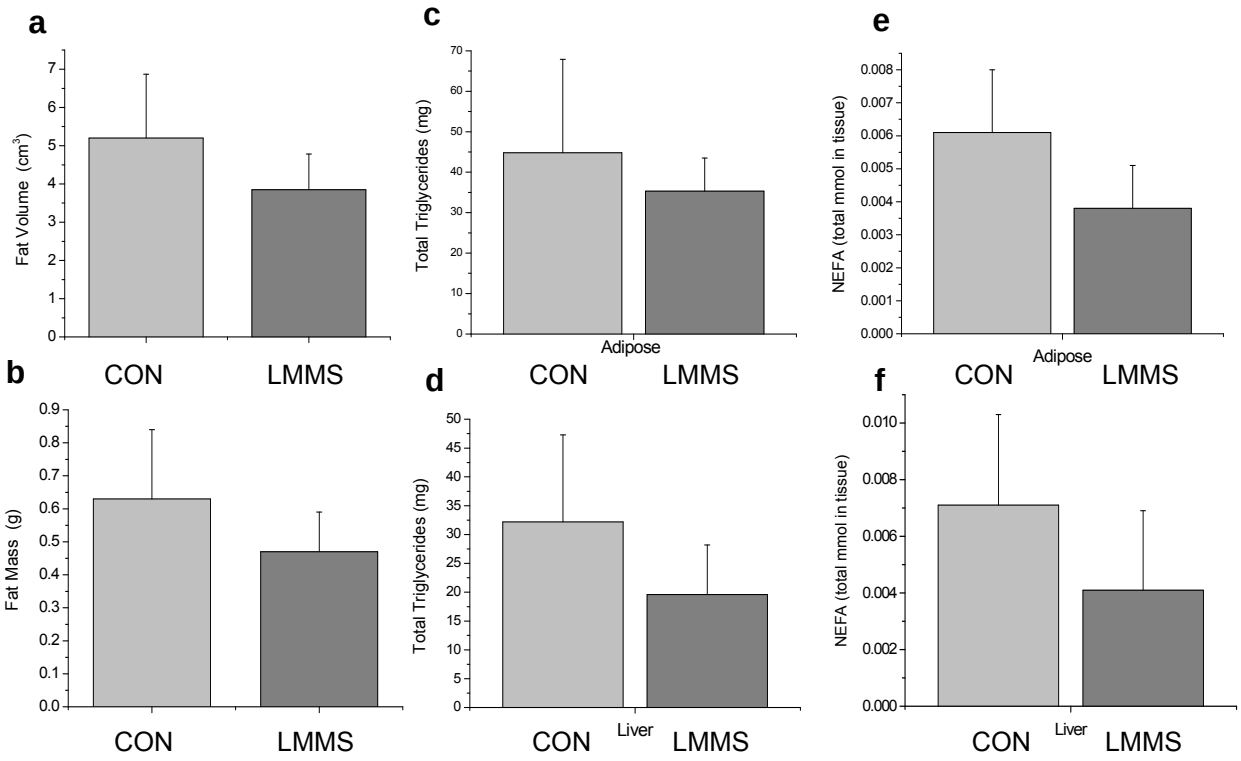

Fig. 16. Mean ± standard deviations of fat volume in the torso of CON and LMMS mice, as measured by *in vivo* microCT (n = 15 each, **a**), as well as the measured mass of the epididymal fat pad (n = 15 each, **b**). Also shown are total triglycerides and non-esterified free fatty acids in adipose tissue (n = 8 each, **c, e**) and TG's and NEFA in liver (n = 12 each, **d, f**). For all comparisons of CON to LMMS, $p<0.05$ except TG in adipose.

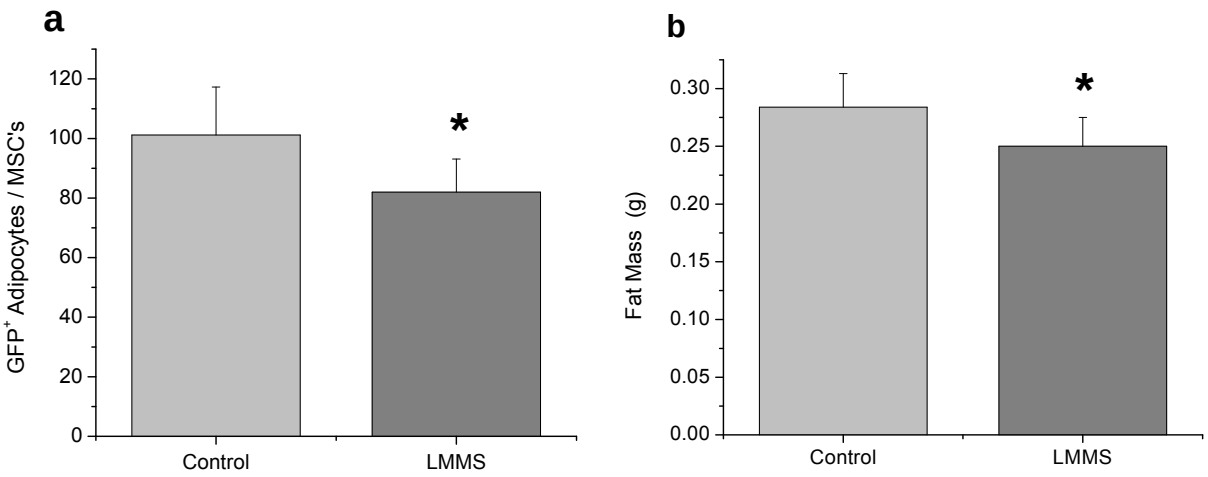

Fig 17. The ratio of GFP^+ adipocytes to GFP^+ mesenchymal stem cells (**a**), to be compared to the weight of the epididymal fat pad (**b**). * signifies $p<0.05$. The significant 19% decrease in this ratio in LMMS animals in part explains a reduced adipose burden as fewer transplanted cells have differentiated into adipocytes.

DISCUSSION

Obese children are more prone to develop type II diabetes(144) and increase their lifetime risk of cardiovascular disease.(145) Overweight adults, not yet even obese, are more susceptible to chronic, debilitating diseases and increased risk of death.(146) While exercise remains the most readily available and generally accepted means of curbing weight gain and the onset of type II diabetes, compliance is poor, and the means by which these metabolic and mechanical cues conspire to suppress adiposity and diabetes are not fully understood. In contrast to the perception that physical signals must be large and endured over a long period of time to offset caloric input and control

insulin production, the results presented here indicate that the cell population(s) and physiologic process(es) responsible for establishing fat mass and, perhaps indirectly, free fatty acid and triglyceride production, are readily influenced by mechanical signals barely large enough to be perceived, an attribute achieved within a short period of time.

The brevity of the signal, and that loading challenge of LMMS is low relative even to normal weightbearing, indicate that the inhibition of adipogenesis is achieved by pathways other than an exercise-mediated increase in metabolic activity. Instead, data from the GFP^+ recipient mice, indicate that the reduced adiposity resulting from LMMS is achieved through influencing the differentiation of adipocytes. Despite a similar diet, it appears that LMMS curbs the gain of fat by "simply" avoiding the creation of adipocytes. There is recent *in vitro* evidence that high levels of mechanical stretch can influence mesenchymal stem cells to drive towards an osteoblastogenic lineage, in preference over adipocytes.(15) Here, in an *in vivo* system, we were able to demonstrate that physical signals need not be large to influence differentiation, and can be delivered non-invasively to influence the phenotype of the entire organism. Certainly, acceleration as a means of delivering mechanical information to a biologic system is an efficient means of notifying a cell population of physical challenges.(68)

In any case, the inhibition of adipogenesis by low-level mechanical signals, considered along with the anabolic potential of these stimuli to bone and muscle, (69) support the presence of a systems-interdependent benefit of exercise, and the systemic consequences of a sedentary lifestyle. Arguably, these data indicate that mesenchymal precursors perceive and respond to these mechanical "demands" as stimuli to differentiate down a musculoskeletal pathway rather than "defaulting" to adipose tissues, and may, to a certain extent, etiologically interconnect age-related increases in obesity, osteopenia and sarcopenia.

In parallel with the lower adiposity realized by LMMS, the production of non-esterified free fatty acids and triglycerides in adipose and liver tissue, key biochemical factors related to type II diabetes, were suppressed. Numerous studies have demonstrated that dyslipidemia can have major negative impact on metabolism, growth and development. In particular, intra-tissue lipid accumulation (liver steatosis) and intra-myocellular lipids have been closely linked to insulin resistance, and is considered the best predictor for the future development of insulin resistance.(147) The ability to suppress adipose tissue expansion by mechanical signals, as well as limit NEFA and triglyceride production, may provide a simple, non-pharmacologic approach to limit obesity in a manner sufficient to prevent the consequences of dyslipidemia.

In summary, our findings indicate that brief exposure to high frequency, low magnitude mechanical signals, inducing forces and accelerations far below those which arise even during walking, markedly suppress adipogenesis, triglyceride and free fatty acid production, and could ultimately provide a unique, non-pharmacologic intervention for the control of obesity and its sequelae, such as type II diabetes. That the signals are so low, and so brief, yet with such striking response in the phenotype of the growing animal, suggest a means of suppressing adipogenesis independent of a metabolic pathway, and that a mechanical signal anabolic to bone may simultaneously inhibit fat production would couple the prevention of obesity to the prevention of osteoporosis.

Chapter 5

PROMOTION OF MESENCHYMAL STEM CELL PROLIFERATION AND DIFFERENTIATION POTENTIAL CAN CIRCUMVENT THE DEVELOPMENT OF DIETARY INDUCED OBESITY BY PROMOTING OSTEOGENESIS

ABSTRACT

Mesenchymal stem cells (MSCs), a population of adult stem cells, are defined by their ability to self-renew and differentiate into the cells forming mesodermal tissues In young male C57BL/6J mice, 6w of extremely low magnitude mechanical signals (LMMS) increased the bone marrow stem cell population by 37% and the number of MSCs by 46% relative to sham controls. Concomitant with the increase in number of stem cells, the differentiation potential of the MSCs was strongly biased towards osteoblastic over adipogenic differentiation, as reflected by Runx2 expression, a key transcription factor in osteoblastogenesis, was upregulated in the bone marrow by 72%, while PPARγ, a gene central to adipogenesis, was downregulated by 27%, paralleled by a 29% increase in the number of osteoprogenitor cells in the marrow space. The ability of LMMS to influence MSC lineage determination was demonstrated in a mouse model of high fat diet induced obesity (DIO), where 14w of LMMS suppressed visceral adipose tissue formation in the torso by 28% while simultaneously increasing trabecular bone volume fraction in the tibia by 11%. The inability of LMMS to *reduce* fat in mice that were already obese indicates that the *prevention* of obesity in DIO was achieved primarily by mechanical influence of developmental pathways. Mechanical modulation of stem cell proliferation and differentiation indicates a unique therapeutic target for tissue regenerative therapy, and represents the basis of a non-pharmacologic strategy to simultaneously prevent obesity and osteoporosis, diseases linked by a common precursor.

INTRODUCTION

Bone marrow houses a diverse population of cells belonging to several lineages, including stem cells of both hematopoietic and mesenchymal origin. Pluripotent mesenchymal stem cells (MSCs) are considered ideal therapeutic targets in regenerative medicine, as they hold the capacity to differentiate into osteoblasts, adipocytes, fibroblasts, chondrocytes, and myocytes. However, the pertinent environmental cues that regulate the lineage selection of MSCs remain largely unknown, making it difficult to harness this potential for clinical application.(79;148;149)

When the bone marrow stem cell population is driven to differentiate towards one cell fate, the establishment of another cell type is inherently suppressed. More specifically, MSCs express small amounts of both adipogenic and osteogenic factors, which cross regulate to retain the cell in an undifferentiated state.(33) When oncostatin, a member of the IL-6 family, is used to promote osteogenesis it simultaneously inhibits adipogenesis.(150) Conversely, anti-diabetic thiazolidinediones such as Rosiglitazone, a potent activator of PPARγ, promotes adipogenesis while suppressing osteogenesis.(138;151;152) Hyper-physiologic levels of tensile strain will increase proliferation of bone marrow cells,(43) and can down-regulate PPARγ in the local bone marrow, thus favoring osteoblastogenesis over adipogenesis.(15) These examples indicate an inversely coupled relationship of adipocytes and osteoblast differentiation, as dependent on fate decisions of their common precursor, the MSC.

The potential to harness MSCs as a means of prevention and treatment of disease is dependent on an improved understanding of the means by which exogenous signals regulate their activity, and the ability of these stimuli to influence either/both proliferation and differentiation.(123) Pharmacologic enhancement of stem cell proliferation has recently been demonstrated *in vivo*,(153) while extremely low

magnitude mechanical signals (LMMS) were shown to suppress adipogenesis in the growing animal without the use of drugs.(93) Utilizing a model of dietary induced obesity (DIO), the work presented here demonstrates that non-invasive mechanical signals can markedly elevate the total number of stem cells in the marrow, and can bias their differentiation towards osteoblastogenesis, resulting in both an increase in bone density and less visceral fat. A pilot trial on young osteopenic women provides preliminary evidence that the therapeutic potential of low magnitude mechanical signals can be translated to the clinic, with an enhancement of bone and muscle mass, and a concomitant suppression of visceral fat formation.

METHODS

Animal Model to Prevent Diet Induced Obesity. All animal procedures were reviewed and approved by the Stony Brook University animal care and use committee. The overall experimental design consisted of two similar protocols, differing in the duration of treatment to assess mechanistic responses of cells to LMMS (6w of LMMS compared to control, n=8 per group) or to characterize the phenotypic effects (14w of LMMS compared to control). Two models of DIO were employed: 1. to examine the ability of LMMS to prevent obesity, a “Fat Diet” condition (n=12 each, LMMS and CON) was evaluated where LMMS and DIO were initiated simultaneously, and 2. to examine the ability of LMMS to reverse obesity, an “Obese” condition (n=8 each, LMMS and CON) was established, whereby LMMS treatment commenced 3 weeks after the induction of DIO, and compared to sham controls.

Mechanical Enhancement of Stem Cell Proliferation and Differentiation in DIO. Beginning at 7w of age, C57BL/6J male mice were given free access to a high fat diet (45% kcal fat, # 58V8, Research Diet, Richmond, IN). The mice were randomized into two groups defined as LMMS (5d/w of 15min/d of a 90Hz, 0.2g mechanical signal, where 1.0g is earth's gravitational field, or 9.8m/s^2), and placebo sham controls (CON). The LMMS protocol(93) provides low magnitude, high frequency mechanical signals by a vertically oscillating platform,(140) and generates strain levels in bone tissue of less than five microstrain, several orders of magnitude below peak strains generated during strenuous activity.(154) Food consumption was monitored by weekly weighing of food.

Status of MSC Pool by Flow Cytometry. Cellular and molecular changes in the bone marrow resulting from 6w LMMS (n=8 animals per group, CON or LMMS) were determined at sacrifice from bone marrow harvested from the right tibia and femur (animals at 13w of age). Red blood cells in the bone marrow aspirate were removed by room temperature incubation with Pharmlyse (BD Bioscience) for 15 mins. Single cell suspensions were prepared in 1% sodium azide in PBS, stained with the appropriate primary and (when indicated) secondary antibodies, and fixed at a final concentration of 1% formalin in PBS. Phycoerythrin (PE) conjugated rat anti-mouse Sca-1 antibody and isotype control were purchased from BD Pharmingen and used at 1:100. Rabbit anti-mouse Pref-1 antibody and FITC conjugated secondary antibody were purchased from Abcam (Cambridge, MA) and used at 1:100 dilutions. Flow cytometry data was collected using a Becton Dickinson FACScaliber flow cytometer (San Jose, CA).

RNA Extraction and Real-Time RT-PCR. At sacrifice, the left tibia and femur were removed and marrow flushed into an RNAlater solution (Ambion, Foster City, CA). Total RNA was harvested from the bone marrow using a modified TRIspin protocol. Briefly,

TRIzol reagent (Life Technologies, Gaithersburg, MD) was added to the total bone marrow cell suspension and the solution homogenized. Phases were separated with chloroform under centrifugation. RNA was precipitated via ethanol addition and applied directly to an RNeasy Total RNA isolation kit (Qiagen, Valencia, CA). DNA contamination was removed on column with RNase free DNase. Total RNA was quantified on a Nanodrop spectrophotometer and RNA integrity monitored by agarose electrophoresis. Expression levels of candidate genes was quantified using a real-time RT-PCR cycler (Lightcycler, Roche, IN) relative to the expression levels of samples spiked with exogenous cDNA.(155) A "one-step" kit (Qiagen) was used to perform both the reverse transcription and amplification steps in one reaction tube.

qRT-PCR with Content Defined 96 Gene Arrays. PCR arrays were obtained from Bar Harbor Biotech (Bar Harbor, ME), with each well of a 96 well PCR plate containing gene specific primer pairs. The complete gene list for the osteoporosis array can be found at www.bhbio.com, and include genes that contribute to bone mineral density through bone resorption and formation, genes that have been linked to osteoporosis, as well as biomarkers and gene targets associated with therapeutic treatment of bone loss. cDNA samples were reversed transcribed (Message Sensor RT Kit, Ambion, Foster City, CA) from total RNA harvested from bone marrow cells and used as the template for each individual animal. Data were generated using an Applied Biosystems 7900HT real-time PCR machine, and analyzed by Bar Harbor Biotech.

Body Habitus Established by *In Vivo* Micro-Computed Tomography (µCT)

Phenotypic effects of DIO, for both the "prevention" and "reversal" of obesity test conditions were defined after 12 and 14w of LMMS. At 12w, *in vivo* µCT scans were used to establish fat, lean, and bone volume of the torso (VivaCT 40, Scanco Medical,

Bassersdorf, Switzerland). Scan data was collected at an isotropic voxel size of 76 μm (45 kV, 133 μA, 300-ms integration time), and analyzed from the base of the skull to the distal tibia for each animal. Threshold parameters were defined during analysis to segregate and quantify fat and bone volumes. Lean volume was defined as animal volume that is neither fat nor bone, and includes muscle and organ compartments. (Refer to Chapter 2). Detailed CT scanning protocol and analysis techniques are reported elsewhere.(101;156)

Bone Phenotype Established by *Ex Vivo* Micro-computed Tomography. Trabecular bone morphology of the proximal region of the left tibia of each mouse was established by μCT at 12μm resolution (μCT 40, Scanco Medical, SUI). The metaphyseal region spanned 600 μm, beginning 300μm distal to the growth plate. Bone volume fraction (BV/TV), connectivity density (Conn.D), trabecular number (Tb.N), trabecular thickness (Tb.Th), trabecular separation (Tb.Sp), and the structural model index (SMI) were determined.

Serum and Tissue Biochemistry. Blood collection was performed after overnight fast by cardiac puncture with the animal under deep anesthesia. Serum was harvested by centrifugation (14,000 rpm, 15 min, 4°C). Mice were euthanized by cervical dislocation, and the different tissues (i.e., epididymal fat pad and subcutaneous fat pads from the lower torso, liver, and heart) were excised, weighed, frozen in liquid nitrogen, and stored at -80°C. Total lipids from white adipose tissue (epididymal fat pad) and liver were extracted and purified based on a chloroform–methanol extraction. Total triglycerides (TG) and non-esterified free fatty acids (NEFA) were measured on serum (n=10 per group) and lipid extracts from adipose tissue (n=5 or 6 per group) and liver (n=10 per group) using enzymatic colorimetric kits (TG Kit from Sigma, Saint Louis, MO; and NEFA

C from Wako Chemicals, Richmond, VA). ELISA assays were utilized to determine serum concentrations of leptin, adiponectin, resistin (all from Millipore, Chicago, IL), osteopontin (R&D Systems, Minneapolis, MN), and osteocalcin (Biomedical Technologies Inc, Stoughton, MA), using a sample size of n=10 per group.

Statistical analyses. All data are shown as mean ± standard deviation, unless noted. To determine significant differences between LMMS and CON groups, two tailed t-tests (significance value set at 5%) were used throughout. Animal outliers were determined based on animal weight at baseline (before the start of any treatment) as animals falling outside of two standard deviations from the total population, or in each respective group at the end of 6 or 14 weeks LMMS (or sham CON) by failure of the Weisberg one-tailed t-test (alpha = 0.01), regarded as an objective tool for showing consistency within small data sets.(157) No outliers were identified in the 6w CON and LMMS groups. Two outliers per group (CON and LMMS) were identified in the Fat Diet model (14w LMMS study) and removed. Data from these animals were not included in any analyses, resulting in a sample size of n=10 per group for all data, unless otherwise noted. No outliers were identified in the 14w Obese model (n=8).

RESULTS

Bone marrow stem cell population is promoted by LMMS. Flow cytometric measurements using antibodies against Stem Cell Antigen-1 (Sca-1) indicated that in animals in the “prevention” DIO group, 6w of LMMS treatment significantly increased the overall stem cell population relative to controls, as defined by cells expressing Sca-1.

Analysis focused on the primitive population of cells with low forward (FSC) and side scatter (SSC), indicating the highest Sca-1 staining for all cell populations. Cells in this region demonstrated a 37.2% (p=0.028) increase in LMMS stem cell numbers relative to sham CON animals. Mesenchymal stem cells as represented by cells positive for Sca-1 and Preadipocyte Factor-1 (Pref-1),(79) represented a much smaller percentage of the total cells. Identified in this manner, in addition to the increase in the overall stem cell component, LMMS treated animals had a 46.1% (p=0.022) increase in mesenchymal stem cells relative to CON (**Fig 18**).

LMMS biases marrow environment and lineage commitment towards osteogenesis. After six weeks, cells expressing only the Pref-1 label, considered committed preadipocytes, were elevated by 18.5% (p=0.25) in LMMS treated animals relative to CON (**Fig 19**). Osteoprogenitor cells in the bone marrow population, identified as Sca-1 positive with high FSC and SSC,(158) were 29.9% greater (p=0.23) greater when subject to LMMS. This trend indicating that differentiation in the marrow space of LMMS animals had shifted towards osteogenesis was confirmed by gene expression data, which demonstrated that transcription of Runx2 in total bone marrow isolated from LMMS animals was upregulated 72.5% (p=0.021) relative to CON. In these same LMMS animals, expression of PPARγ was downregulated by 26.9% (p=0.042) relative to CON (**Fig 20**).

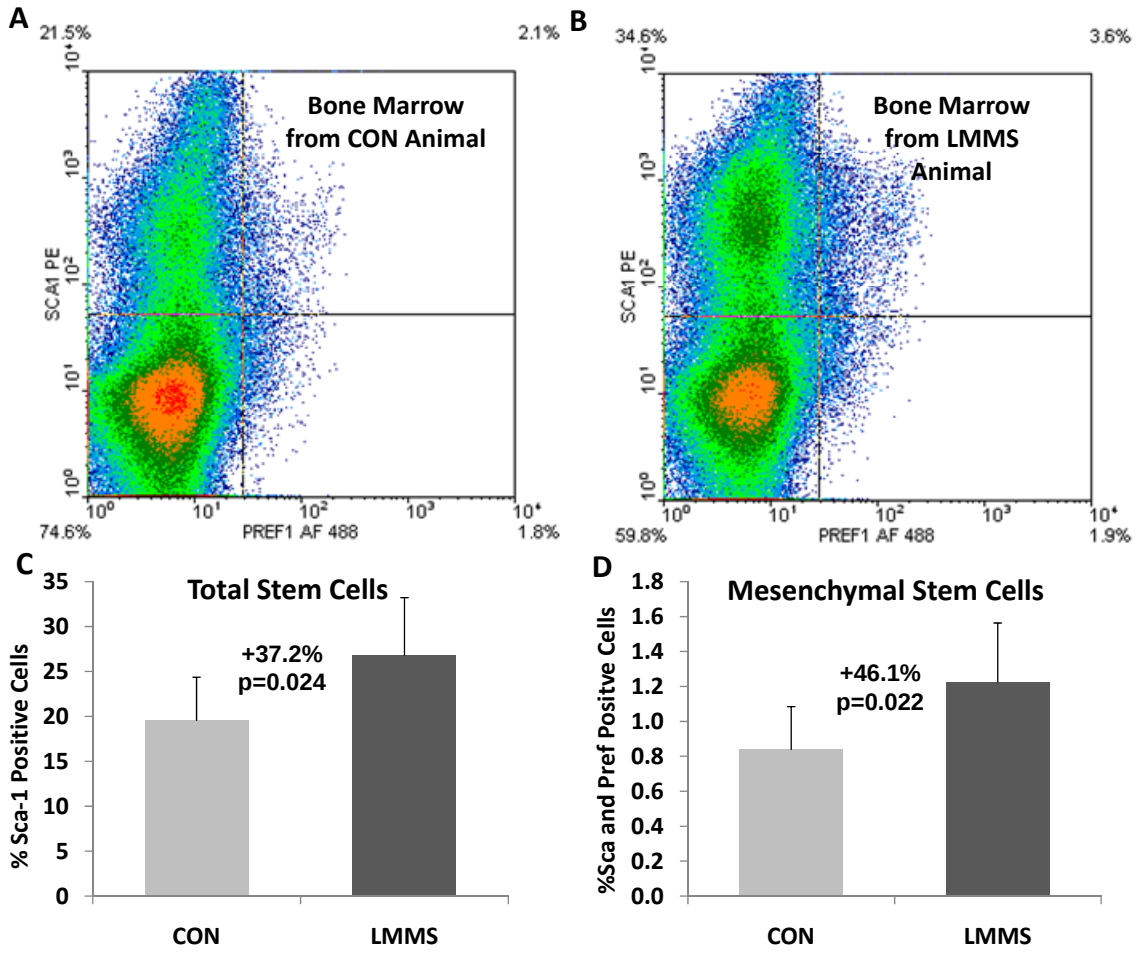

Fig 18. As compared to Control animals (A), low level mechanical signals increase the number of stem cells in the bone marrow of LMMS animals (B). Representative dot plots from flow cytometry experiments indicate the ability of LMMS to increase the number of stem cells in general (Sca-1 single positive, upper quadrants), and MSCs specifically (both Sca-1 and Pref-1 positive, upper right quadrant). The actual increase in total stem cell number was calculated as % positive cells/total cells for the cell fraction showing highest intensity staining (C). The effect of LMMS enhancement of MSC proliferation is even greater (D).

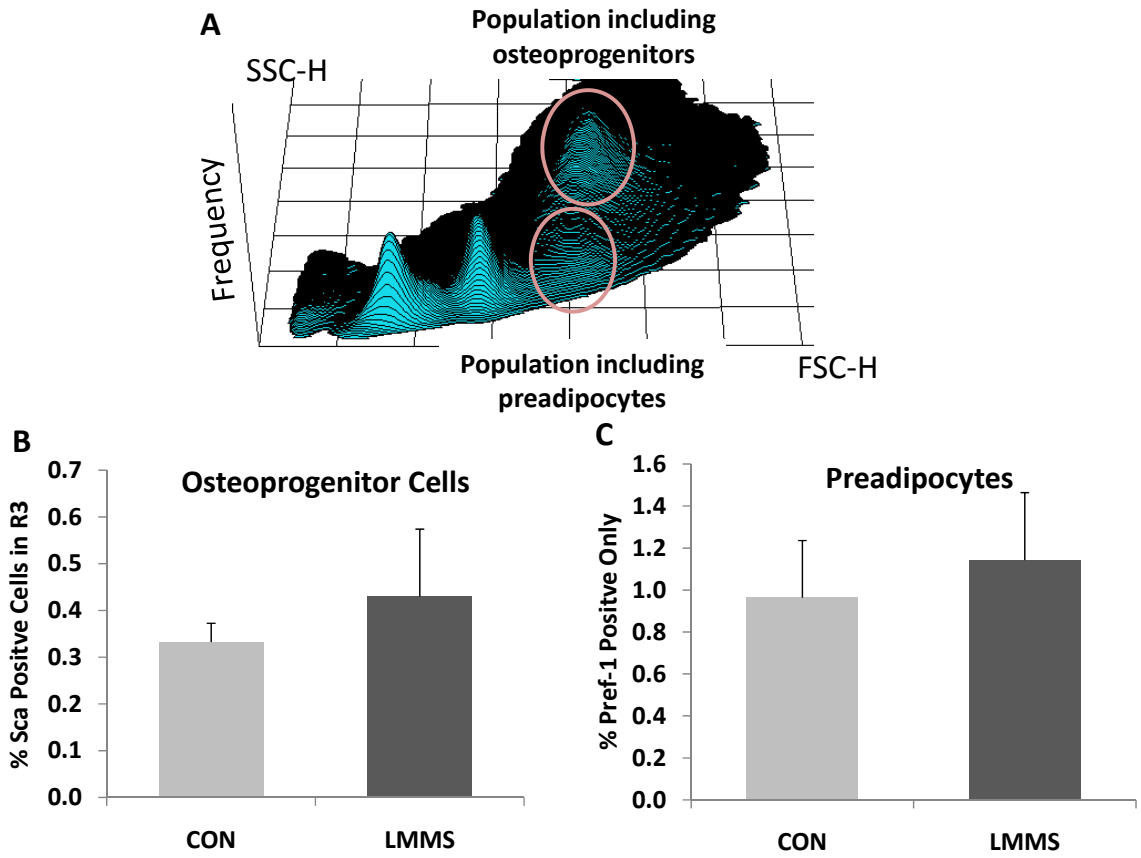

Fig 19. LMMS influences on stem cells was focused on the distinct cell populations identified in flow cytometry (A), with stem cells being identified as low forward (FSC) and side (SSC) scatter. Osteoprogenitor cells were identified as Sca-1(+) cells, residing in the region highlighted as high FSC and SSC, and were 29.9% (p=0.23) more abundant in the bone marrow of LMMS treated animals (B). The preadipocyte population, identified as Pref-1 (+), Sca-1 (-), demonstrated a trend (+18.5%; p=0.25) towards an increase in LMMS relative to CON animals (C).

Gene expression data on bone marrow samples were also tested on a 96 gene "osteoporosis" array, which included genes that contribute to bone mineral density through bone resorption and formation, and genes that have been linked to osteoporosis through association studies. Samples for both CON and LMMS groups expressed 83 of the 94 genes present on the array. qRT-PCR arrays reported decreases in genes such as Pon1 (paraoxonase-1), is known to be associated with high density lipoproteins (-137%, p = 0.263), and sclerostin (-258%, p=0.042), which antagonizes bone formation

by acting on Wnt signaling.(159) Genes such as estrogen related receptor (Esrra; +107%, p=0.018) and Pomc-1 (pro-opiomelanocortin, +68%, p=0.055) were up-regulated by LMMS.

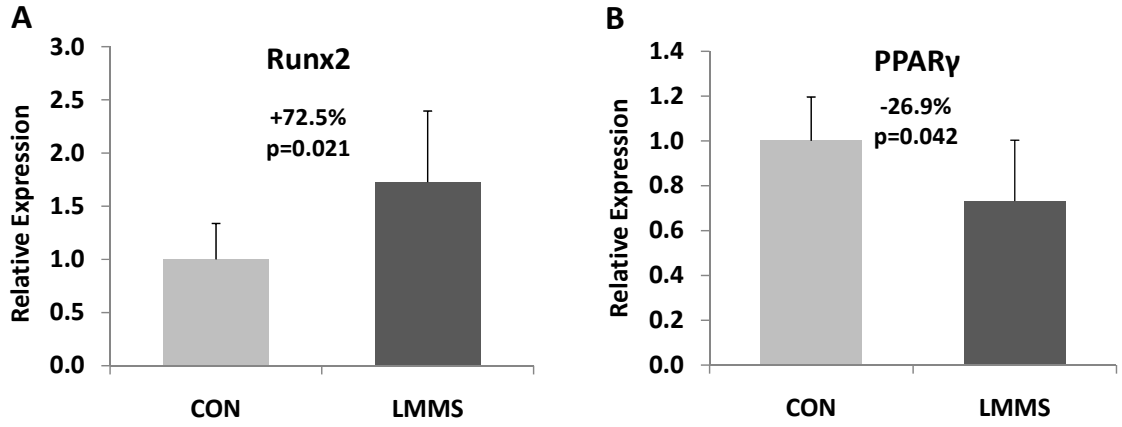

Fig 20. LMMS shifts the bone marrow environment towards osteogenesis. Real Time RT-PCR analysis of bone marrow samples harvested from animals subject to 6 weeks LMMS treatment of sham control indicated a significant upregulation of the osteogenic gene Runx2 (A) and downregulation of the adipogenic gene PPARγ (B).

LMMS enhancement of bone quantity and quality. The ability of LMMS induced changes in proliferation and differentiation of MSCs to elicit phenotypic changes in the skeleton was first measured at 12w by *in vivo* μCT scanning of the whole mouse (neck to distal tibia). Animals subject to LMMS showed a 7.3% (p=0.055) increase in bone volume fraction of the axial and appendicular skeleton (BV/TV) over sham CON. Post-sacrifice, 12 μm resolution μCT scans of the isolated proximal tibia of the LMMS animals showed 11.1% (p=0.024) greater bone volume fraction than CON (**Fig 21**). The micro architectural properties were also enhanced in LMMS as compared to CON, as evidenced by 23.7% greater connectivity density (p=0.037), 10.4% higher trabecular

number (p=0.022), 11.1% smaller separation of trabeculae (p=0.017) and a 4.9% lower structural model index (SMI, p=0.021; **Table 3**).

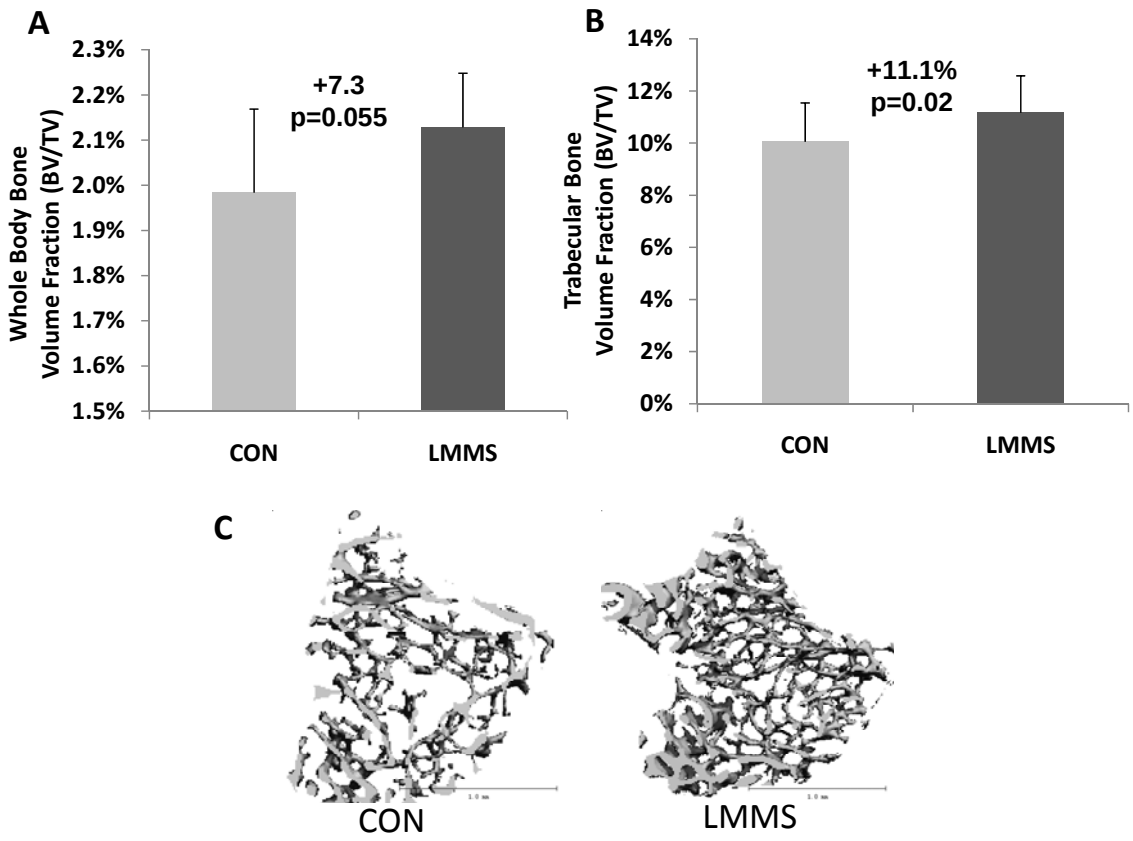

Fig 21. Bone volume fraction, as measured *in vivo* by low resolution μCT, indicated that LMMS increased bone volume fraction across the entire torso of the animal (A). Post-sacrifice, high resolution CT of the proximal tibia indicated a significant increase in trabecular bone density (B). As compared to controls (C), representative μCT reconstructions at the proximal tibia indicate the enhanced morphological properties of LMMS animals (D).

	CON	LMMS	% diff	p-value
Conn.D ($1/mm^3$)	105.3 ± 34.2	130.3 ± 28.9	**23.7**	**0.037**
Tb.N (1/mm)	3.06 ± 0.45	3.38 ± 0.37	**10.4**	**0.022**
Tb.Th (mm)	0.029 ± 0.001	0.030 ± 0.001	1.0	0.398
Tb.Sp (mm)	0.304 ± 0.046	0.270 ± 0.035	**-11.1**	**0.017**
SMI	2.93 ± 0.22	2.78 ± 0.14	**-4.9**	**0.021**

Table 3. Micro-architectural parameters of trabecular bone in fat diet animals measured at 14w (mean ± s.d., n=10) demonstrate the enhanced structural quality of bone in the proximal tibia of LMMS treated animals as compared to controls.

Prevention of obesity by LMMS: At 12w, neither body mass gains nor the average weekly food intake differed significantly between the LMMS or CON groups (**Table 4**). At this point, (19w of age), CON weighed 32.9g ± 4.2g, while LMMS mice were 6.8% lighter at 30.7g ± 2.1g (p=0.15). CON were 15.0% heavier than mice of the same strain, gender and age that were fed a regular chow diet, (93) and increase in body mass due to high fat feeding was comparable to previously reported values. (160) Adipose volume from the abdominal region (defined as the area encompassing the lumbar spine) was segregated as either subcutaneous or visceral adipose tissue (SAT or VAT, respectively). LMMS animals had 28.5% (p=0.021) less VAT by volume, and 19.0% (p=0.016) less SAT by calculated volume. Weights of epididymal fat pads harvested at sacrifice (14w) correlated strongly with fat volume data obtained by CT. The epididymal fat pad weight was 24.5% (p=0.032) less in LMMS than CON, while the subcutaneous fat pad at the lower back region was 26.1% (p=0.018) lower in LMMS (**Table 4**).

	CON	LMMS	% diff	p-value
Animal Weight at 12 weeks (grams)	32.9 ± 4.12	30.7 ± 2.74	-6.8	0.152
Weekly Food Consumption (grams)	18.9 ± 1.57	18.5 ± 1.47	-2.5	0.406
Visceral Adipose Tissue (VAT, cm^3)	2.3 ± 0.72	1.6 ± 0.34	**-28.5**	**0.021**
Subcutaneous Adipose Tissue (SAT, cm^3)	0.84 ± 0.16	0.68 ± 0.08	**-19.0**	**0.016**
Epididymal Fat Pad (grams)	1.85 ± 0.52	1.40 ± 0.32	**-24.5**	**0.032**
Subcutaneous Fat Pad (grams)	0.67 ± 0.17	0.50 ± 0.12	**-26.1**	**0.018**
Liver (grams)	0.99 ± 0.16	0.94 ±0.07	-4.9	0.399

Table 4: Despite similar body mass and weekly food consumption, phenotypic parameters of the fat diet animals after 12w of LMMS or at sacrifice (14w, mean ± s.d., n=10) demonstrate a leaner body habitus, as the adipose burden (visceral and subcutaneous fat) is significantly lower in the LMMS animals.

LMMS prevents increased biochemical indices of obesity. Triglycerides (TG) and non-esterified free fatty acids (NEFA) measured in plasma, epididymal adipose tissue, and liver were all lower in LMMS as compared to CON (**Table 5**). Liver TG levels decreased by 25.6% (p=0.19) in LMMS animals, paralleled by a 33.0% (p=0.022) decrease in NEFA levels. Linear regressions of adipose and liver TG and NEFA values to μCT visceral volume (VAT) demonstrated strong positive correlations for CON animals, with R^2 =0.96 (p=0.002) for adipose TG, R^2 =0.85 (p=0.027) for adipose NEFA, R^2 =0.64 (p=0.006) for liver TG and R^2 =0.80 (p=0.003) for liver NEFA (**Fig 22**). LMMS resulted in weaker correlations between all TG and NEFA levels to increases in VAT.

	CON	LMMS	% diff	p-value
TG Liver (total mg)	31.8 ± 14.3	23.6 ± 12.7	-25.6	0.195
NEFA Liver (total mol)	7.5 ± 2.7	5.0 ± 1.5	**-33.0**	**0.022**
TG Adipose (total mg)	91.6 ± 34.6 (n=5)	72.9 ± 18.1 (n=6)	-20.4	0.321
NEFA Adipose (total mmol)	18.1 ± 5.8 (n=5)	15.3 ± 2.4 (n=6)	-15.8	0.345
TG Serum (mg/dl)	46.2 ± 17.0	47.0 ± 18.4	1.6	0.928
NEFA Serum (mmol/l)	0.68 ± 0.10	0.64 ± 0.14	-5.3	0.526
Leptin Serum (ng/mL)	15.9 ± 7.2	10.1 ± 4.7	**-37.6**	**0.049**
Resistin Serum (ng/mL)	4.3 ± 1.2	3.6 ± 1.0	-15.8	0.200
Adiponectin Serum (μg/mL)	9.2 ± 1.7	7.0 ± 1.4	**-23.5**	**<0.01**
Osteopontin Serum (ng/mL)	197.8 ± 22.8	183.0 ± 39.6	-7.5	0.409
Osteocalcin Serum (ng/mL)	55.7 ± 17.2	47.6 ± 7.8	-14.6	0.218

Table 5: Biochemical parameters of the fat diet animals (mean ± s.d., n=10) highlight lower level of TG, NEFA, and circulating adipokines following 14w of LMMS stimulation as compared to controls.

At sacrifice, fasting serum levels of adipokines were lower in LMMS as compared to CON. Circulating levels of leptin were 35.3% (p=0.05) lower, adiponectin was 21.8% (p=0.009) lower, and resistin was 15.8% lower (p=0.26) than CON (**Table 5**). Circulating serum osteopontin (-7.5%, p=0.41) and osteocalcin (-14.6%, p=0.22) levels were not significantly affected by the mechanical signals.

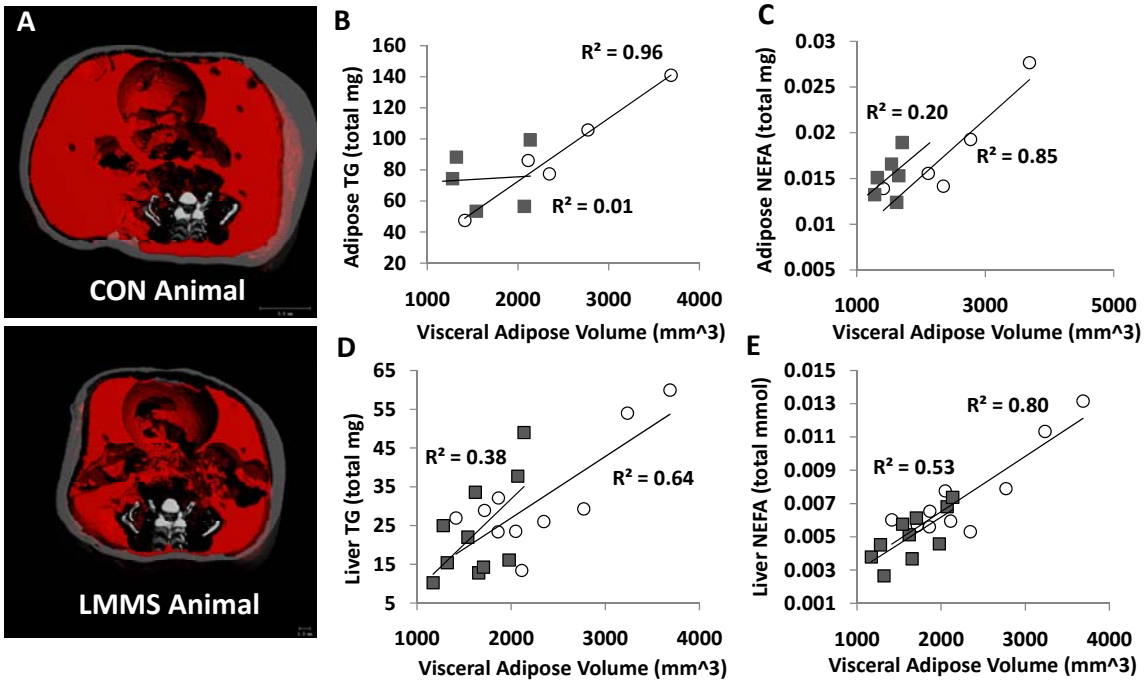

Fig 22. *In vivo* µCT images used to discriminate visceral and subcutaneous adiposity in the abdominal region of a CON and LMMS animal (A). Visceral fat is shown in red, subcutaneous fat in gray (A). Linear regressions of calculated visceral adipose tissue (VAT) volume against adipose and liver biochemistry values demonstrated strong positive correlations in CON, and weak correlations in LMMS, as well as generally lower levels for all LMMS biochemical values. N=6 for adipose (B), N=10 for liver (C,D). Regressions for adipose TG (p=0.002), adipose NEFA (p=0.03), liver TG (p=0.006) and liver NEFA (p=0.003) were significant for CON animals, but only liver NEFA (p=0.02) was significant for LMMS. Overall, LMMS mice exhibited lower, non-significant correlations in liver TG (p=0.06), adipose TG (p=0.19), and adipose NEFA (p=0.37) to increases in visceral adiposity. CON =○, LMMS = ■

LMMS fails to reduce existing adiposity. In the "reversal" model of obesity, 4w old animals were started on a high fat diet for 3w prior to beginning the LMMS protocol at 7w of age. These "obese" animals were on average 3.7 grams heavier ($p < 0.001$) than chow fed regular diet animals (baseline) at the start of the protocol. The early-adolescent obesity in these mice translated to adulthood, such that by the end of the 12w protocol, they weighed 21% more than the CON animals who begun the fat diet at 7w of age ($p < 0.001$). In stark contrast to the "prevention" animals, where LMMS realized a 22.2% ($p=0.03$) lower overall adipose volume relative to CON (distal tibia to the base of the skull), no differences were seen for fat (-1.1%, $p=0.92$), lean (+1.3%, $p=0.85$), or bone volume (-0.2%, $p=0.94$) between LMMS and sham control groups after 12w of LMMS for these already obese mice (**Fig 23**).

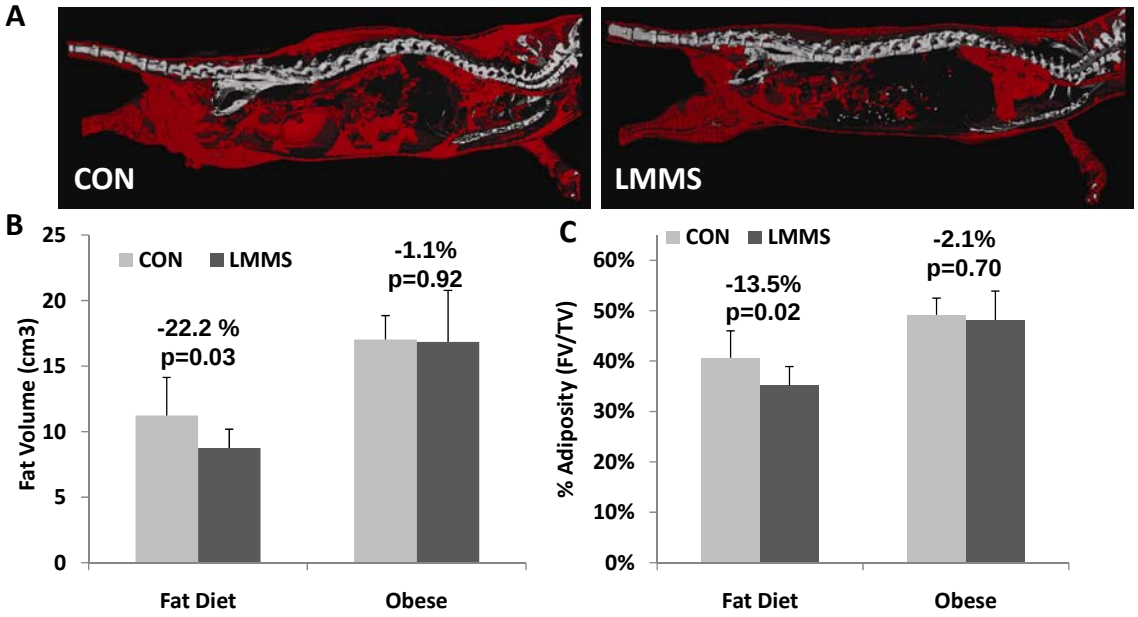

Fig 23. Suppression of the obese phenotype was achieved to a degree by stem cells preferentially diverting from an adipogenic lineage. Reconstructed *in vivo* μCT images of total body fat (red; A) indicate that following 12w, animals which began LMMS at the time that the high fat diet was introduced exhibited 22.2% less fat volume as compared to control. In contrast, animals allowed a high fat diet for 4w prior to LMMS failed to demonstrate any reduction of fat volume (B). Shown as a relative percentage of fat to total animal volume, LMMS reduced the percent animal adiposity by 13.5% (p=0.017), while the lack of a response in the already obese animals reinforces a conclusion that the mechanical signal works primarily at the stem cell development level, as existing fat is not metabolized by LMMS stimulation.

DISCUSSION

The experiments reported here indicate that extremely low magnitude mechanical signals, well below those generated during locomotion, will promote the number of stem cells residing in the marrow. Further, these subtle mechanical signals biased the differentiation of the MSC cohort towards osteoblastogenesis over adipogenesis, such that obesity was prevented while the formation of bone was simultaneously promoted. These data provide support for the growing body of evidence of an inversely coupled

relationship between pre-osteoblasts and pre-adipocytes in the marrow cavity, and osteogenesis and adipogenesis overall.(4)

Cell surface expression of Sca-1 was used to give a general indication of the status of the bone marrow cell population, representing both HSCs and MSCs. The relative increase in the overall bone marrow stem cell population induced by LMMS reflected an enhancement of stem cells of both hematopoietic and mesenchymal lineages. The method utilized for bone marrow harvesting (flushing of bones) does not remove the significant portion (33%) of hematopoietic stem cells (HSCs) that resides in proximity to the endosteal surface of the bone,(161) and thus the influence of LMMS on HSC's is likely underestimated in this model. Cells expressing both Sca-1 and Pref-1 are more specific in identifying mesenchymal stem cells, and while accordingly these cells occur less frequently, this population demonstrated a larger increase in response to LMMS than that measured in the overall stem cell population. In all, these data indicate that the stem cell pool has been positively influenced by mechanical signals, resulting in an increase in total number of cells.

At the molecular level, LMMS induced a clear shift in the biological balance of key osteogenic and adipogenic factors, including a marked increase in the expression levels of Runx2, and a significant decrease in the level of PPARγ. Together, this change in balance would conspire to push stem cells in the undifferentiated state preferentially towards the formation of bone and away from fat.(4) PPARγ activation has been shown to change marrow structure and function by decreasing the multipotential character of mesenchymal stem cells.(152) Reduced levels of PPARγ are known to be permissive to osteoblastogenesis and lead to higher trabecular bone volume,(162) by promoting the osteoblastic lineage decision of MSCs.(163) Data from the PCR arrays highlights that – despite the marked changes in bone and fat phenotype, relatively few genes have changed expression in response to the LMMS, emphasizing that the adaptive response

of the organism is quite subtle, particularly when considered relative to repair.(164) That said, those genes that were upregulated (i.e. Esrra, Pomc1) have been shown to be osteogenic and/or protective of obesity, while those genes that were down-regulated (ie. sclerostin, Pon1) are related to osteoclast and lipid activity. While the full mechanistic pathway by which LMMS is sensed and transduced in the bone marrow environment is as of yet undetermined, the data indicate that genes implicated in signaling cascades controlling bone development are up-regulated, and those influencing adipose development are down-regulated, all by a physical signal transduced to the marrow.

While not statistically significant, the increased percentage of cells in the osteoprogenitor and preadipocyte populations in bone marrow from the LMMS animals showed trends which support a conclusion that lineage selection of cells has been altered by the mechanical signal. There is evidence suggesting that preadipocytes, through expression of the plasma membrane protein Pref-1, are responsive to differentiation signals from the extracellular environment,(165) with Pref-1 expression actually being *inhibitory* of adipogenesis and terminal adipocyte differentiation.(166) The ultimate fate of marrow preadipocytes and their ability to migrate to other adipose tissue depots has not been definitively addressed and ultimately may highlight the inherent difficulty in harnessing stem cell plasticity as a therapeutic endpoint.(167;168)

While the influence of LMMS has been evaluated in bone marrow derived stem cells, it is important to recognize that the mechanical signal is delivered systemically and thus does not preclude other cell populations from being subject to the stimulus. Indeed, we do not categorically conclude that the phenotypic changes measured in fat and bone are exclusively the result of regulating the bone marrow stem cell population, and changes in visceral fat, etc., may be through influencing other stem cell populations. What is apparent, however, is that LMMS increases the size of the precursor pool, and biases them away from adipogenesis and towards higher order connective tissues. We

believe these data support a conclusion that the mechanical biasing of MSC lineage selection towards osteoblastogenesis inherently suppresses adipogenesis because the stem cell can only make a “single pathway” commitment. Indeed, even though adipose tissue mass was more than twenty percent greater in the controls relative to the LMMS animals, animal weights differed by less than seven percent, as the reduced fat mass of the LMMS animals was to a degree, compensated by the increase in bone mass, and further emphasized the binary nature of the differentiation process.

While these data indicate a critical role of development in obesity, they do not preclude an influence on the overall metabolic state of the animal, as increased adiposity alters the systemic physiology by changing the endocrine and metabolic state of the fat tissue.(105) The marked disparities of fat mass measured between control and LMMS groups will inevitably influence their susceptibility to the metabolic consequences of obesity, particularly considering the capacity of LMMS to suppress visceral adipose tissue (VAT). VAT is an important risk factor to metabolic complications which afflict the obese, with adiposity positively correlating with fasting plasma insulin, triglyceride (TG), low-density lipoprotein (LDL) and apolipoprotein B (apo B) levels, as well as the cholesterol (CHOL)/high-density lipoprotein (HDL)-CHOL ratio.(83) Increased abdominal adiposity is also known to be a significant risk factor for type 2 diabetes.(80) Control animals presented with these same positive correlations of TG and NEFA levels in adipose tissue and the liver to visceral adipose accumulation, while adipose gains in LMMS treated animals did not translate into proportional increases, suggesting that suppression of adipogenesis and/or adiposity inhibited associated sequelae.

Serum levels of osteopontin were measured to assay systemic changes in bone tissue, as osteopontin is secreted by osteoblasts and acts to activate osteoclasts in the normal process of bone remodeling. Additionally, osteopontin has been reported as a potent constraining factor on hematopoietic stem cell proliferation.(45) That osteopontin

is unaffected by LMMS treatment highlights the general promotion of stem cell proliferation (HSC and MSC), but the specificity of the proposed mechanism to MSC differentiation as biasing the formation of osteoprogenitors did not examine if osteoclasts, which derive from HSCs, were activated. Circulating levels of the key adipokines leptin, adiponectin and resistin are known to be elevated under conditions of DIO, as these molecules are secreted by white adipose tissue. (160;169) Animals with greater adipose volume demonstrate correspondingly higher serum adipokine levels. These molecules each exhibit pleiotropic effects, with implications for inflammatory and immune responses.(170) In light of the similar food intake between groups, the markedly reduced levels of circulating adipokines in LMMS animals may best reflect the reduced adipose burden in these mice.

In evaluating the ability of LMMS to prevent obesity, these data clearly indicate that these mechanical signals were effective at the molecular, cellular and tissue level, as indicated by a distinct bias towards osteogenesis after 6w, translating at 12 and 14w into clear phenotypic differences in bone and fat volume. In contrast, mice allowed to become obese (4w of a high fat diet) before being subject to LMMS indicated not only the inability of these mechanical signals to reverse obesity in animals that were already fat, it failed to influence their bone mass, despite receiving the same mechanical signal as the “prevention” group. This could either mean that the stem cell population in the “pre-obese” mice was already committed towards adipogenesis by the time the mechanical signal was introduced, or that the adipogenic environment catalyzed by a high fat diet supersedes the ability of other exogenous signals to drive MSCs towards specific lineages. Certainly, the inability to coax adipose tissue away from the obese animal emphasizes the starkly different challenges of a developmental strategy to prevent obesity versus the metabolic realities of reversing it. A similar scenario may well be evident in preventing versus reversing age-related bone loss with mechanical signals,

as the deterioration of the marrow based stem cell population which parallels aging may undermine the ability of any intervention to harness the potential of stem cells to treat disease.(171)

Aging animals demonstrate a significant reduction in their stem cell population and their regenerative capacity,(172) while simultaneously predisposing this environment towards adipogenesis in the remaining MSCs.(173) Extending this “aging” related deterioration to disuse, inactivity and microgravity markedly reduce osteoblastogenesis in the MSC pool,(174) while the actual number of osteoprogenitor cells is also severely compromised.(175) Thus, both age and activity are determinants of the viability of the stem cell population, and independently or together may conspire towards a reduced regenerative capacity. This deterioration can be somewhat mitigated by replenishment of the bone marrow stem cell population, either directly or via exposure to a “young” environment, showing promise as a intervention to restore musculoskeletal health.(176;177) When considering this in the context of the data presented here, where LMMS increased bone mass while simultaneously suppressing visceral adiposity, suggests that susceptibility to diseases such as obesity and osteoporosis may be more closely linked than previously thought, due – potentially - to a failure to drive stem cells towards the “right” fate.

It has been estimated that 80% of obese adolescents develop into obese adults,(178) contributing to the conclusion by the American Heart Association that primary prevention is the key to constraining the societal impact,(179) as treatments once an individual is obese are limited. The differential response to LMMS in the two animal models presented herein further highlights this disparity, in that prevention of obesity via developmental control was achievable, but that reversal of an obese state, once cell fate had been pre-determined, was not realized. Rather than a metabolic pathway, these data indicate a developmentally mediated mechanism by which the

suppression of fat and the enhancement of bone is coupled, as linked to mechanical influences on stem cell populations. Indeed, the mechanically mediated increase in the number of progenitor cells, taken together with the ability of these mechanical signals to drive commitment choices, indicates a viable means to enhance an organism's regenerative capacity and reduce susceptibility to disease, achieved by exploiting stem cell sensitivity to physical signals.

Chapter 6

36 WEEKS OF DAILY LMMS TREATMENT PROTECTS AGAINST AGE-RELATED LOSS OF STEM CELLS AND DIET INDUCED FATTY LIVER DIESEASE

ABSTRACT

The increased fragility of the human body in response to aging, including diminished immunity and regenerative capacity, exact great health consequences in the elderly. Further potentiating the negative effects of aging is the increasing prevalence of obesity, which independently compromises the regenerative potential by decreasing the number of stem cells. Herein we characterized the dual effects of both diet and long term LMMS in a mouse model of obesity and aging, and investigated the ability of LMMS to mitigate the loss of stem cells associated with both these pathologies. Suppression of adiposity during DIO is observed in young animals (-20.4%, p=0.05) after 12 wks of LMMS stimulation, but animals equalized over the ensuing 24 wks such that there were no significant differences in fat volume between CON and LMMS groups at 36 wks. However, the benefit of 36 wks of LMMS was seen in the prevention of obesity related hepatomegaly and fatty liver disease. Livers from the CON animals demonstrated an average weight of 2.78 ± 0.30 g whereas livers of LMMS treated animals weighed 1.98 ± 0.61 g, demonstrating a 28.7% (p=0.022) mass reduction. Qualitative histological examination revealed the presence of numerous large lipid deposits infiltrating the hepatocellular space on CON animals, but livers from LMMS animals displayed relatively few and smaller-sized lipid vesicles. Quantitative assays for TG and FFA demonstrated 46.2% (p=0.013) and 42.1% (p=0.020) reductions in LMMS stimulated animals compared to CON. Mechanistically, the protection against fatty liver disease seen in LMMS stimulated animals is perhaps partially explained by the mesenchymal stem cell population, which saw a 36.4% (p=0.039) increase over CON animals. Taken together, these results give preliminary indication of the ability of LMMS to ameliorate the long term health consequences of obesity and the gradual accumulation of damage due to aging by protection of the stem cell population.

INTRODUCTION

Of great health consequence to an aging population is the increased fragility of the human body in response to aging, and the compromised immunity and regenerative capacity. Emerging evidence suggests that diverse tissue-specific stem cell reserves decline with advancing age, with consequences that contribute to accumulation of damage to tissues and organs. (23) Diseases such as Type II osteoporosis result from dysregulated bone remodeling during aging. Anemia and sarcopenia are also likely the result of an imbalance between cell loss and renewal, (180) with the weakening of the musculoskeletal system contributing to a generalized fragile state in older individuals. Another age-related change in physiology contributing to a state of fragility is the change in size and distribution of body fat, with the visceral and subcutaneous fat deposits generally decreasing and marrow fat increasing. The intricate balance of bone and fat development due to the interaction of many factors, as they become altered during aging, all conspire and contribute to the high incidence of both osteoporosis and bone marrow adiposity in elderly subjects. (3) It has been reported that decreases in bone volume correlate to increased bone marrow adiposity. (181) The clinical presentations of old age comprise an entire field of medicine – gerontology, and yet the molecular mechanisms – and hence development of potential palliative treatments – for aging are still not well characterized nor fully realized.

The clear changes in physiology due to aging are driven at the cellular and molecular levels by changes in the various tissues, including the bone marrow derived stem cell populations. MSCs undergo age related changes, underlying a fundamental shift of the marrow environment to a pro-adipocytic program via shifts in TGF-β and BMP signaling pathways. (121) Changes in cell proliferation and signaling result in the diminished capacity of the undifferentiated stem cell population to maintain tissue

homeostasis, and retain their multipotency. Adipocytes which are mostly absent in the bone marrow of young individuals, can come to occupy up to 90% of the bone marrow cavity of older individuals. (182) This metabolically inactive and potentially toxic marrow fat releases adipokines and fatty acids (171) which surely would interact with and further diminish the already altered marrow stem cell population.

Further potentiating the negative effects of aging is the increasing prevalence of obesity, which independently compromises the regenerative potential by decreasing the number of stem cells (Chapter 3). As the number of obese individuals continues to increase, and these individuals begin to age, the long term consequences of excess adiposity and the subsequent acceleration of the otherwise gradual process of age-related accumulation of tissue damage will need to be addressed. At the heart of these changes, both in terms of cause and effect, is the mesenchymal stem cell which becomes an attractive therapeutic target. Even as it gives rise to mature adipocytes and osteoblasts, once differentiated the presence of mature cells can affect the further proliferation and differentiation of the MSC. The ability of low magnitude mechanical stimulation (LMMS) to specifically promote MSC proliferation has been shown in the preceding chapters. Herein we characterized the dual effects of both diet and aging in a mouse model of obesity, and demonstrate the ability of LMMS to mitigate the loss of stem cells associated with these pathologies, providing protection against at least one significant obesity pathology, fatty liver disease.

MATERIALS AND METHODS

Animal Model and Experimental Design. Beginning at 8w of age, single-housed C57BL/6J male mice were given free access to a high fat diet (45% kcal fat, # 58V8,

Research Diet, Richmond, IN), and were randomized into two groups defined as LMMS (5 d/w of 15 min/d of a 90 Hz, 0.2 g mechanical signal) and age-matched sham handled controls (CON). Refer to Chapters 4 and 5 for detailed LMMS protocol. Animal mass and food consumption were monitored weekly.

In vivo μCT scans were used to establish fat, lean, and bone volume of the torso at 12, 24, and 36 wks (VivaCT 40 for 12 and 24 wk time points, VivaCT 75 for 36 wk time point, both systems from Scanco Medical, SUI). Refer to Chapter 2 for detailed CT scanning protocol and analysis techniques. Scan data was collected at low resolution (76-82 μm), and reported fat volumes are based on an analysis region from the neck to the distal tibia for each animal. (101;156)

Serum and Liver Biochemistry. Blood collection was performed after overnight fast by cardiac puncture with the animal under deep anesthesia. Mice were euthanized by cervical dislocation, and the liver was excised, weighed, frozen in liquid nitrogen, and stored at -80°C. Total lipids from liver were extracted and purified based on a chloroform–methanol extraction. Total triglycerides (TG) and non-esterified free fatty acids (NEFA) were measured on total lipid extracts from liver using enzymatic colorimetric kits (TG Kit from Sigma, Saint Louis, MO; and NEFA C from Wako Chemicals, Richmond, VA). An ELISA assay was used to determine serum resistin (Millipore, Chicago, IL).

Flow Cytometry Analysis for Stem Cell Identification. Cellular composition of the bone marrow was determined at sacrifice from bone marrow harvested from the right tibia and femur by flushing. Refer to Chapter 3 for detailed methodology for marrow harvest and preparation. Phycoerythrin (PE) conjugated rat anti-mouse Sca-1 antibody, FITC conjugated rat anti-mouse CD 90.2 (aka Thy 1.2) and isotype controls were

purchased from BD Pharmingen. Flow cytometry data was collected using a Becton Dickinson FACScaliber flow cytometer (San Jose, CA).

Statistical Analysis. All data are shown as mean ± standard deviation, unless noted. To determine significant differences between LMMS and CON groups, two tailed t-tests (significance value set at 5%) were used throughout. Two animals (one from each group, CON and LMMS) were euthanized shortly before the 36 week scan due to some form of dermatitis. No scan data is available for these animals at the last time point. One additional animal from the LMMS group expired during the course of the last scan at 36 weeks due to anesthesia overdose, and the scan data for this animal is reported. Tissue samples were not harvested for these three animals, and the final sample size for all reported *ex-vivo* tissue analyses is n=7 for CON, n=6 for LMMS.

RESULTS

LMMS Slows the Rate of Weight Gain in Long Term Obesity. In a 36 week long study to assess the long term benefits of LMMS treatment to suppress fat accumulation, weekly measurements of animal mass demonstrated that the rate of weight accumulation was decreased by 24.8% (p=0.128) during the first 12 weeks of treatment, and was continually suppressed even as the animals aged. The maximum weight suppression was seen at 18 weeks of LMMS (animals at 25 weeks of age), where animals exhibited a 5.8 g weight difference (p=0.019) between groups. By the end of the 36 week LMMS protocol, treated animals (48.4 ± 4.2 g) were still on average 4.1 grams lighter than sham handled CON animals (52.5 ± 2.3 g, p=0.067) even as the rate of animal growth had decreased by approximately 50% compared to the early time

points for both groups. CON animals consistently ate more on a weekly basis, ($p<0.05$ at wks 8, 16, and 34) compared the LMMS animals. Comparison of the total food consumption during the entire study (sum of weekly averages for the entire 36 wks) demonstrated a 5.7% increase ($p = 0.021$) in total food consumption over LMMS animals.

Inverse Interdependence of Fat and Bone Volumes. Induced by a large caloric excess to develop obesity, the suppression of adipogenesis in LMMS animals was observed in longitudinal microCT scan data collected at 3, 6, and 9 months of the study (**Fig 24a**). Similar to the fat diet data reported in Chapter 5, 12 weeks of LMMS suppressed adipose development in the mouse body by -20.4% ($p=0.05$). After 6 months of high fat feeding, LMMS was still able to reduce the adipose volume by -9.8% ($p=0.15$). Nine months of a high fat diet, coupled with the increased age of the animals, attenuated the initial differences seen between LMMS and CON groups -7.8% ($p=0.13$), confirming that the maximal fat suppression was seen in the earliest phases of LMMS, during the phase of maximal animal development.

MicroCT data analyzed for bone volume from the same scans showed the inverse response, where the largest total body bone volume fraction was measured at 3 months and gradually declined as the animals increased in fat volume. Compared to data at the 3 month time point, the bone volume fraction had decreased by -18.0% ($p<0.001$) by 9 months for the CON animals. Relative to the same 3 month CON value, LMMS was able to protect against some of the age and diet induced bone loss, with treated animals only losing 10.0% ($p=0.042$) bone volume fraction. Comparisons between CON and LMMS at each time point are shown in **Fig 25.**

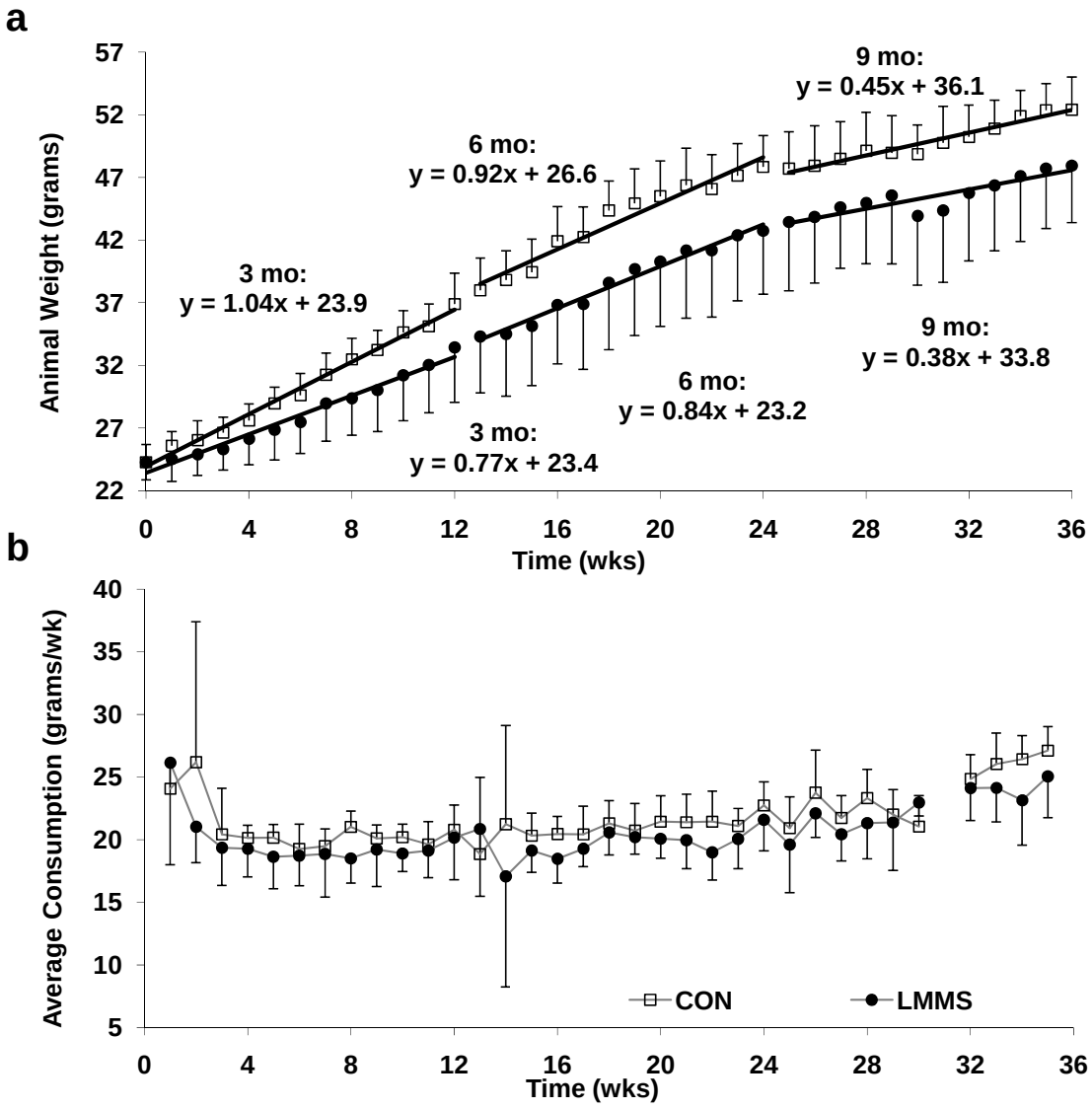

Fig 24. Average weekly animal weights (**a**) and food consumption (**b**) for CON and LMMS animals over the 36 week study period (n=8 per group). Rate of growth was established as the slope of a linear fit line and assessed in 3 month increments to coincide with the longitudinal microCT scans performed at 3, 6 and 9 months, and demonstrated high correlations for both groups of animals (all R^2-values ≥0.95 except for LMMS animals at 9 months R^2 =0.081). LMMS animals demonstrated a trend towards reductions in mass accumulation due to DIO, with 24.8% (p=0.128) suppression in the growth rate during the first 3 months (0 and 12 wks on study). CON animals consistently ate more on a weekly basis, (p<0.05 at wks 8, 16, and 34) and summed for the entire 36 wks demonstrated a 5.7% increase (p = 0.021) in total food consumption over LMMS animals.

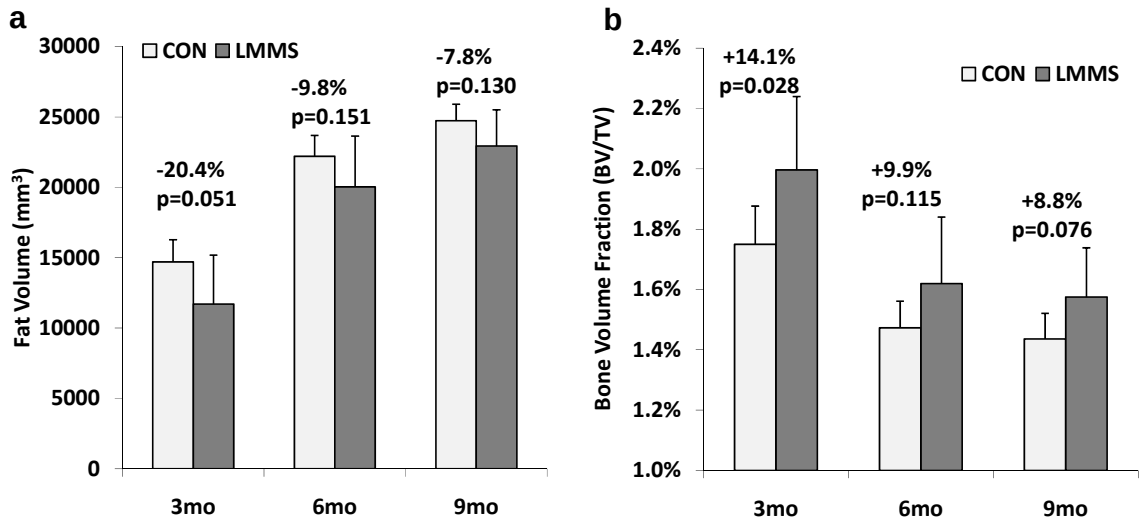

Fig 25. The inverse development and maintenance of adipose (**a**) and bone (**b**) tissue for animals on a high fat diet was monitored by longitudinal *in vivo* microCT at 3, 6, and 9 months. Daily LMMS treatment demonstrated maximal fat suppression at the 3 month time point, with a -20.4% (p=0.051) reduction in LMMS animals compared to CON. The greatest promotion of bone was also seen during this early phase, during the period of maximal animal growth as they achieve peak bone mass. Differences in fat volume between CON and LMMS groups attenuated over time, as LMMS animals "caught up" in fat development by 6 months on the high fat diet due to the large caloric excess. Compared to data at 3 months, the bone volume fraction had decreased by -18.0% ($p<0.001$) by 9 months for the CON animals. Relative to the same 3 month CON value, LMMS was able to protect against some of the age and diet induced bone loss, with treated animals only losing 10.0% (p=0.042) bone volume fraction.

LMMS Decreases Liver Size. Even as animal weights had begun to equilibrate after long term, high fat feeding, the long term effects of LMMS treatment were clearly seen in the significant -28.7% ($p=0.022$) reduction in liver weights of LMMS animals (**Fig 26a**). The average liver weight of the CON group was 2.78 ± 0.30 g while the LMMS group weighed 1.98 ± 0.61 g. The disparity of "fat" content in the livers of CON and LMMS animals harvested at sacrifice was visually evident, as CON livers showed a "speckling" pattern where fat had deposited, in contrast to the clear, bright red color of LMMS livers (**Fig 26b**). Histological sections cut from frozen liver and stained with hematoxylin and eosin further supported the decrease in fat content of LMMS livers, as qualitatively large lipid vacuoles (macrovesicles) were seen throughout the CON tissue, but were much smaller and less prevalent in LMMS tissue (**Fig 26c**). The size and prevalence of lipid infiltration into the tissue based on histological sections has not been quantified.

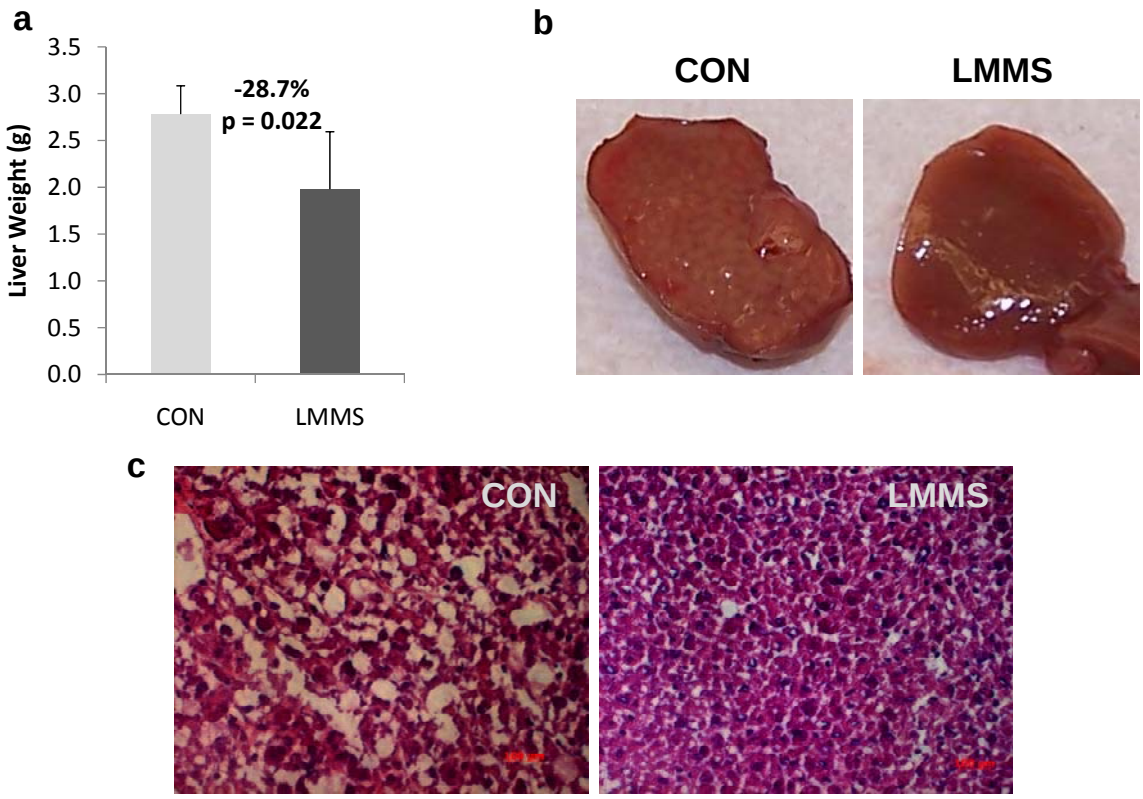

Fig 26. LMMS provided significant protection against hepatomegaly (liver enlargement) associated with long term dietary induced obesity. (**a**) Liver weight after 36 wks LMMS treatment was on average 0.8 grams (-28.7%, p=0.022) less that the CON group. The reduction in liver weight was observed in conjunction with improved appearance of the liver, both in terms of gross morphology (**b**, speckling, color) and histologically (**c**). CON livers contained large lipid deposits (macrovesicles) infiltrated within and between the hepatocytes, whereas LMMS livers show a more typical packing of cells, with smaller and fewer lipid vacuoles.

Accumulation of Triglycerides and Free Fatty Acids in Liver is Suppressed by LMMS. In addition to the reduction in liver weight, the concentration of total liver triglycerides also saw a -27.4% (p=0.041) decrease (**Fig 27a**). The concentration of free fatty acids in the liver was reduced -24.7% (p=0.081, **Fig 27c**). Taking into account both the reduction in liver weight coupled with the reduction in concentration, the total amount of triglycerides in the liver saw a 46.2% (p=0.013, **Fig 27b**) overall decrease. Similarly, the total NEFA amount for each animal in the liver experienced an overall -42.1% (p=0.020) decrease (**Fig 27d**).

Age-induced Loss of Mesenchymal Stem Cells is Mitigated by 36 wks of Daily LMMS Stimulation. To characterize age-related changes in the overall stem cell population, flow cytometry data from bone marrow samples from the current study, harvested at sacrifice after 36 wks, was compared to data reported for animals in Chapter 3 fed a high fat diet for 6 wks. Comparing CON animals at each time point that were not subject to any mechanical stimulation, the total bone marrow derived stem cell population was reduced by -53.2% ($p<0.001$) after 36 wks of the high fat diet when compared to 6 wks (**Fig 28a**). Whereas at 13 wks of age (6 wk study) the Sca-1 positive population represented 19.5 ± 4.9% of the total cell population in the region of interest (R1, refer to Chapter 3 for definitions of regions), this value had declined to 9.1 ± 1.0% by 44 wks of age.

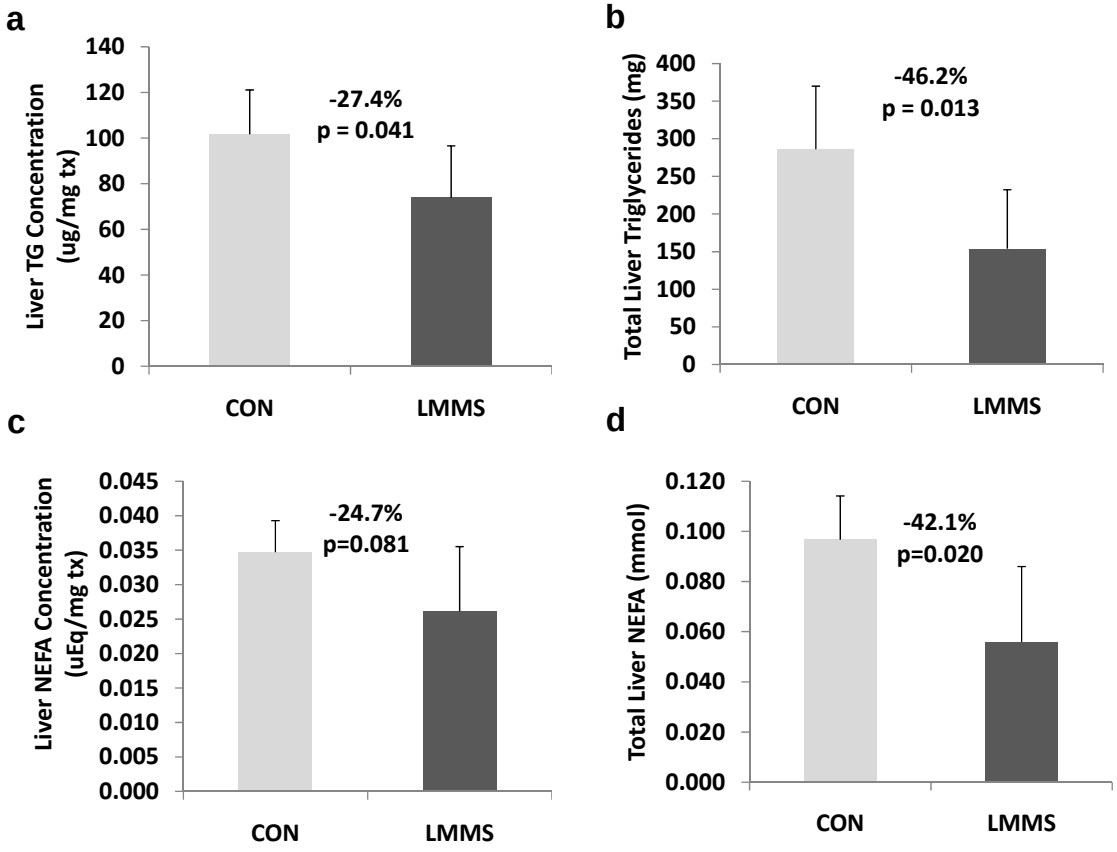

Fig 27. The reduction in liver size and weight can be somewhat accounted for by the reduction of fatty infiltration (as approximated by TG and NEFA content) in LMMS animals. The concentration (per mg of tissue) of these compounds were both decreased by ~25% (**a,c**), and taken in parallel with the 29% decrease liver weight translated into 46.2%, (p=0.013) reduction in total triglycerides in the liver (**b**) and 42% overall decrease in total liver NEFA (**d**) of LMMS animals, compared to the sham CON group. Based on the concentrations of TG levels and % decreases, the reduction in just the triglyceride component of the liver accounted for 132 mg of the decrease in liver weight.

Comparing the effect of the LMMS signal on either the overall stem cell population (**Fig 28b**) or specifically the MSC population (**Fig 28c**) it was evident that the MSC cell population exhibits a greater responsiveness to mechanical stimulation over the long term. While the overall percentage of bone marrow derived stem cells were non-significantly affected by LMMS, MSCs saw a 36.4% (p=0.039) increase due to 36 wks of daily stimulation. In contrast to the previous studies where MSCs were identified

by Sca-1 and Pref-1 positivity, these studies utilized Thy 1.2 and Sca-1 to label the MSC population and thus no data on the preadipocyte population was obtained. However, the osteoblast progenitor population could now be identified based on expression of both markers. (183) Identified in this more stringent manner, a trend towards increase of osteoprogenitors (+5.7%, p=0.528) was observed.

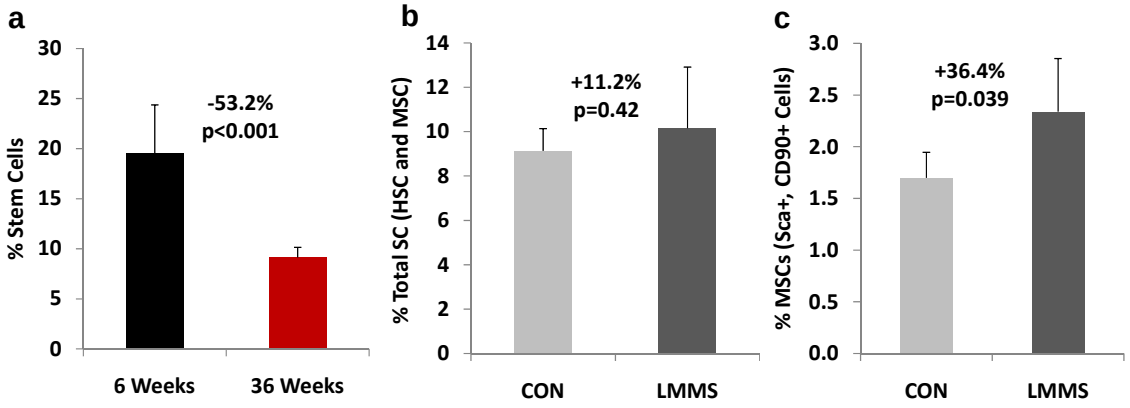

Fig 28. Flow cytometry data tracking the surface labeling of Sca-1, a marker present on both HSC and MSC, illustrate the age-related decline in the number of multipotent progenitor cells (**a**). Data were compared between CON subjects (6 wk: n=8 , 36 wk: n=7), fed a high fat diet for either 6 or 36 weeks. Comparing the effect of the LMMS signal on either the overall stem cell population (**b**) or specifically the MSC population (**c**) it was evident that the MSC cell population exhibits a greater responsiveness mechanical stimulation over the long term. While overall stem cells were non-significantly affected by LMMS, MSCs saw a 36.4% (p=0.039) increase highlighting the ability of the LMMS signal to some degree counter the age-induced loss of stem cells and regenerative potential.

DISCUSSION

Evidence suggests that DNA damage, accumulated over time, contributes significantly to stem cell decline in aging. (180) While we have reported that diet induced obesity likewise causes a decline in number of stem cells, the actual cause of obesity induced stem cell loss has not been examined by us nor other researchers.

Obesity and old age increase an individuals risk of mortality, but excess fat and/or the fragile state are not the actual causes of death. Rather, the downstream effects of these conditions in the overall reduction of the organism's capacity to resist disease, and repair the damages of disease lead to ultimate and fatal failure of tissues and organ systems. In other words, an individual likely will not die of obesity, but obesity related diseases such as cardiac failure. Similarly, the colloquial usage of the expression "dying of old age" typically refers to the fact that an elderly individual has succumbed to an injury or disease that their body was not capable of repairing. A 2004 statistic from the CDC reports that for mortalities in individuals aged 65 and over, 30% were from heart disease, 22% from cancer, and 7% from stroke as the underlying cause of death.(184)

Our characterization of the interaction between diet and aging in a mouse model of obesity clearly show the diet potentiated development of at least one pathological condition: nonalcoholic fatty liver disease. From our previous studies, we have observed that liver weights of normal animals of the C57BL/6J strain typically are on the order of approximately 1.5 grams (Chapter 4), and enlargements in the liver are associated with a number of pathologies. Primarily, nonalcoholic fatty liver disease (NAFLD) is a very common disorder that is documented in up to 10-15% of normal weight individuals, but is exacerbated by excess adiposity as 70 to 80 percent of obese individuals are afflicted. (119) Evidence indicates that this disease is the hepatic component of the obesity induced metabolic syndrome, with gradual weight loss as the primary therapeutic component for treatment. Left untreated, NAFLD could lead to end-stage liver disease, as well as an increased risk of heptocellular carcinoma. (119) NAFLD is characterized by macrovesicular steatosis, like those observed in livers from the CON animals in this study. The biosynthesis of triglycerides typically occurs in adipocytes, and occurrence other tissues is typically linked to various disease states. The accumulation of TG in non-adipocytic cells facilities that formation of molecules that

eventually induce apoptosis and lipotoxicity. (120) As such, the increase quantity of TG and FFA in the liver represents a state of hepatic steatosis that compromises liver function.

Our data clearly indicate that the development and/or progression of fatty liver disease is prevented LMMS. The protection against liver enlargement by LMMS, and significant reductions in TG and FFA production in the liver give indication of improved function even though *in vivo* functional assays (glucose production and insulin suppression tests) were not conducted out of concern that the stress of these procedures could affect the development of adiposity. The reduction in liver FFAs and TG levels in long term obesity represents improved health of these animals, an effect we believe to be due to the synergistic interaction of a reduced adipose burden early in life and the long term maintenance of the stem cell population against diet and age-induced losses.

Of note between these analyses of older animals, compared to our previous studies that utilized primarily young adult animals, was the differential response of the various stem cell populations. We had previously noted that in young animals, the LMMS promotion of stem cell number was greater in the MSC population than when HSC and MSC were classified together (Chapter 6) even as both quantifications were increased significantly after 6 weeks of treatment. In response to 36 weeks of LMMS, an increase in MSC number was still experienced, but the overall stem cell population did not exhibit any significant difference. This data certainly highlights the need for a more thorough analysis of the LMMS effect specifically on HSC, and a more rigorous identification of this cell type, but is consistent with the current understanding of the HSC niche, and the potential divergence in response from the MSC niche. Yet extensive evidence indicates that HSC numbers increase substantially with advancing age in common strains of lab mice. (185) Even as the number of resident stem cells might or

might not be diminished during aging, HSCs from old mice display impaired bioactivity and numerous functional deficiencies.(186)

For this study, the full assessment of experimental outcomes is still a work in progress, and the effects of diet and aging, and the ability of LMMS to counteract some of the deleterious changes is currently under study in other tissues. The fatty infiltration into muscles will be assessed in terms of TG and FFA in soleus and gastrocnemius muscles and well as examined histologically. The adipose content of the bone marrow cavity will be examined both quantitatively by methods such as microMRI (with specificity to quantify fat in the marrow space) and histology. Further, cortical and trabecular bone quantity and micro-architectural quality in the tibia and lumbar vertebrae will be determined.

The idea of a possible negative synergy between diet and aging is illustrated via examination of the opposite end of the diet spectrum. Caloric restriction (CR) is the only intervention known to actually extend longevity. This anti-aging effect is seen along with improved HSC function in aged animals. (187) Energy restriction has been successfully utilized to restore the impaired immune response induced by dietary obesity. (188) These studies lend insight into the complexity of interaction between diet, aging, and the stem cell population and in part explain why exercise is so often generally indicated for treatment even as the mechanisms involved have not been isolated.

Studies have shown that exercise can greatly decrease the risk of metabolic disease and improve the complications of Type 2 diabetes mellitus by the reduction of key adipokines and inflammatory factors.(134;189) Body composition changes and improved musculoskeletal health resulting from exercise can reduce aging associated insulin resistance, (190) the risk of infectious disease, and improve vaccine efficacy. (191) However, in obese and/or elderly individuals exercise might not be a feasible treatment. For most diabetic men over 55 years old, physical training aside from very

low intensity exercise is not possible because of complications and hindrance from interfering diseases. (192) The benefit of exercise in cancer patients has been shown, but in the case of elderly patients (where 78% of all new cancers are diagnosed) the participation in and adherence to exercise programs is low. (193) For patients where exercise is logistically difficult, perhaps LMMS could represent a viable alternative to exacting some of the same benefits and promotion of not only musculoskeletal health, but also protection against age and obesity related sequelae via maintenance of the stem cell population.

Chapter 7

IMPLICATIONS AND LIMITATIONS

SUMMARY

The studies and experiments reported in this dissertation were designed to explore the hypothesis that MSCs represent a common mechano-responsive element upstream of osteoblast and adipocyte differentiation that could potentially be targeted for the control and treatment of both obesity and osteoporosis. We proposed that low magnitude mechanical signals (LMMS) could non-pharmacologically and non-invasively promote stem cell proliferation, and thus an organism's healing and regenerative potential. In Chapter 1, the current strategies for the treatment of obesity and osteoporosis were reviewed. Focus on the emerging understanding of the role of the progenitor stem cell population in the development of these diseases, and control of the stem cell population by mechanical signals highlighted the potential of LMMS to influence the cell lineage commitment.

In the second chapter, the development of a robust methodology to non-invasively quantify adiposity in a live animal was detailed. MicroCT calculated fat volumes demonstrated excellent correlation to explanted fat pad weights, validating the method as a surrogate assessment of *in vivo* adipose burden, which could further be delineated and quantified as visceral or subcutaneous fat. This methodology was applied to assessing the development of excess adiposity by a dietary signal to induce obesity. Aside from the contribution of the caloric excess to the process of adipogenesis, the impact of a high fat diet on the resident stem cell population, as a possible contributing factor in the pathophysiology of obesity was examined in Chapter 3. We show that the MSC population was significantly diminished in animals fed a high fat diet for six weeks, and that the reduction in number of bone marrow derived stem cells correlated to the mass of the epididymal fat pad.

The ability and applicability of LMMS to reduce the adipose burden and key biochemical factors such as adipokines (leptin, adiponectin, and resistin), triglycerides and free fatty acids that are known to be elevated in obese individuals was demonstrated in Chapter 4. Results for the bone marrow transplantation experiments provided the first indication that the applied LMMS signal was increasing the proliferation of bone marrow derived stem cells. Data from flow cytometry and real-time PCR from animals on a model of dietary induced obesity in Chapter 5 provided clear indication that indeed the marrow environment had changed in LMMS treated animals, with an increase in stem cell number and a shift towards osteogenesis. Taken together, the data in Chapters 3, 4 and 5 highlight that while the high fat diet decreased the MSC population, LMMS increased the proliferation of MSC's and was able to recover the diet-induced decrease in cell numbers. In addition, the marrow environment in LMMS animals had shifted towards osteogenesis both in cell number and gene expression, providing a mechanism of LMMS action based on the selective differentiation of MSC's into osteoprogenitors. Finally, data from a long term study (36 week of LMMS treatment, Chapter 6) provided preliminary evidence of the benefit of LMMS in mitigating some the deleterious effects of dietary induced obesity and aging. Specifically, the 36 weeks of high fat diet promoted the development of fatty liver disease in CON animals, whereas LMMS animals subject to the same dietary challenge were largely protected against liver enlargement and fatty infiltration.

Cumulatively these studies provide insight into the role of MSCs in the development of bone and fat. Further, the utility of low magnitude mechanical signals as a preventative measure in the development of obesity and osteoporosis is demonstrated in normal animals and several animal models of obesity and aging. The changes in the cellular and molecular composition of the bone marrow highlight the important pathological features intrinsically arising from a high fat diet and aging. These two

factors are remarkably similar in that they negatively impact the stem cell population, which affects both the immune response (by decreasing the HSC population) and the ability to regenerate and repair damaged tissues (by decreasing the MSC population). The mechanical promotion of the number of progenitor cells, as well as driving commitment choices, suggests a means to enhance an organism's regenerative capacity as achieved by exploiting stem cell sensitivity to physical signals. The remarkable specificity of LMMS to promote the MSC and tune its differentiation towards osteogenesis highlights the vast clinical applications of this technology.

The relevance and translation of LMMS to bone is currently being explored (and in some cases has already seen application) in various patient populations including young osteopenic women, post-menopausal women, and astronauts to protect against bone loss during space flight. Our results demonstrating the suppression of adipogenesis in young animals highlight the utility of LMMS as a primary prevention to the development of childhood obesity. While we have not shown that it can in and of itself reverse or treat a state of obesity, in combination with lifestyle and dietary modifications it would surely boost health and immunity and perhaps even synergistically promote weight loss in adults. For the various disease states and obesity related pathologies where weight loss is the primary treatment indication, LMMS could serve as a powerful adjunct therapy to that end. Further, the field of obesity research is undergoing a fundamental paradigm shift, where in contrast to the long-held belief that once formed fat cells in an individual do not renew, recent findings definitively demonstrate that adipocytes do indeed turn over in humans. By analysis of integration of ^{14}C into genomic DNA, Spalding *et al* determined that approximately 10% of fat cells are renewed annually in adults, via a balance of adipocyte death and generation. (194) Based on the ability of LMMS to slow and deter the development of stem cells into fat,

perhaps even adult obesity could be treated via capitalizing on the normal process of adipocyte death if the development of new adipocytes could be suppressed.

The potential applications of non-invasive, non-pharmacologic, *in vivo* LMMS promotion of bone marrow derived stem cells, and specifically mesenchymal stem cells which are able to be recruited to various biological sites are incredibly vast. To date, no negative outcomes due to LMMS have been noted, and the long term usage of the stimulation for preventative treatments would be indicated. The list of disorders that could benefit from LMMS, and we believe comprise the eventual applications of LMMS, include:

- To promote an enhanced and robust capacity to fight and resist disease in the overall population by promotion of the HSC population.
- To accelerate the ability to repair and regenerate after injury and tissue damage by enhancement of the MSC population.
- To protect against development of obesity and age related disorders such as liver disease and neurodegenerative disorders such as Alzheimers and Parkinsons.
- To serve as an adjunct therapy to cancer patients undergoing chemotherapy and/or radiation to help boost innate immunity.
- To elderly individuals as either treatment or prophylaxes for age-related decline in overall health.

Although our identifications of the HSC and MSC populations are not exact and are quantified based on the cells being members of a population enriched for stem cell activity, this common limitation has yet to be overcome by stem cell researchers.(22) Further, while our results clearly demonstrate an effect and interaction between bone,

fat, and the undifferentiated stem cells in the marrow in response to LMMS, the precise mechanism and order of events has yet to be uncovered. We do not conclude that the proposed mechanism is exclusive, but rather hypothesize that it is complementary to the many theories put forth by the many experts in the fields of bone, fat, and stem cell research. Indeed, based on the abundant and often contradictory reports in the literature on the interaction of stem cells in certain niches, with the differentiated tissues that form the micro-environment – any phenotypic observation is likely resultant of a complex interplay with feedback and regulatory factors yet unknown. Beyond the binary choice to differentiate either into osteoblasts or adipocytes, the development of chondrocytes, and myocytes are also likely affected by the low magnitude mechanical signals and need to be examined. Stem cell populations residing outside of the bone marrow need to be assessed, to determine if there is a site and/or lineage specificity of LMMS promotion of proliferation.

The quantifications of stem cell and progenitor populations are all reported as percentage changes relative to the total population in suspension, and due to technical limitations of the cell harvesting and flow cytometry procedures absolute quantification of cell numbers are difficult. With the manual harvesting of bone marrow by flushing of the marrow cavity, it is not possible to ensure that the same amounts of marrow (and therefore cells) are collected from each animal. Further, the marrow fat is typically (although perhaps not consistently) lost during the preparation of cells for flow cytometry during the numerous washing steps as the lower density of these cells cause them to float rather than pellet during centrifugation. As such, additional methods to quantify the cell types, whether histologically or with *in vitro* experiments will be needed to corroborate these findings. Further work with the models of bone marrow transplants to track cell fate, specifically via injections of sorted populations of cells identified for

surface expression of specific markers in flow cytometry, would greatly enhance the functional characterizations *in vivo* of the cell populations.

While mouse models of disease are excellent research tools, the applicability of these findings and their uncertain translation to the human disease state represents another current limitation of this work. Indeed, even the identifying markers of stem cells in mice and in humans show large disparity, with surface antigens such as Sca-1 expressed on mouse cells and not human cells. (195) As such, the characterization of LMMS effects on mesenchymal stem cell populations will have to necessarily rely on other markers to identify human mesenchymal and hematopoietic stem cells.

The eventual translation of stem cell technologies to clinical application is hampered by numerous challenges including the inability to isolate a homogenous population of MSCs, and expansion of the cell population without compromising the differentiation potential.(23) Further, the plasticity of MSCs and their ability to transdifferentiate make most attempts at *in vitro* functional characterization difficult.(196) As such, we believe that our findings represent a significant advance in that the *in vivo* application of LMMS can be directly measured in clear and beneficial changes in animal phenotype and physiology.

REFERENCES

Reference List

(1) Wolf AM, Colditz GA. Current estimates of the economic cost of obesity in the United States. Obes Res 1998 March;6(2):97-106.

(2) Ray NF, Chan JK, Thamer M, Melton LJ, III. Medical expenditures for the treatment of osteoporotic fractures in the United States in 1995: report from the National Osteoporosis Foundation. J Bone Miner Res 1997 January;12(1):24-35.

(3) Zhao LJ, Jiang H, Papasian CJ, Maulik D, Drees B, Hamilton J, Deng HW. Correlation of obesity and osteoporosis: effect of fat mass on the determination of osteoporosis. J Bone Miner Res 2008 January;23(1):17-29.

(4) Gimble JM, Zvonic S, Floyd ZE, Kassem M, Nuttall ME. Playing with bone and fat. J Cell Biochem 2006 May 15;98(2):251-66.

(5) Hoiberg M, Nielsen TL, Wraae K, Abrahamsen B, Hagen C, Andersen M, Brixen K. Population-based reference values for bone mineral density in young men. Osteoporos Int 2007 May 30.

(6) Dehghan M, Akhtar-Danesh N, Merchant AT. Childhood obesity, prevalence and prevention. Nutr J 2005 September 2;4(1):24.

(7) Kirk S, Scott BJ, Daniels SR. Pediatric obesity epidemic: treatment options. J Am Diet Assoc 2005 May;105(5 Suppl 1):S44-S51.

(8) Padwal RS, Majumdar SR. Drug treatments for obesity: orlistat, sibutramine, and rimonabant. Lancet 2007 January 6;369(9555):71-7.

(9) Close P, Neuprez A, Reginster JY. Developments in the pharmacotherapeutic management of osteoporosis. Expert Opin Pharmacother 2006 August;7(12):1603-15.

(10) Valverde P. Pharmacotherapies to manage bone loss-associated diseases: a quest for the perfect benefit-to-risk ratio. Curr Med Chem 2008;15(3):284-304.

(11) Khosla S, Westendorf JJ, Oursler MJ. Building bone to reverse osteoporosis and repair fractures. J Clin Invest 2008 February;118(2):421-8.

(12) Schwab P, Klein RF. Nonpharmacological approaches to improve bone health and reduce osteoporosis. Curr Opin Rheumatol 2008 March;20(2):213-7.

(13) Nelson-Dooley C, la-Fera MA, Hamrick M, Baile CA. Novel treatments for obesity and osteoporosis: targeting apoptotic pathways in adipocytes. Curr Med Chem 2005;12(19):2215-25.

(14) Cheng SL, Shao JS, Charlton-Kachigian N, Loewy AP, Towler DA. MSX2 promotes osteogenesis and suppresses adipogenic differentiation of

multipotent mesenchymal progenitors. J Biol Chem 2003 November 14;278(46):45969-77.

(15) David V, Martin A, Lafage-Proust MH, Malaval L, Peyroche S, Jones DB, Vico L, Guignandon A. Mechanical loading down-regulates peroxisome proliferator-activated receptor gamma in bone marrow stromal cells and favors osteoblastogenesis at the expense of adipogenesis. Endocrinology 2007 May;148(5):2553-62.

(16) Porada CD, Zanjani ED, meida-Porad G. Adult mesenchymal stem cells: a pluripotent population with multiple applications. Curr Stem Cell Res Ther 2006 September;1(3):365-9.

(17) Liu M, Han ZC. Mesenchymal stem cells: Biology and clinical potential in Type 1 Diabetes Therapy. J Cell Mol Med 2008 February 24.

(18) Giordano A, Galderisi U, Marino IR. From the laboratory bench to the patient's bedside: an update on clinical trials with mesenchymal stem cells. J Cell Physiol 2007 April;211(1):27-35.

(19) Rosen CJ, Bouxsein ML. Mechanisms of disease: is osteoporosis the obesity of bone? Nat Clin Pract Rheumatol 2006 January;2(1):35-43.

(20) Shiota M, Heike T, Haruyama M, Baba S, Tsuchiya A, Fujino H, Kobayashi H, Kato T, Umeda K, Yoshimoto M, Nakahata T. Isolation and characterization of bone marrow-derived mesenchymal progenitor cells with myogenic and neuronal properties. Exp Cell Res 2007 March 10;313(5):1008-23.

(21) Bar-Shavit Z. The osteoclast: a multinucleated, hematopoietic-origin, bone-resorbing osteoimmune cell. J Cell Biochem 2007 December 1;102(5):1130-9.

(22) Morrison SJ, Spradling AC. Stem cells and niches: mechanisms that promote stem cell maintenance throughout life. Cell 2008 February 22;132(4):598-611.

(23) Kassem M. Stem cells: potential therapy for age-related diseases. Ann N Y Acad Sci 2006 May;1067:436-42.

(24) Hachisuka H, Mochizuki Y, Yasunaga Y, Natsu K, Sharman P, Shinomiya R, Ochi M. Flow cytometric discrimination of mesenchymal progenitor cells from bone marrow-adherent cell populations using CD34/44/45(-) and Sca-1(+) markers. J Orthop Sci 2007 March;12(2):161-9.

(25) Wong SH, Lowes KN, Bertoncello I, Quigley AF, Simmons PJ, Cook MJ, Kornberg AJ, Kapsa RM. Evaluation of Sca-1 and c-Kit as selective markers for muscle remodelling by nonhemopoietic bone marrow cells. Stem Cells 2007 June;25(6):1364-74.

(26) Okuno Y, Iwasaki H, Huettner CS, Radomska HS, Gonzalez DA, Tenen DG, Akashi K. Differential regulation of the human and murine CD34 genes in hematopoietic stem cells. Proc Natl Acad Sci U S A 2002 April 30;99(9):6246-51.

(27) Yoshimoto M, Chang H, Shiota M, Kobayashi H, Umeda K, Kawakami A, Heike T, Nakahata T. Two different roles of purified CD45+c-Kit+Sca-1+Lin- cells after transplantation in muscles. Stem Cells 2005 May;23(5):610-8.

(28) Joseph NM, Morrison SJ. Toward an understanding of the physiological function of Mammalian stem cells. Dev Cell 2005 August;9(2):173-83.

(29) Stenderup K, Rosada C, Justesen J, Al-Soubky T, gnaes-Hansen F, Kassem M. Aged human bone marrow stromal cells maintaining bone forming capacity in vivo evaluated using an improved method of visualization. Biogerontology 2004;5(2):107-18.

(30) Biankin SA, Collector MI, Biankin AV, Brown LJ, Kleeberger W, Devereux WL, Zahnow CA, Baylin SB, Watkins DN, Sharkis SJ, Leach SD. A histological survey of green fluorescent protein expression in 'green' mice: implications for stem cell research. Pathology 2007 April;39(2):247-51.

(31) Kratchmarova I, Blagoev B, Haack-Sorensen M, Kassem M, Mann M. Mechanism of divergent growth factor effects in mesenchymal stem cell differentiation. Science 2005 June 3;308(5727):1472-7.

(32) Abdallah BM, Jensen CH, Gutierrez G, Leslie RG, Jensen TG, Kassem M. Regulation of human skeletal stem cells differentiation by Dlk1/Pref-1. J Bone Miner Res 2004 May;19(5):841-52.

(33) Rosen ED, MacDougald OA. Adipocyte differentiation from the inside out. Nat Rev Mol Cell Biol 2006 December;7(12):885-96.

(34) Orr AW, Helmke BP, Blackman BR, Schwartz MA. Mechanisms of mechanotransduction. Dev Cell 2006 January;10(1):11-20.

(35) Ko KS, McCulloch CA. Intercellular mechanotransduction: cellular circuits that coordinate tissue responses to mechanical loading. Biochem Biophys Res Commun 2001 August 3;285(5):1077-83.

(36) Ingber DE. Cellular mechanotransduction: putting all the pieces together again. FASEB J 2006 May;20(7):811-27.

(37) Avram MM, Avram AS, James WD. Subcutaneous fat in normal and diseased states 3. Adipogenesis: from stem cell to fat cell. J Am Acad Dermatol 2007 March;56(3):472-92.

(38) Kubo Y, Kaidzu S, Nakajima I, Takenouchi K, Nakamura F. Organization of extracellular matrix components during differentiation of adipocytes in long-term culture. In Vitro Cell Dev Biol Anim 2000 January;36(1):38-44.

(39) Rubin J, Rubin C, Jacobs CR. Molecular pathways mediating mechanical signaling in bone. Gene 2006 February 15;367:1-16.

(40) Xiao Z, Zhang S, Mahlios J, Zhou G, Magenheimer BS, Guo D, Dallas SL, Maser R, Calvet JP, Bonewald L, Quarles LD. Cilia-like structures and

polycystin-1 in osteoblasts/osteocytes and associated abnormalities in skeletogenesis and Runx2 expression. J Biol Chem 2006 October 13;281(41):30884-95.

(41) You L, Temiyasathit S, Lee P, Kim CH, Tummala P, Yao W, Kingery W, Malone AM, Kwon RY, Jacobs CR. Osteocytes as mechanosensors in the inhibition of bone resorption due to mechanical loading. Bone 2008 January;42(1):172-9.

(42) Qin YX, Kaplan T, Saldanha A, Rubin C. Fluid pressure gradients, arising from oscillations in intramedullary pressure, is correlated with the formation of bone and inhibition of intracortical porosity. J Biomech 2003 October;36(10):1427-37.

(43) Song G, Ju Y, Shen X, Luo Q, Shi Y, Qin J. Mechanical stretch promotes proliferation of rat bone marrow mesenchymal stem cells. Colloids Surf B Biointerfaces 2007 April 6.

(44) Terraciano V, Hwang N, Moroni L, Park HB, Zhang Z, Mizrahi J, Seliktar D, Elisseeff J. Differential response of adult and embryonic mesenchymal progenitor cells to mechanical compression in hydrogels. Stem Cells 2007 November;25(11):2730-8.

(45) Haylock DN, Nilsson SK. Osteopontin: a bridge between bone and blood. Br J Haematol 2006 September;134(5):467-74.

(46) Papayannopoulou T, Scadden DT. Stem-cell ecology and stem cells in motion. Blood 2008 April 15;111(8):3923-30.

(47) Calvi LM, Adams GB, Weibrecht KW, Weber JM, Olson DP, Knight MC, Martin RP, Schipani E, Divieti P, Bringhurst FR, Milner LA, Kronenberg HM, Scadden DT. Osteoblastic cells regulate the haematopoietic stem cell niche. Nature 2003 October 23;425(6960):841-6.

(48) Taichman RS, Reilly MJ, Emerson SG. Human osteoblasts support human hematopoietic progenitor cells in vitro bone marrow cultures. Blood 1996 January 15;87(2):518-24.

(49) Borer KT. Physical activity in the prevention and amelioration of osteoporosis in women : interaction of mechanical, hormonal and dietary factors. Sports Med 2005;35(9):779-830.

(50) BASSETT CA, BECKER RO. Generation of electric potentials by bone in response to mechanical stress. Science 1962 September 28;137:1063-4.

(51) Burger EH, Klein-Nulend J. Mechanotransduction in bone--role of the lacuno-canalicular network. FASEB J 1999;13 Suppl:S101-S112.

(52) Lanyon LE, Rubin CT. Static vs dynamic loads as an influence on bone remodelling. J Biomech 1984;17(12):897-905.

(53) Rubin CT, Lanyon LE. Regulation of bone formation by applied dynamic loads. J Bone Joint Surg Am 1984 March;66(3):397-402.

(54) Turner CH, Owan I, Takano Y. Mechanotransduction in bone: role of strain rate. Am J Physiol 1995 September;269(3 Pt 1):E438-E442.

(55) Robling AG, Duijvelaar KM, Geevers JV, Ohashi N, Turner CH. Modulation of appositional and longitudinal bone growth in the rat ulna by applied static and dynamic force. Bone 2001 August;29(2):105-13.

(56) Turner CH, Forwood MR, Rho JY, Yoshikawa T. Mechanical loading thresholds for lamellar and woven bone formation. J Bone Miner Res 1994 January;9(1):87-97.

(57) Mosley JR, Lanyon LE. Strain rate as a controlling influence on adaptive modeling in response to dynamic loading of the ulna in growing male rats. Bone 1998 October;23(4):313-8.

(58) Rubin CT, Lanyon LE. Regulation of bone mass by mechanical strain magnitude. Calcif Tissue Int 1985 July;37(4):411-7.

(59) Forwood MR. Physical activity and bone development during childhood: insights from animal models. J Appl Physiol 2008 April 17.

(60) Umemura Y, Ishiko T, Yamauchi T, Kurono M, Mashiko S. Five jumps per day increase bone mass and breaking force in rats. J Bone Miner Res 1997 September;12(9):1480-5.

(61) Robling AG, Burr DB, Turner CH. Partitioning a daily mechanical stimulus into discrete loading bouts improves the osteogenic response to loading. J Bone Miner Res 2000 August;15(8):1596-602.

(62) Macdonald HM, Kontulainen SA, Khan KM, McKay HA. Is a school-based physical activity intervention effective for increasing tibial bone strength in boys and girls? J Bone Miner Res 2007 March;22(3):434-46.

(63) Macdonald HM, Kontulainen SA, Petit MA, Beck TJ, Khan KM, McKay HA. Does a novel school-based physical activity model benefit femoral neck bone strength in pre- and early pubertal children? Osteoporos Int 2008 March 21.

(64) Rubin C, Judex S, Qin YX. Low-level mechanical signals and their potential as a non-pharmacological intervention for osteoporosis. Age Ageing 2006 September;35 Suppl 2:ii32-ii36.

(65) Rubin C, Turner AS, Bain S, Mallinckrodt C, McLeod K. Anabolism: Low mechanical signals strengthen long bones. Nature 2001 August 9;412(6847):603-4.

(66) Xie L, Rubin C, Judex S. Enhancement of the adolescent murine musculoskeletal system using low-level mechanical vibrations. J Appl Physiol 2008 April;104(4):1056-62.

(67) Eisman JA. Good, good, good... good vibrations: the best option for better bones? Lancet 2001 December 8;358(9297):1924-5.

(68) Garman R, Gaudette G, Donahue LR, Rubin C, Judex S. Low-level accelerations applied in the absence of weight bearing can enhance trabecular bone formation. J Orthop Res 2007 June;25(6):732-40.

(69) Gilsanz V, Wren TA, Sanchez M, Dorey F, Judex S, Rubin C. Low-level, high-frequency mechanical signals enhance musculoskeletal development of young women with low BMD. J Bone Miner Res 2006 September;21(9):1464-74.

(70) Christiansen BA, Silva MJ. The effect of varying magnitudes of whole-body vibration on several skeletal sites in mice. Ann Biomed Eng 2006 July;34(7):1149-56.

(71) Person RS, Kudina LP. Discharge frequency and discharge pattern of human motor units during voluntary contraction of muscle. Electroencephalogr Clin Neurophysiol 1972 May;32(5):471-83.

(72) Fritton SP, McLeod KJ, Rubin CT. Quantifying the strain history of bone: spatial uniformity and self- similarity of low-magnitude strains. J Biomech 2000 March;33(3):317-25.

(73) Judex S, Lei X, Han D, Rubin C. Low-magnitude mechanical signals that stimulate bone formation in the ovariectomized rat are dependent on the applied frequency but not on the strain magnitude. J Biomech 2007;40(6):1333-9.

(74) Brockmann GA, Bevova MR. Using mouse models to dissect the genetics of obesity. Trends Genet 2002 July;18(7):367-76.

(75) Magnusson ML, Pope MH, Wilder DG, Areskoug B. Are occupational drivers at an increased risk for developing musculoskeletal disorders? Spine 1996 March 15;21(6):710-7.

(76) Kiiski J, Heinonen A, Jarvinen T, Kannus P, Sievanen H. Transmission of Vertical Whole Body Vibration to the Human Body. J Bone Miner Res 2008 March 18.

(77) International Standards Organization. Evaluation of Human Exposure to Whole-Body Vibration. Geneva; 1985 Jan. Report No.: 2631/1.

(78) Kuo LE, Kitlinska JB, Tilan JU, Li L, Baker SB, Johnson MD, Lee EW, Burnett MS, Fricke ST, Kvetnansky R, Herzog H, Zukowska Z. Neuropeptide Y acts directly in the periphery on fat tissue and mediates stress-induced obesity and metabolic syndrome. Nat Med 2007 July;13(7):803-11.

(79) Gesta S, Tseng YH, Kahn CR. Developmental origin of fat: tracking obesity to its source. Cell 2007 October 19;131(2):242-56.

(80) Haffner SM. Abdominal adiposity and cardiometabolic risk: do we have all the answers? Am J Med 2007 September;120(9 Suppl 1):S10-S16.

(81) Robert J.Seely, Louis Munyakazi, Thomas F.Curry, Heather Simmerman, W.Heath Rushing, John Haury. Application of the Weisberg t-test for Outliers. Pharmaceutical Technology Europe . 2003.
Ref Type: Magazine Article

(82) Fox CS, Massaro JM, Hoffmann U, Pou KM, Maurovich-Horvat P, Liu CY, Vasan RS, Murabito JM, Meigs JB, Cupples LA, D'Agostino RB, Sr., O'Donnell CJ. Abdominal visceral and subcutaneous adipose tissue compartments: association with metabolic risk factors in the Framingham Heart Study. Circulation 2007 July 3;116(1):39-48.

(83) Despres JP. Cardiovascular disease under the influence of excess visceral fat. Crit Pathw Cardiol 2007 June;6(2):51-9.

(84) Imbeault P, Lemieux S, Prud'homme D, Tremblay A, Nadeau A, Despres JP, Mauriege P. Relationship of visceral adipose tissue to metabolic risk factors for coronary heart disease: is there a contribution of subcutaneous fat cell hypertrophy? Metabolism 1999 March;48(3):355-62.

(85) Chiba Y, Saitoh S, Takagi S, Ohnishi H, Katoh N, Ohata J, Nakagawa M, Shimamoto K. Relationship between visceral fat and cardiovascular disease risk factors: the Tanno and Sobetsu study. Hypertens Res 2007 March;30(3):229-36.

(86) Maurovich-Horvat P, Massaro J, Fox CS, Moselewski F, O'Donnell CJ, Hoffmann U. Comparison of anthropometric, area- and volume-based assessment of abdominal subcutaneous and visceral adipose tissue volumes using multi-detector computed tomography. Int J Obes (Lond) 2007 March;31(3):500-6.

(87) Calderan L, Marzola P, Nicolato E, Fabene PF, Milanese C, Bernardi P, Giordano A, Cinti S, Sbarbati A. In vivo phenotyping of the ob/ob mouse by magnetic resonance imaging and 1H-magnetic resonance spectroscopy. Obesity (Silver Spring) 2006 March;14(3):405-14.

(88) Reed DR, Bachmanov AA, Tordoff MG. Forty mouse strain survey of body composition. Physiol Behav 2007 August 15;91(5):593-600.

(89) Taicher GZ, Tinsley FC, Reiderman A, Heiman ML. Quantitative magnetic resonance (QMR) method for bone and whole-body-composition analysis. Anal Bioanal Chem 2003 November;377(6):990-1002.

(90) Muller R, Hahn M, Vogel M, Delling G, Ruegsegger P. Morphometric analysis of noninvasively assessed bone biopsies: comparison of high-resolution computed tomography and histologic sections. Bone 1996 March;18(3):215-20.

(91) Ruegsegger P, Koller B, Muller R. A microtomographic system for the nondestructive evaluation of bone architecture. Calcif Tissue Int 1996 January;58(1):24-9.

(92) Garcia MC, Wernstedt I, Berndtsson A, Enge M, Bell M, Hultgren O, Horn M, Ahren B, Enerback S, Ohlsson C, Wallenius V, Jansson JO. Mature-onset obesity in interleukin-1 receptor I knockout mice. Diabetes 2006 May;55(5):1205-13.

(93) Rubin CT, Capilla E, Luu YK, Busa B, Crawford H, Nolan DJ, Mittal V, Rosen CJ, Pessin JE, Judex S. Adipogenesis is inhibited by brief, daily exposure to high-frequency, extremely low-magnitude mechanical signals. Proc Natl Acad Sci U S A 2007 October 24.

(94) Bastie CC, Zong H, Xu J, Busa B, Judex S, Kurland IJ, Pessin JE. Integrative metabolic regulation of peripheral tissue fatty acid oxidation by the SRC kinase family member Fyn. Cell Metab 2007 May;5(5):371-81.

(95) Gesta S, Bluher M, Yamamoto Y, Norris AW, Berndt J, Kralisch S, Boucher J, Lewis C, Kahn CR. Evidence for a role of developmental genes in the origin of obesity and body fat distribution. Proc Natl Acad Sci U S A 2006 April 25;103(17):6676-81.

(96) Parekh PI, Petro AE, Tiller JM, Feinglos MN, Surwit RS. Reversal of diet-induced obesity and diabetes in C57BL/6J mice. Metabolism 1998 September;47(9):1089-96.

(97) Eguchi M, Tsuchihashi K, Saitoh S, Odawara Y, Hirano T, Nakata T, Miura T, Ura N, Hareyama M, Shimamoto K. Visceral obesity in Japanese patients with metabolic syndrome: reappraisal of diagnostic criteria by CT scan. Hypertens Res 2007 April;30(4):315-23.

(98) Lublinsky S, Ozcivici E, Judex S. An automated algorithm to detect the trabecular-cortical bone interface in micro-computed tomographic images. Calcif Tissue Int 2007 October;81(4):285-93.

(99) Buie HR, Campbell GM, Klinck RJ, MacNeil JA, Boyd SK. Automatic segmentation of cortical and trabecular compartments based on a dual threshold technique for in vivo micro-CT bone analysis. Bone 2007 October;41(4):505-15.

(100) Canny J. *A Computational Approach to Edge Detection*. IEEE Transactions on Pattern Analysis and Machine Intelligence 1986 November;8(6).

(101) Lublinsky S, Luu YK, Rubin CT, Judex S. An Automated Algorithm to Separate Visceral from Subcutaneous Fat in Micro Computed Tomographies. J Digital Imaging. In press 2008.

(102) Kanaley JA, Giannopoulou I, Ploutz-Snyder LL. Regional differences in abdominal fat loss. Int J Obes (Lond) 2007 January;31(1):147-52.

(103) Rins M, Diez I, Calpena AC, Obach R. Skin density in the hairless rat. Evidence of regional differences. Eur J Drug Metab Pharmacokinet 1991;Spec No 3:456-7.

(104) Kodera T, McGaha TL, Phelps R, Paul WE, Bona CA. Disrupting the IL-4 gene rescues mice homozygous for the tight-skin mutation from embryonic death and diminishes TGF-beta production by fibroblasts. Proc Natl Acad Sci U S A 2002 March 19;99(6):3800-5.

(105) Weisberg SP, McCann D, Desai M, Rosenbaum M, Leibel RL, Ferrante AW, Jr. Obesity is associated with macrophage accumulation in adipose tissue. J Clin Invest 2003 December;112(12):1796-808.

(106) Hausman DB, DiGirolamo M, Bartness TJ, Hausman GJ, Martin RJ. The biology of white adipocyte proliferation. Obes Rev 2001 November;2(4):239-54.

(107) Brehm BJ, D'Alessio DA. Weight loss and metabolic benefits with diets of varying fat and carbohydrate content: separating the wheat from the chaff. Nat Clin Pract Endocrinol Metab 2008 March;4(3):140-6.

(108) Esposito K, Ceriello A, Giugliano D. Diet and the metabolic syndrome. Metab Syndr Relat Disord 2007 December;5(4):291-6.

(109) Giugliano D, Ceriello A, Esposito K. The effects of diet on inflammation: emphasis on the metabolic syndrome. J Am Coll Cardiol 2006 August 15;48(4):677-85.

(110) Albala C, Yanez M, Devoto E, Sostin C, Zeballos L, Santos JL. Obesity as a protective factor for postmenopausal osteoporosis. Int J Obes Relat Metab Disord 1996 November;20(11):1027-32.

(111) Davidson P, Goulding A, Chalmers D. Biomechanical analysis of arm fracture in obese boys. J Paediatr Child Health 2003 December;39(9):657-64.

(112) Goulding A. Risk factors for fractures in normally active children and adolescents. Med Sport Sci 2007;51:102-20.

(113) Goulding A, Grant AM, Williams SM. Bone and body composition of children and adolescents with repeated forearm fractures. J Bone Miner Res 2005 December;20(12):2090-6.

(114) Hausman GJ, Hausman DB. Search for the preadipocyte progenitor cell. J Clin Invest 2006 December;116(12):3103-6.

(115) Ward WE, Kim S, Robert BW. A western-style diet reduces bone mass and biomechanical bone strength to a greater extent in male compared with female rats during development. Br J Nutr 2003 September;90(3):589-95.

(116) Parhami F, Tintut Y, Beamer WG, Gharavi N, Goodman W, Demer LL. Atherogenic high-fat diet reduces bone mineralization in mice. J Bone Miner Res 2001 January;16(1):182-8.

(117) Hirasawa H, Tanaka S, Sakai A, Tsutsui M, Shimokawa H, Miyata H, Moriwaki S, Niida S, Ito M, Nakamura T. ApoE gene deficiency enhances the reduction of bone formation induced by a high-fat diet through the stimulation of p53-

mediated apoptosis in osteoblastic cells. J Bone Miner Res 2007 July;22(7):1020-30.

(118) Center for Disease Control. Defining Overweight and Obesity. Department of Health and Human Services 2008;Available from: URL: http://www.cdc.gov/nccdphp/dnpa/obesity/defining.htm

(119) Duvnjak M, Lerotic I, Barsic N, Tomasic V, Virovic JL, Velagic V. Pathogenesis and management issues for non-alcoholic fatty liver disease. World J Gastroenterol 2007 September 14;13(34):4539-50.

(120) Fonseca-Alaniz MH, Takada J, onso-Vale MI, Lima FB. Adipose tissue as an endocrine organ: from theory to practice. J Pediatr (Rio J) 2007 November;83(5 Suppl):S192-S203.

(121) Moerman EJ, Teng K, Lipschitz DA, Lecka-Czernik B. Aging activates adipogenic and suppresses osteogenic programs in mesenchymal marrow stroma/stem cells: the role of PPAR-gamma2 transcription factor and TGF-beta/BMP signaling pathways. Aging Cell 2004 December;3(6):379-89.

(122) Hilton MJ, Tu X, Wu X, Bai S, Zhao H, Kobayashi T, Kronenberg HM, Teitelbaum SL, Ross FP, Kopan R, Long F. Notch signaling maintains bone marrow mesenchymal progenitors by suppressing osteoblast differentiation. Nat Med 2008 March;14(3):306-14.

(123) Dazzi F, Horwood NJ. Potential of mesenchymal stem cell therapy. Curr Opin Oncol 2007 November;19(6):650-5.

(124) Spaeth E, Klopp A, Dembinski J, Andreeff M, Marini F. Inflammation and tumor microenvironments: defining the migratory itinerary of mesenchymal stem cells. Gene Ther 2008 April 10.

(125) Yakar S, Nunez NP, Pennisi P, Brodt P, Sun H, Fallavollita L, Zhao H, Scavo L, Novosyadlyy R, Kurshan N, Stannard B, East-Palmer J, Smith NC, Perkins SN, Fuchs-Young R, Barrett JC, Hursting SD, LeRoith D. Increased tumor growth in mice with diet-induced obesity: impact of ovarian hormones. Endocrinology 2006 December;147(12):5826-34.

(126) Amar S, Zhou Q, Shaik-Dasthagirisaheb Y, Leeman S. Diet-induced obesity in mice causes changes in immune responses and bone loss manifested by bacterial challenge. Proc Natl Acad Sci U S A 2007 December 18;104(51):20466-71.

(127) Calle EE, Rodriguez C, Walker-Thurmond K, Thun MJ. Overweight, obesity, and mortality from cancer in a prospectively studied cohort of U.S. adults. N Engl J Med 2003 April 24;348(17):1625-38.

(128) Lazar MA. How obesity causes diabetes: not a tall tale. Science 2005 January 21;307(5708):373-5.

(129) Stumvoll M, Goldstein BJ, van Haeften TW. Type 2 diabetes: principles of pathogenesis and therapy. Lancet 2005 April 9;365(9467):1333-46.

(130) Colombo M, Gregersen S, Kruhoeffer M, Agger A, Xiao J, Jeppesen PB, Orntoft T, Ploug T, Galbo H, Hermansen K. Prevention of hyperglycemia in Zucker diabetic fatty rats by exercise training: effects on gene expression in insulin-sensitive tissues determined by high-density oligonucleotide microarray analysis. Metabolism 2005 December;54(12):1571-81.

(131) Slentz CA, Aiken LB, Houmard JA, Bales CW, Johnson JL, Tanner CJ, Duscha BD, Kraus WE. Inactivity, exercise, and visceral fat. STRRIDE: a randomized, controlled study of exercise intensity and amount. J Appl Physiol 2005 October;99(4):1613-8.

(132) Adult participation in recommended levels of physical activity--United States, 2001 and 2003. MMWR Morb Mortal Wkly Rep 2005 December 2;54(47):1208-12.

(133) Atlantis E, Barnes EH, Singh MAF. Efficacy of exercise for treating overweight in children and adolescents: a systematic review. Int J Obes 2006 March 14;30(7):1027-40.

(134) Frank LL, Sorensen BE, Yasui Y, Tworoger SS, Schwartz RS, Ulrich CM, Irwin ML, Rudolph RE, Rajan KB, Stanczyk F, Bowen D, Weigle DS, Potter JD, McTiernan A. Effects of exercise on metabolic risk variables in overweight postmenopausal women: a randomized clinical trial. Obes Res 2005 March;13(3):615-25.

(135) Tanabe Y, Koga M, Saito M, Matsunaga Y, Nakayama K. Inhibition of adipocyte differentiation by mechanical stretching through ERK-mediated downregulation of PPARgamma2. J Cell Sci 2004 July 15;117(Pt 16):3605-14.

(136) Baynard T, Franklin RM, Goulopoulou S, Carhart R, Jr., Kanaley JA. Effect of a single vs multiple bouts of exercise on glucose control in women with type 2 diabetes. Metabolism 2005 August;54(8):989-94.

(137) Xie L, Jacobson JM, Choi ES, Busa B, Donahue LR, Miller LM, Rubin CT, Judex S. Low-level mechanical vibrations can influence bone resorption and bone formation in the growing skeleton. Bone 2006 July 4.

(138) Crossno JT, Jr., Majka SM, Grazia T, Gill RG, Klemm DJ. Rosiglitazone promotes development of a novel adipocyte population from bone marrow-derived circulating progenitor cells. J Clin Invest 2006 December;116(12):3220-8.

(139) Lakka TA, Bouchard C. Physical activity, obesity and cardiovascular diseases. Handb Exp Pharmacol 2005;(170):137-63.

(140) Fritton JC, Rubin CT, Qin YX, McLeod KJ. Whole-body vibration in the skeleton: development of a resonance-based testing device. Ann Biomed Eng 1997 September;25(5):831-9.

(141) Folch J, Lees M, SLOANE STANLEY GH. A simple method for the isolation and purification of total lipides from animal tissues. J Biol Chem 1957 May;226(1):497-509.

(142) SEIFTER S, DAYTON S, . The estimation of glycogen with the anthrone reagent. Arch Biochem 1950 January;25(1):191-200.

(143) Watts GF, Chan DC, Barrett PH. Adipose tissue compartments and the kinetics of very-low-density lipoprotein apolipoprotein B-100 in non-obese men. Metabolism 2002 September;51(9):1206-10.

(144) Cara JF, Chaiken RL. Type 2 diabetes and the metabolic syndrome in children and adolescents. Curr Diab Rep 2006 June;6(3):241-50.

(145) Freedman DS, Mei Z, Srinivasan SR, Berenson GS, Dietz WH. Cardiovascular Risk Factors and Excess Adiposity Among Overweight Children and Adolescents: The Bogalusa Heart Study. J Pediatr 2007 January;150(1):12-7.

(146) Adams KF, Schatzkin A, Harris TB, Kipnis V, Mouw T, Ballard-Barbash R, Hollenbeck A, Leitzmann MF. Overweight, Obesity, and Mortality in a Large Prospective Cohort of Persons 50 to 71 Years Old. The New England Journal of Medicine 2006 August 22;NEJMoa055643.

(147) Unger RH. Minireview: weapons of lean body mass destruction: the role of ectopic lipids in the metabolic syndrome. Endocrinology 2003 December;144(12):5159-65.

(148) Ghosh K, Ingber DE. Micromechanical control of cell and tissue development: Implications for tissue engineering. Adv Drug Deliv Rev 2007 August 16.

(149) Rehfeldt F, Engler AJ, Eckhardt A, Ahmed F, Discher DE. Cell responses to the mechanochemical microenvironment-Implications for regenerative medicine and drug delivery. Adv Drug Deliv Rev 2007 August 14.

(150) Song HY, Jeon ES, Kim JI, Jung JS, Kim JH. Oncostatin M promotes osteogenesis and suppresses adipogenic differentiation of human adipose tissue-derived mesenchymal stem cells. J Cell Biochem 2007 January 16.

(151) De CP, Milan G, Scarda A, Boldrin L, Centobene C, Piccoli M, Pozzobon M, Pilon C, Pagano C, Gamba P, Vettor R. Rosiglitazone modifies the adipogenic potential of human muscle satellite cells. Diabetologia 2006 August;49(8):1962-73.

(152) Lazarenko OP, Rzonca SO, Hogue WR, Swain FL, Suva LJ, Lecka-Czernik B. Rosiglitazone Induces Decreases in Bone Mass and Strength that Are Reminiscent of Aged Bone. Endocrinology 2007 June;148(6):2669-80.

(153) Mukherjee S, Raje N, Schoonmaker JA, Liu JC, Hideshima T, Wein MN, Jones DC, Vallet S, Bouxsein ML, Pozzi S, Chhetri S, Seo YD, Aronson JP, Patel C, Fulciniti M, Purton LE, Glimcher LH, Lian JB, Stein G, Anderson KC, Scadden DT. Pharmacologic targeting of a stem/progenitor population in vivo is

associated with enhanced bone regeneration in mice. J Clin Invest 2008 February 1;118(2):491-504.

(154) Rubin CT, Lanyon LE. Dynamic strain similarity in vertebrates; an alternative to allometric limb bone scaling. J Theor Biol 1984 March 21;107(2):321-7.

(155) Gilsbach R, Kouta M, Bonisch H, Bruss M. Comparison of in vitro and in vivo reference genes for internal standardization of real-time PCR data. Biotechniques 2006 February;40(2):173-7.

(156) Luu YK, Lublinsky S, Ozcivici E, Capilla E, Pessin JE, Rubin CT, Judex S. Determination of Subcutaneous and Visceral Fat Distribution by In Vivo Micro Computed Tomography. Medical Engineering and Physics. In press 2008.

(157) Robert J.Seely, Louis Munyakazi, Thomas F.Curry, Heather Simmerman, W.Heath Rushing, John Haury. Application of the Weisberg t-test for Outliers. Pharmaceutical Technology Europe . 2003.
Ref Type: Magazine Article

(158) Van VP, Falla N, Snoeck H, Mathieu E. Characterization and purification of osteogenic cells from murine bone marrow by two-color cell sorting using anti-Sca-1 monoclonal antibody and wheat germ agglutinin. Blood 1994 August 1;84(3):753-63.

(159) Li X, Zhang Y, Kang H, Liu W, Liu P, Zhang J, Harris SE, Wu D. Sclerostin binds to LRP5/6 and antagonizes canonical Wnt signaling. J Biol Chem 2005 May 20;280(20):19883-7.

(160) Lin S, Thomas TC, Storlien LH, Huang XF. Development of high fat diet-induced obesity and leptin resistance in C57Bl/6J mice. Int J Obes Relat Metab Disord 2000 May;24(5):639-46.

(161) Haylock DN, Williams B, Johnston HM, Liu MC, Rutherford KE, Whitty GA, Simmons PJ, Bertoncello I, Nilsson SK. Hemopoietic stem cells with higher hemopoietic potential reside at the bone marrow endosteum. Stem Cells 2007 April;25(4):1062-9.

(162) Akune T, Ohba S, Kamekura S, Yamaguchi M, Chung UI, Kubota N, Terauchi Y, Harada Y, Azuma Y, Nakamura K, Kadowaki T, Kawaguchi H. PPARgamma insufficiency enhances osteogenesis through osteoblast formation from bone marrow progenitors. J Clin Invest 2004 March;113(6):846-55.

(163) Takada I, Suzawa M, Matsumoto K, Kato S. Suppression of PPAR transactivation switches cell fate of bone marrow stem cells from adipocytes into osteoblasts. Ann N Y Acad Sci 2007 November;1116:182-95.

(164) Hadjiargyrou M, Rightmire EP, Ando T, Lombardo FT. The E11 osteoblastic lineage marker is differentially expressed during fracture healing. Bone 2001 August;29(2):149-54.

(165) Sul HS, Smas C, Mei B, Zhou L. Function of pref-1 as an inhibitor of adipocyte differentiation. Int J Obes Relat Metab Disord 2000 November;24 Suppl 4:S15-S19.

(166) Gregoire FM, Smas CM, Sul HS. Understanding adipocyte differentiation. Physiol Rev 1998 July;78(3):783-809.

(167) Koh YJ, Kang S, Lee HJ, Choi TS, Lee HS, Cho CH, Koh GY. Bone marrow-derived circulating progenitor cells fail to transdifferentiate into adipocytes in adult adipose tissues in mice. J Clin Invest 2007 December 3;117(12):3684-95.

(168) Scadden DT. The weight of cell identity. J Clin Invest 2007 December;117(12):3653-5.

(169) Gregoire FM. Adipocyte differentiation: from fibroblast to endocrine cell. Exp Biol Med (Maywood) 2001 December;226(11):997-1002.

(170) Lago F, Dieguez C, Gomez-Reino J, Gualillo O. Adipokines as emerging mediators of immune response and inflammation. Nat Clin Pract Rheumatol 2007 December;3(12):716-24.

(171) Duque G. Will reducing adopogenesis in bone increase bone mass?: PPARgamma2 as a key target in the treatment of age-related bone loss. Drug News Perspect 2003 July;16(6):341-6.

(172) Liu H, Fergusson MM, Castilho RM, Liu J, Cao L, Chen J, Malide D, Rovira II, Schimel D, Kuo CJ, Gutkind JS, Hwang PM, Finkel T. Augmented Wnt signaling in a mammalian model of accelerated aging. Science 2007 August 10;317(5839):803-6.

(173) Astudillo P, Rios S, Pastenes L, Pino AM, Rodriguez JP. Increased adipogenesis of osteoporotic human-mesenchymal stem cells (MSCs) characterizes by impaired leptin action. J Cell Biochem 2007 October 31.

(174) Zayzafoon M, Gathings WE, McDonald JM. Modeled microgravity inhibits osteogenic differentiation of human mesenchymal stem cells and increases adipogenesis. Endocrinology 2004 May;145(5):2421-32.

(175) Basso N, Bellows CG, Heersche JN. Effect of simulated weightlessness on osteoprogenitor cell number and proliferation in young and adult rats. Bone 2005 January;36(1):173-83.

(176) Takada K, Inaba M, Ichioka N, Ueda Y, Taira M, Baba S, Mizokami T, Wang X, Hisha H, Iida H, Ikehara S. Treatment of senile osteoporosis in SAMP6 mice by intra-bone marrow injection of allogeneic bone marrow cells. Stem Cells 2006 February;24(2):399-405.

(177) Conboy IM, Conboy MJ, Wagers AJ, Girma ER, Weissman IL, Rando TA. Rejuvenation of aged progenitor cells by exposure to a young systemic environment. Nature 2005 February 17;433(7027):760-4.

(178) Schonfeld-Warden N, Warden CH. Pediatric obesity. An overview of etiology and treatment. Pediatr Clin North Am 1997 April;44(2):339-61.

(179) Eckel RH, Krauss RM. American Heart Association call to action: obesity as a major risk factor for coronary heart disease. AHA Nutrition Committee. Circulation 1998 June 2;97(21):2099-100.

(180) Rossi DJ, Jamieson CH, Weissman IL. Stems cells and the pathways to aging and cancer. Cell 2008 February 22;132(4):681-96.

(181) Chan GK, Duque G. Age-related bone loss: old bone, new facts. Gerontology 2002 March;48(2):62-71.

(182) Gimble JM, Robinson CE, Wu X, Kelly KA. The function of adipocytes in the bone marrow stroma: an update. Bone 1996 November;19(5):421-8.

(183) Chen XD, Qian HY, Neff L, Satomura K, Horowitz MC. Thy-1 antigen expression by cells in the osteoblast lineage. J Bone Miner Res 1999 March;14(3):362-75.

(184) Gorina Y, Lentzner H. Aging Trends: Multiple Causes of Death in Old Age. Centers for Disease Control and Prevention, National Center for Health Statistics 2008;Available from: URL: http://www.cdc.gov/nchs/data/ahcd/agingtrends/09causes.htm

(185) Morrison SJ, Wandycz AM, Akashi K, Globerson A, Weissman IL. The aging of hematopoietic stem cells. Nat Med 1996 September;2(9):1011-6.

(186) Laird DJ, von Andrian UH, Wagers AJ. Stem cell trafficking in tissue development, growth, and disease. Cell 2008 February 22;132(4):612-30.

(187) Chen J, Astle CM, Harrison DE. Hematopoietic senescence is postponed and hematopoietic stem cell function is enhanced by dietary restriction. Exp Hematol 2003 November;31(11):1097-103.

(188) Lamas O, Martinez JA, Marti A. Energy restriction restores the impaired immune response in overweight (cafeteria) rats. J Nutr Biochem 2004 July;15(7):418-25.

(189) DiPenta JM, Green-Johnson JM, Murphy RJ. Type 2 diabetes mellitus, resistance training, and innate immunity: is there a common link? Appl Physiol Nutr Metab 2007 December;32(6):1025-35.

(190) Ryan AS. Insulin resistance with aging: effects of diet and exercise. Sports Med 2000 November;30(5):327-46.

(191) Senchina DS, Kohut ML. Immunological outcomes of exercise in older adults. Clin Interv Aging 2007;2(1):3-16.

(192) Zierath JR, Wallberg-Henriksson H. Exercise training in obese diabetic patients. Special considerations. Sports Med 1992 September;14(3):171-89.

(193) Courneya KS, Karvinen KH. Exercise, aging, and cancer. Appl Physiol Nutr Metab 2007 December;32(6):1001-7.

(194) Spalding KL, Arner E, Westermark PO, Bernard S, Buchholz BA, Bergmann O, Blomqvist L, Hoffstedt J, Naslund E, Britton T, Concha H, Hassan M, Ryden M, Frisen J, Arner P. Dynamics of fat cell turnover in humans. Nature 2008 May 4.

(195) Bonyadi M, Waldman SD, Liu D, Aubin JE, Grynpas MD, Stanford WL. Mesenchymal progenitor self-renewal deficiency leads to age-dependent osteoporosis in Sca-1/Ly-6A null mice. Proc Natl Acad Sci U S A 2003 May 13;100(10):5840-5.

(196) Caplan AI. Adult mesenchymal stem cells for tissue engineering versus regenerative medicine. J Cell Physiol 2007 November;213(2):341-7.